ADAPTIVE OPTIMAL MONTHLY PEAK BUILDING DEMAND LIMITING STRATEGY CONSIDERING LOAD UNCERTAINTY

XU LEI

PhD

The Hong Kong Polytechnic University

2019

Temporary Binding for Examination Purposes

The Hong Kong Polytechnic University

Department of Building Services Engineering

ADAPTIVE OPTIMAL MONTHLY PEAK BUILDING DEMAND LIMITING STRATEGY CONSIDERING LOAD UNCERTAINTY

Xu Lei

A thesis submitted in partial fulfillment of the requirements for the degree of Doctor of Philosophy

Mar 2019

CERTIFICATE OF ORIGINALITY

I hereby declare that this thesis is my own work and that, to the best of my knowledge and belief, it reproduces no material previously published or written, nor material that has been accepted for the award of any other degree or diploma, except where due acknowledgment has been made in the text.

_____(Signed)

Xu Lei (Name of student)

ABSTRACT

Abstract of thesis entitled: Adaptive Optimal Monthly Peak Building Demand Limiting Strategy considering Load Uncertainty

Submitted by: Xu Lei

For the degree of: Doctor of Philosophy

at The Hong Kong Polytechnic University in March 2019

Peak demand limiting is an efficient means to reduce the electricity cost over a billing cycle (typically a month) in cases where peak demand charge is applied. However, most previous studies focus on the daily peak demand limiting without considering load uncertainty, which is a big challenge in making proper and reliable decisions in applications. The daily peak demand limiting might not achieve the maximum cost saving in a month due to the partial/complete offset between the peak demand cost reduction and the costs of associated limiting efforts. Therefore, a monthly peak demand limiting strategy is needed. Besides, load prediction is usually an inevitable part of peak demand limiting strategy. For individual buildings, there exists great load uncertainty, mainly due to uncertain peak loads and uncertain weather conditions. As for load uncertainty, probabilistic load forecasting can provide more comprehensive information for decision-making compared with the traditional deterministic load forecasting and it draws increasing attention recently.

This study presents an adaptive optimal monthly peak demand limiting strategy considering load uncertainty. The developed strategy includes the probabilistic load forecasting model, the

optimal threshold resetting scheme, and the proactive-adaptive demand limiting control scheme. A new probabilistic building load forecasting model is proposed considering uncertainties in weather forecasts and abnormal peak load. Two basic function components are developed, including the probabilistic normal load forecasting and the probabilistic uncertain peak load (or abnormal peak load) forecasting. The probabilistic normal load forecasting model is built using the artificial neural network (ANN) and the probabilistic temperature forecasts. The probabilistic abnormal peak load forecasting model consists of two models quantifying the probabilistic occurrence and magnitude of the peak abnormal differential load, respectively. Based on the building load model, an optimal threshold resetting scheme is proposed for monthly peak demand limiting considering load uncertainty, which involves two major functions as follows. The uncertain economic benefits (i.e., gains and losses) of a demand limiting control are quantified on the basis of probabilistic load forecasts. The optimal monthly limiting threshold is identified using the expectation metric based on the quantified economic benefits. The scheme optimizes and updates the monthly limiting threshold by adapting it to the ever-changing weather forecast and actual peak power use. Based on the building load model and the optimal threshold resetting scheme, a proactive-adaptive demand limiting control scheme is developed for online demand limiting threshold reset and online demand limiting control, which is especially effective when only small-scale storages are available.

Validation tests are conducted on the probabilistic load forecasting model, the optimal threshold resetting scheme, and the proactive-adaptive demand limiting control scheme, respectively.

The test results show that the ANN deterministic load forecasting model can achieve satisfactory performance. The probabilistic occurrence model can forecast the occurrence frequency of the peak abnormal differential load with the satisfactory agreement, and the probabilistic magnitude model can well forecast the magnitudes of the peak abnormal differential load. Furthermore, real-time application case studies are conducted by different means of using probabilistic weather forecasts. Results show that the probabilistic normal load forecasts have satisfactory accuracies and the load forecasts based on the one-day-ahead probabilistic weather forecasts are the best. In validating the optimal threshold resetting scheme, case studies are conducted, and the results show that demand limiting based on this scheme can effectively reduce the monthly peak demand cost under load uncertainty in different seasons. Moreover, sensitivity analysis of the means of demand limiting and electricity demand charge on the cost benefits of demand limiting with the resetting scheme is conducted. In validating the proactive-adaptive demand limiting control scheme, case studies are conducted, and the results show that this proactive-adaptive demand limiting control scheme can effectively reduce the monthly peak demand cost for buildings with small-scale thermal storages under load uncertainty.

In summary, an adaptive optimal monthly peak demand limiting strategy is proposed to reduce building peak demands over a month (or a billing cycle) considering load uncertainties, which includes the following three main components. A building load model is developed to quantify load uncertainties from weather forecasting uncertainty and uncertain peak loads. An optimal

threshold resetting scheme is developed to identify an adaptive optimal monthly limiting threshold. A proactive-adaptive demand limiting control scheme is developed to conduct proactively online demand limiting control, even when small-scale thermal storages are available. Validation tests are conducted, and the test results show the adaptive optimal monthly peak demand limiting strategy can achieve significant peak demand reduction under load uncertainties, even when only small-scale active thermal storages are available.

PUBLICATIONS ARISING FROM THIS THESIS

Journal Papers

2019 **L. Xu**, S. W. Wang, R. Tang. (2019) Probabilistic load forecasting for buildings considering weather forecasting uncertainty and uncertain peak load. Applied Energy 2019;237:180-195.

2019 **L. Xu**, S. W. Wang, F. Xiao. (2019) An adaptive optimal monthly peak building demand limiting strategy considering load uncertainty. Applied Energy (under review).

2019 **L. Xu**, S. W. Wang, F. Xiao. (2019) A proactive-adaptive monthly peak demand limiting strategy for buildings with small-scale thermal storages considering load uncertainty. Science and Technology for the Built Environment.

ACKNOWLEDGMENTS

First and foremost, I would like to express my deepest gratitude to my supervisor Professor Shengwei Wang for offering me the opportunity to undertake my PhD research as a member of his group and for providing me his continuous support and vision through my research. Additionally, I would like to express my greatest appreciation to my co-supervisor Professor Fu Xiao for her support, patience and valuable instructions at every stage (especially the tough stage) of my PhD study.

My sincerest thanks go to Prof. Godfried L. Augenbroe and Prof. Tin Tai Chow for consenting to attend my doctoral examination as co-examiners and for offering their valuable comments on this PhD thesis. Moreover, I would like to appreciate Prof. Hongxing Yang for chairing my PhD examination.

The support and the funding of this PhD research by the Research Grant Council (RGC) of the Hong Kong SAR (Grant no. 152694/16E) and a research grant under strategic focus area (SFA) scheme of the research institute of sustainable urban development (RISUD) in The Hong Kong Polytechnic University are also very much appreciated.

During the course of my PhD research, I also received advice, guidance and help from my office mates, colleagues and friends from The Hong Kong Polytechnic University's Building Services Engineering in Building Energy and Automation. Especially, I would like to thank Howard Zhang, Wenjie Gang, Chengchu Yan, Diance Gao, Kui Shan, Cheng Fan, Rui Tang,

Jing Kang, Maomao Hu, Tao Lu, Chaoqun Zhuang and all the PhD students with whom we shared happy and tough moments together. Thank you for the discussions and the feedback and for being there listen to me when I had to complain. You really made my PhD years memorable.

I would also like to send to the warmest thanks to the basketball team members, Colin Yan, Qi Zhang, Jerry Zheng, Zehua Peng, Fei Xie for their unlimited support and understanding during my PhD years. Their words of support and their help at times when I needed the most owns my greatest appreciation.

I would also like to extend my warmest gratitude towards my parents, my sisters and the rest of my family who have been extremely supportive of me and they were always there for me whenever I needed them.

Finally, there are no words to express my gratitude towards my girlfriend, Ms. Jiannong Li. Thank you for your patience with me and all the ups and downs during this insane PhD journey. Thank you for your endless love, support and encouragement that kept me moving forward. Thank you for believing in me when I had no faith in myself.

TABLE OF CONTENTS

LIST OF FIGURES

LIST OF TABLES

CHAPTER 1 INTRODUCTION

1.1 Background and motivations

Severe heat waves ravaged countries around the world in the summer of 2018. This extremely hot weather caused disastrous consequences, e.g., wildfires, health problems, and intolerable living conditions for citizens and animals. It again warns human of the severity in climate change and global warming. To relieve global warming (i.e., reduce CO2 emissions), fossil fuels as the major primary energy (e.g., petroleum, natural gas and coal) should be less consumed in the future. The confronted great challenge lies in how to balance cutting down the primary energy consumption together with CO2 emissions and guaranteeing human life quality.

Renewable energies are increasingly and massively applied to cope with the challenges from the dramatic growth of energy demand and global climate change. Since the last decade, there has been an enormous interest in many countries on renewable energies for power generation (M. Singh et al., 2011). Additionally, the market liberalization and government's incentives have further accelerated the renewable energy sector growth. The contribution of the renewable energy share of the global final energy consumption in 2014 was about 19.2% of the global electricity consumption. However, the electricity grids could suffer significant voltage fluctuations with integrating large amounts of renewable generation, for that renewable generation capacities heavily depend on unstable climate conditions, e.g., solar radiation and wind speed. Any significant imbalance might pose a threat to the electrical grid network in terms of reliability,

voltage regulation and power quality issues, even cause grid failures.

In order to stabilize the electricity grid, the smart grid, a modern electrical power grid infrastructure, is proposed and used for improving the efficiency, reliability and safety of the grid. The smart grid is capable of smoothly integrating renewable and alternative energy resources through automated control and modern communication technologies. The smart grid can provide effective grid integration in distributed generation (including renewable generation) based on the demand side management (DSM) and energy storage technologies for load balancing (V. C. Gungor et al., 2011).

DSM, an approach for matching supply and demand, plays a vital role in meeting the load imbalance challenges in smart grids. DSM commonly refers to programs implemented by utility companies to control energy consumption and peak load/demand on the consumer/demand side. In most of the DSM programs that have been deployed over the past three decades, the key focus has been on the interaction between the utility company and end consumers (i.e., the demand side) (P. Centolella, 2010; A. Gomes et al., 2007; K. Herter, 2007; C. Triki & A. Violi, 2009). Furthermore, flexibility requires electricity consumers on the demand side (e.g., buildings) to be "grid-friendly" and responsive to the requests or ever-changing conditions from power grids.

Buildings, as the largest electricity consumer worldwide, account for 32% of global final energy consumption and one-third of the Green House Gas emissions (D. Ürge-Vorsatz et al., 2015), even over 90% of total electricity consumption in high-density urban areas like Hong Kong (E

MSD, 2018; D. Ürge-Vorsatz et al., 2015)Electrical and Mechanical Services Department, 2018). The large energy consumption in buildings poses a great challenge for governments and practitioners to achieve energy reduction and carbon dioxide reduction. Besides, peak building demand (load) is another significant issue which results in huge investment in the power grid development and reduces grid efficiency. J. Wells et al. (J. Wells & D. Haas, 2004) estimated that the capacity to meet peak demands during the top 100 hours in a year accounted for nearly 20% of the entire electricity cost. This is because the generation and transmission capacities of power grids have to be provided to meet these peak demands that occur occasionally (G. W. Arnold, 2011).

Tackling these two issues of large building energy consumption and huge peak building demand, utility companies (e.g., in Hong Kong) usually charge the monthly electricity bills of buildings based on these two parts. Although different price structures (including these two parts) are applied in different regions, the monthly peak demand cost of a commercial building always account for a significant part of the monthly electricity bill due to the high peak demand charge (J. E. Seem, 1995). Lowering the peak demand (power) and/or reducing the hours that a demand threshold is exceeded can drastically reduce demand charges (Y. Zhang & G. Augenbroe, 2018). John E. Seem reported that the monthly peak demand cost of a commercial building contributed a considerable part to the monthly electricity bill, sometimes even exceeding 50% in the US (J. E. Seem, 1995), and it is typically above 30% in Hong Kong according to the field survey. Under these price structures, peak demand reduction could contribute to the significant reduction of the

electricity cost over a billing period (e.g., a month). Therefore, peak demand management attracts increasing attention on both demand and the supply sides. For electricity consumers, if they take advantage of the different electricity tariffs, significant money saving and efficient system operation can be achieved by changing their power usages, e.g., limiting peak demands. For utilities, the peak demand of overall grids can be reduced accordingly, which could directly reduce the design capacity, an initial investment of systems in the grid side and increase the stability of power grids.

To effectively develop and implement peak demand limiting/reduction in buildings, the precise building load prediction is needed. In practice, load uncertainty is inevitable due to uncertain weather conditions, special events, etc., and it significantly affects the economic performance of implementing demand limiting (D.-c. Gao et al., 2015). The load uncertainty significantly affects the identification of the proper/optimal or practically doable demand limiting threshold and the actual achievement of monthly peak demand cost reduction. In commercial or non-residential buildings, the energy consumption is mainly affected by the outdoor weather conditions and space usage schedules (e.g., schedule of occupants), and this kind of energy consumption is defined as the normal load in this study. And in a long period (e.g., more than one week), the building load forecasts would have great uncertainty due to the significant uncertainty in the long-period weather forecasts. Besides, the abnormal peak loads (e.g., due to extreme events) in a long period also have significant impacts on peak demand limiting. To achieve an effective demand limiting and maximize the actual cost saving in a month, the load uncertainty needs to

be considered sufficiently and properly. However, no existing study has considered the building load uncertainty from real-time weather forecasting uncertainty and uncertain peak loads in peak building demand limiting in the entire billing cycle of a month.

As for peak demand management, different demand limiting control strategies have been developed to reduce monthly peak demands for commercial or non-residential buildings (T. Chen, 2001; B. Cui et al., 2014; K. H. Drees & J. Braun, 1997; A. Hajiah & M. Krarti, 2012; G. P. Henze et al., 1997; G. P. Henze et al., 2004; K.-h. Lee & J. E. Braun, 2008; D. D. Massie et al., 2004; S. Scalat et al., 1996; Y. Sun et al., 2013; P. Xu et al., 2005; Y. Zhang et al., 2007). These studies focus on the demand shifting/limiting control of the HVAC (heating, ventilation and air-conditioning) systems, as a major part of the energy in commercial buildings is consumed by the HVAC systems (Y. Sun et al., 2013). Four different means have been widely used in the existing demand limiting/shifting control strategies concerning the HVAC systems. These means use the technologies including phase change material (PCM) (S. Scalat et al., 1996; Y. Zhang et al., 2007), the thermal energy storage (TES) (B. Cui et al., 2014; K. H. Drees & J. Braun, 1997; G. P. Henze et al., 1997; D. D. Massie et al., 2004), the building thermal mass (BTM) (T. Chen, 2001; K.-h. Lee & J. E. Braun, 2008; P. Xu et al., 2005), and the combination of TES and BTM (A. Hajiah & M. Krarti, 2012; G. P. Henze et al., 2004). However, most of the control strategies for demand limiting are conducted over a short period, e.g., one day rather than an entire billing cycle. These studies might not achieve the maximum cost saving due to the partial/complete offset between the peak demand cost reduction and the costs of associated limiting efforts in a month. And no

existing study has considered how to develop an optimal demand threshold for demand limiting control under load uncertainty over the billing cycle of a month.

In actual building demand limiting control, small limiting capacity (e.g., using thermal storage) is preferred due to its low initial investment cost and low space cost. But demand limiting with small limiting capacity are very probable of a shortage of backup energy supply in the real-time demand limiting control. Currently, no existing study has concerned how to conduct real-time demand limiting control with small limiting capacity (e.g., using small-scale thermal storages) considering load uncertainty over the billing cycle of a month.

To address the aforementioned issues, the research in this thesis focuses on developing an adaptive optimal monthly peak demand limiting (i.e., reduction) strategy considering load uncertainty for an individual building or buildings associated with a charging account. The major contributions include the development of a probabilistic load forecasting model for individual buildings, an optimal threshold resetting scheme for monthly peak demand limiting considering load uncertainty in a month and a proactive-adaptive demand limiting control scheme considering load uncertainty in a month with small storage capacities.

In this study, active thermal storages integrated with the HVAC system and the billing structure in Hong Kong (with a high demand charge price) are adopted to illustrate the cost-benefit quantification of peak demand limiting. When using other approaches for demand limiting (e.g., indoor room temperature reset), modification should be made in the cost-benefit quantification

of peak demand limiting. Besides, this study can be widely applied for those regions, whose electricity billing structure contains the high demand charge price over the billing cycle.

1.2 Aim and objectives

The aim of this PhD project is to develop an adaptive optimal monthly peak building demand limiting strategy considering load uncertainty for individual buildings. The aim can be accomplished by addressing the following major objectives:

1. To develop and validate a probabilistic normal load forecasting model for individual buildings considering weather forecasting uncertainty. The model parameters can be trained by using the historical building data (measured by the BMS (Building Management System)) and the HKO (Hong Kong Observatory) weather data. The developed load forecasting model is suitable for the applications of adaptive online decision-making and robust control of building energy systems.

2. To develop and validate a probabilistic peak abnormal load forecasting model for individual buildings. The model parameters can be trained by using the historical building data. The developed load forecasting model is applicable for predicting the abnormal peak loads with significant fluctuations.

3. To quantify the uncertainties of economic effect and the probability of success of implementing demand limiting over a billing cycle. This uncertainty quantification is the basis of decision-making for an optimal monthly limiting threshold.

4. To develop and validate an optimal threshold resetting scheme for peak demand limiting considering load uncertainty over the billing cycle of a month. An optimal threshold resetting scheme is capable of identifying an adaptive optimal monthly limiting threshold under the constraints of building load uncertainty from input scenarios and the long limiting duration of a billing cycle. This adaptive optimal threshold would help reduce maximum or near-maximum monthly electricity bill for customers under the above constraints.

5. To conduct sensitivity analysis of the effects of different means of demand limiting (reflected by demand limiting capacity, e.g., thermal storage capacity and limiting effort price, e.g., price of thermal energy use per kWh) and different electricity charge tariffs (e.g., demand charge price) on the monthly economic benefit using the developed optimal threshold resetting scheme for peak demand limiting in a month.

6. To develop and validate a proactive-adaptive demand limiting control scheme for monthly peak demand limiting considering load uncertainty. This scheme is capable of resetting the limiting threshold online and proactively before using up the demand limiting capacity (e.g., thermal storage capacity).

1.3 Organization of the thesis

The thesis is divided into 8 chapters. Figure 1.1 shows the outline of the PhD study.

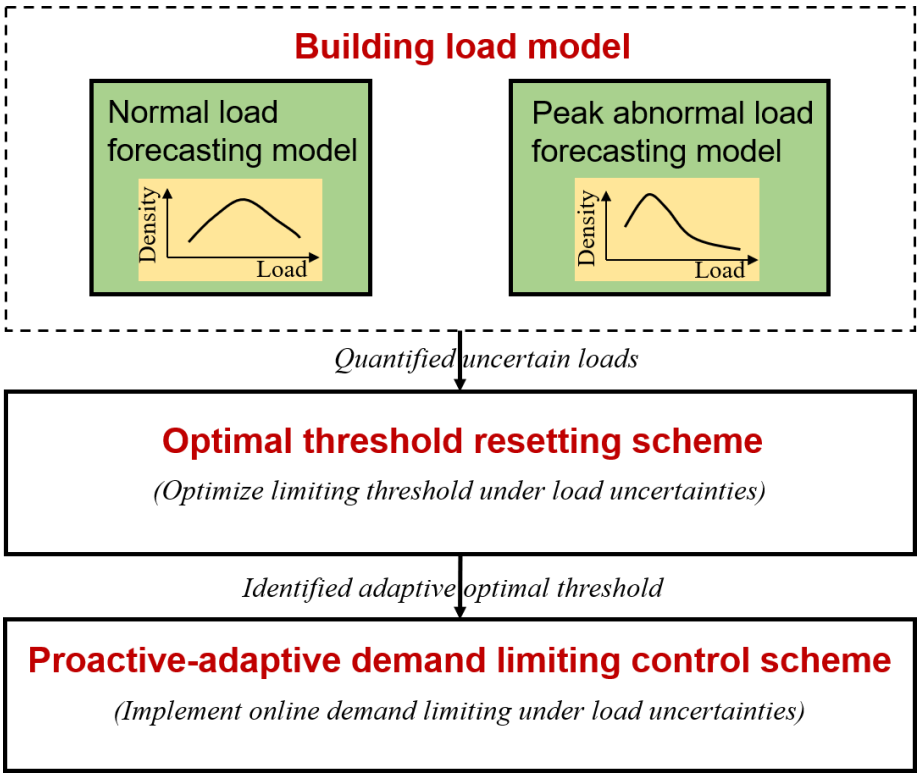

Figure 1.1. Outline of the PhD study.

The main content of each chapter is presented as follows.

Chapter 1: The background and motivation of the present research are outlined by describing the needs of probabilistic load forecasting and monthly peak demand limiting considering load uncertainty. The aim and main objectives are included in this chapter as well.

Chapter 2: A comprehensive literature review is conducted on the state of the art of studies including building load prediction methods (both the deterministic and probabilistic prediction methods), different electric tariffs for demand limiting, existing demand limiting control strategies for buildings and decision-making for demand limiting under uncertainties. This chapter describes the research gaps which are intended to be bridged in this thesis as well.

Chapter 3: This chapter introduces the framework of the adaptive optimal monthly peak building demand limiting strategy. The building data preprocessing is also described in this chapter. Different methods for decomposing the load dataset are introduced and compared. The simple method for normalizing the decomposed load datasets is introduced.

Chapter 4: This chapter presents the development of a new probabilistic building load forecasting model. Two basic function components are developed, including the probabilistic normal load forecasting and the probabilistic uncertain peak load (or abnormal peak load) forecasting. The probabilistic normal load forecasting model is built using the artificial neural network (ANN) and the probabilistic temperature forecast. The probabilistic abnormal peak load forecasting model consists of two models quantifying the probabilistic occurrence and magnitude of the peak abnormal differential load, respectively. The model parameter identification is also introduced.

Chapter 5: This chapter presents an optimal threshold resetting scheme for monthly peak demand limiting considering load uncertainty. The needs and functions of this developed scheme are discussed and illustrated first. Two basic function components are developed and introduced, including the monthly demand limiting threshold optimization and the quantification of economic benefit and probability of success of implementing a demand limiting control. The approach for combining the two kinds of probabilistic load forecasts (i.e., normal load and peak abnormal load forecasts) is introduced.

Chapter 6: This chapter presents a proactive-adaptive demand limiting control scheme for monthly peak demand limiting with small-scale thermal storages considering load uncertainty. Three major functions of the scheme are introduced, respectively. The daily profile prediction is online updated based on a moving average prediction error. The online demand limiting threshold is updated based on the updated demand profile prediction and remaining storage capacity. Based on the updated online limiting threshold, the online demand limiting control is conducted.

Chapter 7: This chapter presents the validation tests of the probabilistic load forecasting model, the optimal threshold resetting scheme and the proactive-adaptive demand limiting control scheme. In the validation of the probabilistic load forecasting model, the ANN model and the probabilistic models of occurrence and magnitude are trained and validated, respectively. Additionally, real-time application case studies are conducted to validate the probabilistic normal load forecasting model by different means of using the probabilistic weather forecasts. In the validation of applying the optimal threshold resetting scheme for monthly peak demand limiting, real-time case studies are conducted in two different seasons (winter and summer). Additionally, sensitivity analysis on the cost benefits of the developed scheme using different means of demand limiting and different electricity demand tariffs is also conducted. In the validation of applying the proactive-adaptive demand limiting control scheme for monthly peak demand limiting, case studies are conducted using small-scale thermal storages in two different seasons.

Chapter 8: Main contributions and conclusions are summarized. Recommendations for the future study are presented as well.

CHAPTER 2 LITERATURE REVIEW

As this research attempts to develop an adaptive monthly peak building demand limiting strategy considering load uncertainty, previous research works are reviewed on building load prediction methods, building demand limiting studies and methods, and demand limiting control under uncertainty. Section 2.1 presents the existing studies on building load prediction methods in two categories: deterministic load prediction and probabilistic load prediction. Section 2.2 presents the building demand limiting studies and methods in two major aspects: demand limiting under different electricity tariffs and existing demand limiting control strategies. Section 2.3 presents an overview of demand limiting control under uncertainty. A summary of the above research reviews is presented in Section 2.4.

2.1 Building load prediction methods

Building load prediction plays a significant role in the optimal planning and control for energy management systems in buildings. In the proceeding years, the conventional deterministic load prediction enables reliable and robust operation of building energy systems, which results in continuous services (e.g., cooling, heating and lighting) to occupants. The operations of building energy systems, e.g., scheduling and maintenance, can be carried out efficiently with accurate load forecast. Effective planning/design of building energy systems depends on the accurate load prediction as well, which can save thousands of dollars.

Moreover, great variability of building use and working conditions, weather conditions as well as extreme events often lead to significant fluctuations of electricity load on the demand side, which results in the needs of the peak load management (or demand limiting) (X. Xue et al., 2014). These fluctuant loads are hard to predict deterministically, sometimes due to lack of knowing precise information about the model inputs, e.g., weather forecasts in a long forecasting horizon like a week. In this case, probabilistic load forecasting has attracted increasing attention due to its capability of providing more comprehensive information in the decision-making process (T. Hong & S. Fan, 2016).

2.1.1 Deterministic load prediction methods

The conventional deterministic load prediction/forecasting can be classified into three categories on the basic time interval, which is acceptable by most of the researchers and shown as follows.

- Short-term load forecast (1 hour to 1 day or 1 week ahead);
- Medium-term load forecast (1 month to 1 year ahead);
- Long-term load forecast (1 year to 10 years ahead).

The short-term load forecast is the major concern in the preceding and existing literature, due to its significant role in the scheduling of energy systems, secure and robust operation of energy systems, cost-effective system control in demand response programs. The medium-term load forecast can be used for efficient operation and maintenance of the building energy systems. The

long-term load forecast can be used for the energy system planning according to the future energy demand prediction and energy policies in the long term.

In the building load forecasting load field, the peak load forecasting in individual buildings is a tough and significant issue. The literature on the building peak load forecasting is quite limited. Most of the previous studies on the peak load forecasting try to construct deterministic models on related information such as weather and historical load data. In 2001, the EUNITE competition was organized aiming to predict the daily maximum load of the next 31 days and several computational techniques (e.g., the support vector machine (B.-J. Chen & M.-W. Chang, 2004), the hybrid artificial intelligence scheme (J. Nagi et al., 2008) and ANN) are used. However, the standard datasets provided in the EUNITE competition only contain the daily maximum load data and the daily average temperature data, which cannot be used for building (i.e., training) the load forecasting model consisting of significant abnormal peak loads. Recently, a least square method is used to predict the monthly peak load based on the historical load data (J. R. G. Sarduy et al., 2016), which also has difficulty predicting the abnormal peak load with good accuracy. In summary, available deterministic models have difficulties in forecasting abnormal peak loads with large fluctuations and little correlation with the weather condition

2.1.2 Probabilistic load prediction methods

Compared to the deterministic load forecasting, the probabilistic load forecasting is presented in the form of density, quantiles, or intervals (T. Hong & S. Fan, 2016). Recently, a tutorial review has summarized the significant development in the probabilistic electric load forecasting,

including notable techniques, methodologies and evaluation methods (T. Hong & S. Fan, 2016). It also concludes that three aspects or any two or three of them can be used to generate the probabilistic load forecasts:

- Simulating input scenarios: An integrated probabilistic electric load forecasting is proposed, which involves the forecast combination of deterministic load forecasting models and temperature scenarios based probabilistic forecasting (J. Xie & T. Hong, 2016).
- Use of probabilistic models (e.g., quantile regression): The probabilistic load forecasts are generated by performing quantile regression averaging on a set of sister deterministic forecasts and the proposed approach leads to dominantly better performance measured by the pinball loss function (B. Liu et al., 2017).
- Converting deterministic forecasts into probabilistic forecasts by residual simulation: A model is presented for probabilistic forecasts of both magnitude and timing (P. E. McSharry et al., 2005).

However, most existing studies on the probabilistic load forecasting for buildings implement temperature scenarios generated from historical climate data, instead of the real probabilistic temperature forecasts, which do not make use of updated online information on future weather condition and cannot provide the best prediction of the building load. In addition, most of these studies are conducted on an aggregation level or system-level loads (Y. Wang et al., 2019). There are very few studies on probabilistic load forecasting for individual load profiles, which have large uncertainties and therefore difficult to be predicted. Recently, a probabilistic individual load

forecasting using pinball loss guided LSTM has been conducted for both residential and commercial buildings (Y. Wang et al., 2019). Also, the probabilistic forecasting of residential electricity consumption of a single household is conducted using the Gaussian Processes (D. W. van der Meer et al., 2018). However, these models are only for short-term probabilistic load forecasting or probabilistic load forecasting of a residential building and neglect the uncertainty of peak load. As for individual commercial/non-residential buildings, the individual load uncertainty significantly depends on the uncertain peak load and the weather forecasting uncertainty (for that the HVAC load is highly related to weather conditions). And up to now, there exist very few existing studies for developing probabilistic forecasting models of uncertain building peak loads over the billing cycle of a month.

2.2 Building demand limiting studies and methods

Building demand limiting control refers to restricting the peak demand of a building in such a way that the maximum demand does not exceed the pre-defined demand in response to the high demand charge tariff. In most tariff mechanisms, high peaks contribute to a higher portion of electricity price. In Hong Kong, the bill mainly consists of two parts. One is the charge for the monthly electrical peak demand (e.g., 120 HK$/kVA), which refers to the maximum energy consumed in a demand interval (i.e., 30 min) for an entire month; the other one is the cost for the overall energy consumption in the month (e.g., 0.6 HK$/kWh). Figure 2.1(A) shows the recent monthly demand profile of a typical office building in Hong Kong, and Figure 2.1(B) shows the corresponding load duration curve. It can be seen that if the demand was controlled during the

5% of the period, there would be a large decrease in the monthly peak demand, and even more dramatic reduction of the monthly electricity charge.

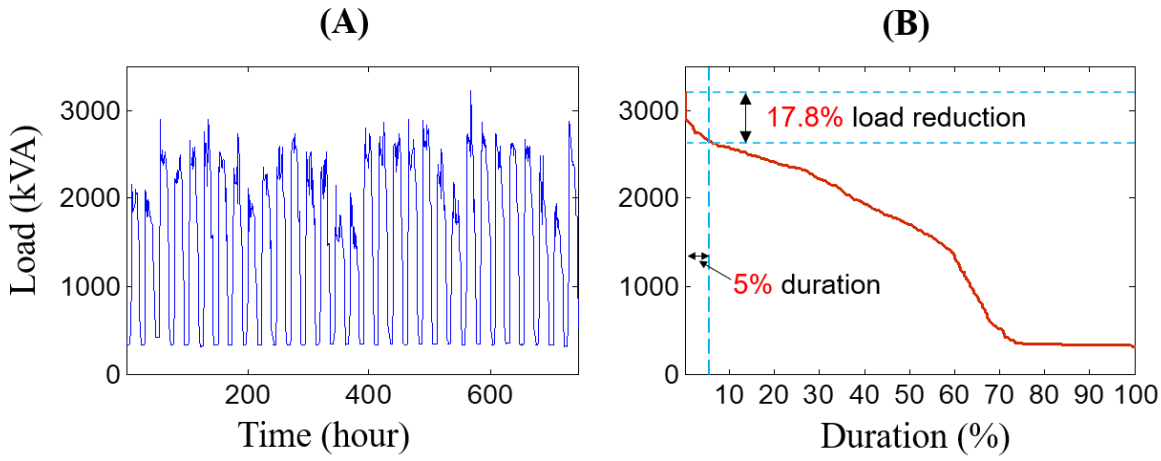

Figure 2.1. A typical office building in Hong Kong with: (A) a typical monthly electricity demand profile and (B) the corresponding the load duration curve in Aug/2015.

Most of the demand limiting control issues in residential buildings can be categorized as an optimal scheduling problem (J. H. Yoon et al., 2014). In contrast, demand limiting control in commercial buildings and other non-residential buildings involves more complex demand management and attracts more attention (D.-c. Gao & Y. Sun, 2016). In commercial buildings, peak demand limiting could breed significant economic benefits to both building owners at the electricity demand side and utilities at the electricity supply side. The owner of a commercial building is charged by both the total amount of electricity it consumes and the peak demand over the billing cycle. Different demand usage profiles are treated with different electric tariffs by the utility company, which results in different means of demand limiting according to their economic benefits. Demand limiting control of the commercial sector is driven by electric tariffs and

achieved through optimizing the operation schedules and controls of the systems/devices.

2.2.1 Demand limiting under different electricity tariffs

The electric load balancing issue at the demand side can be relieved according to different electricity tariffs. These electricity tariffs can automatically induce the customers to limit the peak electric loads during the on-peak period. Several electric tariffs embedded in the demand response programs have already been developed and applied to alter their energy usage behaviors. With these tariffs, building electric demands can be limited based on the occupants' own considerations (e.g., maximum cost saving). A brief introduction is presented on different electricity pricing mechanisms herein.

- Time of use (ToU) denotes that the electricity prices are set for specific periods of the day, e.g., on-peak period and off-peak period. ToU aims to stimulate building owners to shift their power usage from the on-peak period to the off-peak period for economic benefits. Meanwhile, it helps the electrical grid to improve its load factor and reduce the system generation capacity.

- Critical peak pricing (CPP) denotes that the ToU pricing is in effect but with high prices for peak demand hours/days when these prices could be several times of usual prices. CPP is different from the peak demand charge. The latter accounts for the kVA value consumed by the end-users over the billing cycle. The CPP could result in a quite different demand profile through demand limiting control, compared to that according to the ToU pricing.

- Real-time pricing (RTP), also called dynamic pricing, denotes that the electricity prices might

change as often as hourly or even in a shorter time step (e.g., 15 min). The RTP is usually announced one day ahead or a few hours ahead. The actual power profile after the implementation of demand limiting under the day ahead RTP could be unusual and affect the RTP pricing in the next day.

- Direct load control (DLC) program denotes that the electrical utilities own the right to directly regulate the amount of power of the specific building energy systems at certain times based on the previous signed agreements/contracts. The DLC is usually conducted during the on-peak periods with high demand or emergency situations of the electrical grid.

- Demand side bidding (DSB) program denotes that end-users provide their availabilities in demand reduction quantities and the corresponding expected economic benefits in advance, e.g., one day ahead or one hour ahead. Once the electricity market accepts the bid, the end-users are expected to reduce peak demand as promised and will receive the corresponding payments. Otherwise, they will be penalized for breaking the promise to guarantee a certain amount of demand reduction. The DSB involves the short-term discrete alterations into individual load profiles of the end-users, while other electric tariffs for demand limiting involve continuous and permanent alterations into the load profiles.

2.2.2 Existing demand limiting control strategies

As aforementioned, the demand limiting control in commercial buildings is more complex and attracts more attention due to its significant economic benefits. As reported from the International

Energy Agency (IEA), peak demand management in commercial buildings could account for an annual $10-$15 billion for the U.S. market (S. B. Sadineni & R. F. Boehm, 2012). Moreover, the energy usage in the commercial sector increases at a higher speed than that in other sectors. In some high-density urban areas, e.g., Hong Kong, a large share of the total electricity (e.g., 60%) is consumed by commercial buildings, in which the HVAC systems account for about 50% (R. Qi et al., 2012).

The total electric demand/load of a commercial building can be further divided into two major categories: inelastic demands and elastic demands. Generally, it is contributed by various building service systems including HVAC systems, lightings, lifts/elevators and other electrical equipment (C. Yan et al., 2012). Normally, electricity loads of lightings, electrical equipment, lifts and other appliances can be categorized as sheddable loads. In contrast, the electricity loads of HVAC systems are categorized as controllable loads which are possible to be changed via demand management. Load shedding and load shifting are two major means used for peak demand management. Load shedding control reduces peak building demand by turning off non-essential electric loads. Load shifting reduces peak building demand by shifting the on-peak load to off-peak time is more commonly-used for peak demand management.

To reduce the peak building demand, different demand limiting control strategies have been developed. These studies focus on the demand shifting/limiting control of the HVAC (heating, ventilation and air-conditioning) systems, as a major part of the energy in commercial buildings is consumed by the HVAC systems (Y. Sun et al., 2013). Moreover, thermal storages can be

solely used or combined with the HVAC systems to reduce fluctuations of daily demand profiles further and achieve more peak demand reduction. Four different types of thermal storages have been widely used, i.e., the phase change material (PCM) (S. Scalat et al., 1996; Y. Zhang et al., 2007), the thermal energy storage (TES) (B. Cui et al., 2014; K. H. Drees & J. Braun, 1997; G. P. Henze et al., 1997; D. D. Massie et al., 2004), the building thermal mass (BTM) (T. Chen, 2001; K.-h. Lee & J. E. Braun, 2008; P. Xu et al., 2005), and the combination of TES and BTM (A. Hajiah & M. Krarti, 2012; G. P. Henze et al., 2004).

Optimal limiting control strategies using HVAC systems

Building automation provides a convenient way for the supervisory and optimal controls of the devices/systems in conducting peak building demand management. In commercial buildings, it is simple and takes little efforts to conduct demand management in lightings, electrical appliances, escalators and elevators. For instance, proper interaction between the artificial light and the daylight can reduce the electric demand in the lighting systems. In contrast, it is more complex to reduce power demands in the HVAC systems and the amount of the corresponding demand reduction could be far larger. The optimal control of the HVAC systems in commercial buildings is more complicated than that in other building systems.

Energy saving of the HVAC systems can be achieved by two major approaches: the global temperature adjustment and the HVAC system adjustment. The global temperature adjustment is carried out by resetting building zone temperature setpoints during the demand limiting periods.

HVAC system adjustment is conducted via the chiller quantity, duct static pressure set-point, fan quantity and so on to satisfy different demand reduction quantities as required.

- Global temperature adjustment (GTA) allows building operators to adjust the space temperature set-points for an entire facility by a quest from a specific location. In field tests, GTA is demonstrated to be an effective control strategy for building demand limiting (M. A. Piette et al., 2004). In practice, the power consumption of the HVAC systems in commercial buildings is significantly determined by the indoor thermostat set-points (N. Wang et al., 2013).Figure 2.2 illustrates the control logic of indoor air temperature set-point resetting strategy to limit the peak demand. In this case, the set-point at the *k*th time step is continuously updated according to the actual power demands of the chiller plant. This control strategy has the capability of achieving even reduction of service level among all zones and is easy and automatic to activate via remote signals and manually by building operators.

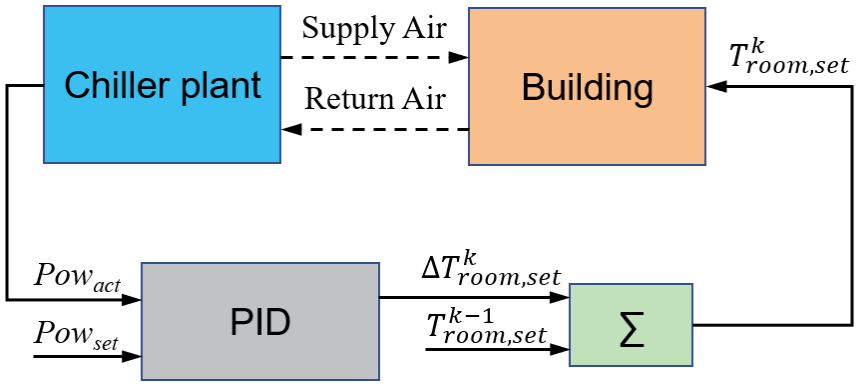

Figure 2.2. Schematics of the PID control algorithm of demand limiting for indoor air temperature set-point reset (Y. Sun et al., 2010).

- Chiller consumes a significant share of the total electricity and has great potential in peak demand limiting. For instance, the power demand of chillers might dramatically increase during the precooling/morning start period. In such a period, the aggregated peak demand and high peak demand charges are derived. Therefore, the optimal start control and sequencing control of chillers are essential in the daily operation of the HVAC systems to restrict peak demand in commercial buildings. Different demand profiles could result from different combinations of the operating number of chillers and precooling lead time (Y. Sun et al., 2010). Identifying the optimal operating number of chillers is an efficient way to conduct electric demand limiting when a certain amount of demand is needed to be reduced. Green scheduling for chillers and thermal storages was adopted to achieve both higher COP by improving the PLR of chillers and the peak demand reduction.

- Duct static pressure (DSP) set-points can be reduced for peak demand limiting without any sacrifice of the indoor thermal comfort. This is due to the fact that the DSP set-points are higher than actual demands and the openings of variable air volume (VAV) boxes approach to be fully closed. But the reduction of the DSP set-points would result in some VAV terminal boxes fully open due to the extremely low DSP set-points.

- Fan quantity reduction can reduce the power demands of air-conditioning systems by shutting down some of the operating air delivery fans. As this approach might speed up the retained fans for the VAV system and brings the burden to these fans, it is solely recommended for the constant air volume (CAV) system, not the VAV system.

- Fan variable frequency drive limit can reduce the power demands of air delivery fans by slowing down the fan's variable frequency drives (VFD). Generally, two major approaches are used for the fan's VFD limit. The first one is to limit the speed of the VFD at a fixed percentage. The second one is to limit the speed of the VFD at a fixed percentage lower than the VFD% prior to the curtailment.

Onsite generation such as the CCHP (combined cooling, heating and power) systems can significantly reduce the peak demand and total energy consumption (P. J. Mago & A. K. Hueffed, 2010; K. Siler-Evans et al., 2012) as well. It was reported that using cogeneration could achieve 13% peak demand reduction and 16% total energy consumption reduction while using cogeneration together with thermal storages could achieve 23% peak demand reduction and 21% total energy consumption reduction (K. Khan et al., 2004).

Building automation system (BAS) is an effective energy management system in the commercial buildings, which allows both the local control and supervisory control of the energy systems. BAS functions to not only record the specific energy information such as heating/cooling loads of buildings and the power demands of other devices/systems for further analysis but also to conduct the optimal controls of electric demands in different levels, i.e., buildings, systems and system components. With the help of the information and communication technologies, BAS can conduct the overall optimization in both the power supply and demand sides by considering the power reliability, energy efficiency and economic benefits. An agent-based building energy simulation process was demonstrated to interact with the aggregate load profile of individual

buildings and the electricity prices of the grid (F. Zhao et al., 2010). The building energy usage behaviors and power demand reduction potentials that are greatly sensitive to electricity prices can significantly affect the aggregate effect of the demand response.

Optimal limiting control strategies using thermal storages

Recently, thermal storages are regarded as one promising technology for peak demand limiting in commercial buildings, which also treated as supplementary sources when integrating with renewable energies (M. Ban et al., 2012; P. Tatsidjodoung et al., 2013). The optimal control of thermal storages is a significant issue in peak demand management since building thermal demand is considered as one of the potential building power demand responses. Generally, thermal storages in commercial buildings can be categorized into two categories: passive thermal storages (e.g., building thermal mass and decentralized PCM) and active thermal storages (e.g., ice storage, water storage and centralized PCM). The passive thermal storages are usually controlled with limitations from the indoor/outdoor conditions. In contrast, the active thermal storages can be controlled on the basis of a stable control variable, e.g., a fixed temperature for energy charging/ discharging, which is free from the constraints of the indoor/outdoor conditions.

Building thermal mass

Existing studies and applications of the building (thermal) mass (BTM) mainly focus on two functions, i.e., night precooling and diurnal peak demand reduction, which are driven by the different electricity usage costs during day and night and primarily stimulated by the ToU prices

and/or CPP prices (Y. Sun et al., 2013). The charge control strategies of the BTM during the precooling period and the discharge control strategies of the BTM during the on-peak period significantly affect the cooling load profile, the power demands of the HVAC systems and the corresponding total energy cost. For instance, the peak load can be effectively reduced by 25% of the cooling capacity by implementing the precooling strategy (K. R. Keeney & J. E. Braun, 1997). Moreover, the indoor air temperature could be maintained at the lower temperature boundary of the comfort region during the office hours and allowed to float to the upper-temperature boundary during the peak hours (P. Xu et al., 2004). Based on this strategy, the chiller power was reduced by 80%-100% without causing any thermal discomfort and complaints. Detailed precooling tests were carried out in eleven buildings, and it was reported that 15%-30% peak demand reduction was achieved during peak hours (R. Yin et al., 2010). Most of the control strategies for demand limiting was conducted over a short period, e.g., one day. These strategies did not consider the tradeoff between the peak demand reduction and the total used energy cost over the billing cycle. This tradeoff might contribute to no economic benefits based on how much this tradeoff could be. Considering such a tradeoff, a power demand limiting strategy was developed based on the prediction of the building monthly peak demand, 8.51%-10.45% of the electricity cost saving could be achieved through peak demand limiting via the BTM (Y. Sun et al., 2010). Figure 2.3 illustrates a typical precooling and discharging control strategies of the BTM during the unoccupied and occupied periods, respectively. The indoor air temperature set-point is reset to a low value aiming to store cold energy in the BTM and then reset to a high value to release that stored cold energy.

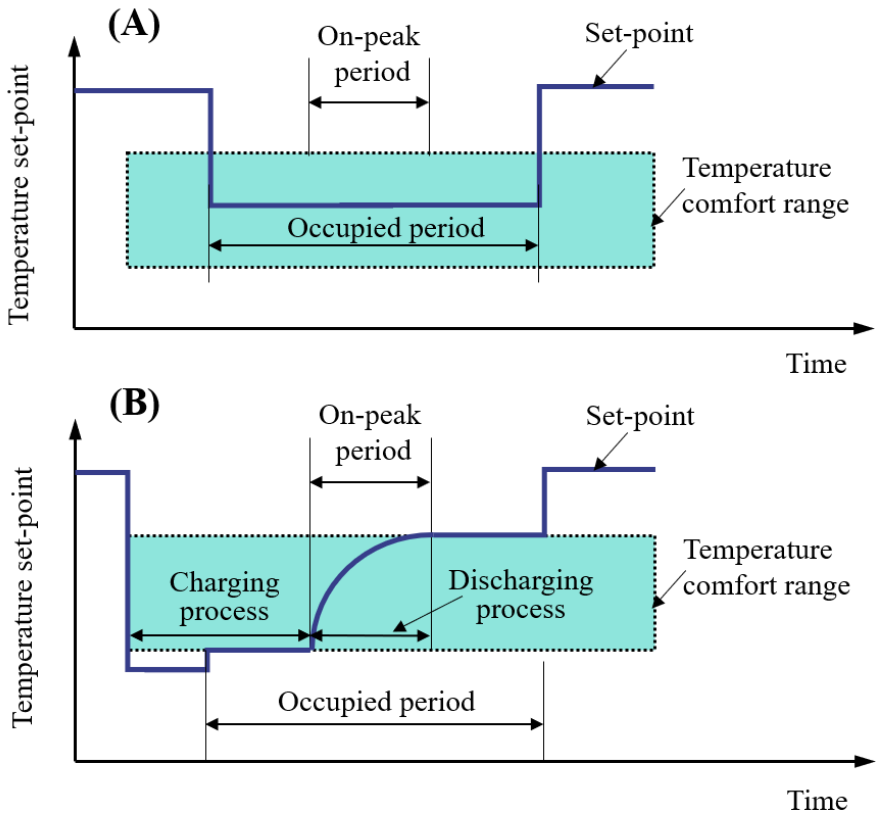

Figure 2.3. Indoor air temperature set-points of (A) conventional night setup control strategy; (B) precooling and demand limiting strategy (K.-h. Lee & J. E. Braun, 2008; Y. Sun et al., 2013).

As demand limiting using the BTM depends on the variations of the indoor air temperature, the actual performance of demand limiting is constrained by several factors such as the performance of the HVAC systems, the thermal capacitance of the BTM, the electricity pricing structure, occupancy thermal comfort, weather conditions, etc. Due to these constraint factors, it is more complicated to develop control strategies of the BTM compared with the active thermal storages. To relieve such complexity, the active thermal storages combined with the passive thermal storages for peak demand limiting were investigated (G. P. Henze et al., 2004; G. Zhou et al.,

2004). Results showed the combined use of the active and passive thermal storages for demand limiting could save energy cost up to 26% compared with the case without the active thermal storage. Moreover, the predictive optimal control of active and passive thermal storages is also significant for the building peak load management due to the fact that building loads suffer the uncertainties from the weather conditions, special events and especially the forecasting models (G. P. Henze, 2005; S. Liu & G. P. Henze, 2004; S. Morgan & P. Moncef Krarti PhD, 2010).

Ice and water storages

Generally, both ice and water storages are implemented as the centralized thermal storages to achieve peak demand limiting. In the U.S., the peak demand cost could be reduced by 27%-31% by using ice storage in different climates (F. Sehar et al., 2012). As for employing the chilled water storage, the chiller capacity and peak demand could be decreased by 50% and 31.2% respectively (S. Boonnasa & P. Namprakai, 2010). Figures 2.4 and 2.5 illustrate the operation principle of a typical thermal storage system for the purpose of cooling. The thermal storages usually charge the cold energy during the off-peak time and discharge the cold energy during the on-peak time to achieve cooling load shifting/ peak demand limiting. It is worth mentioning that the power demand of the HVAC systems usually depends on their provided cooling loads. Hence, the power demand limiting of the HVAC systems is determined by the cooling demand limiting of the systems.

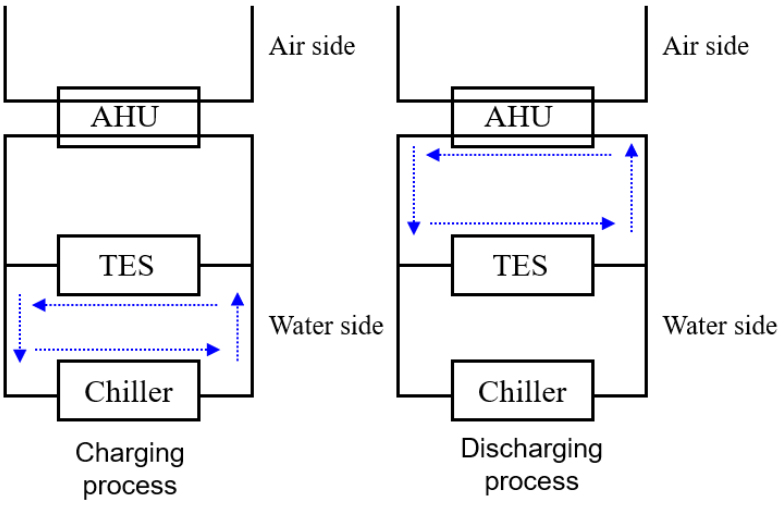

Figure 2.4. Schematics of charging or discharging processes using the thermal storage system (Y. Sun et al., 2013).

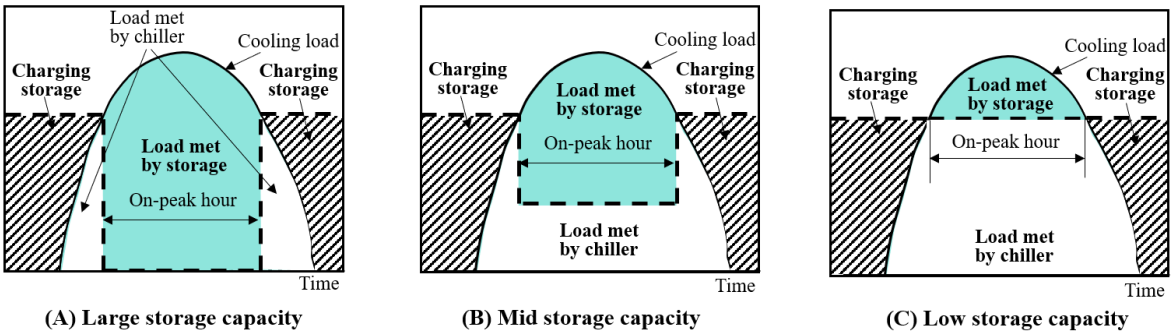

Figure 2.5. Storage capacity based control strategies of the thermal storage system for peak demand limiting (Y. Sun et al., 2013).

Different optimal control strategies and algorithms have been developed to improve the performance of the ice/water storage systems (K. H. Drees & J. E. Braun, 1996). However, most of these optimal control strategies are mainly implemented on day-ahead electricity prices and operation management. These control strategies/algorithms might not fulfill the requirements of peak demand limiting in a long period (e.g., a month), which concerns a different electricity

billing structure and the issue of compromise between the peak demand reduction and accumulated limiting efforts in the long period.

Phase change material

Phase change materials (PCM) are considered as a promising energy storage on the basis of four major functions: utilizing the free cooling at night for daily peak cooling load limiting, reducing diurnal temperature fluctuations concerning the indoor thermal comfort, narrowing the difference between the on-peak and off-peak loads of electricity/energy demand and saving the operation cost of building energy systems under specific tariffs e.g., ToU and CPP (W. A. Qureshi et al., 2011; A. Waqas & Z. U. Din, 2013; Y. Zhang et al., 2007). Many studies have been conducted on the modeling and optimal control of the building integrated PCM. An idealized model for peak load shifting and a simplified EC-model have been respectively developed for investigating the indoor thermal performance, and the results showed that developed models were capable of representing the thermal characteristics of the PCM (A. Waqas & Z. U. Din, 2013; N. Zhu et al., 2010). Studies also pointed out that the occupancy and ventilation patterns could significantly influence the energy performance of the PCM-enhanced envelope (B. M. Diaconu, 2011). It was reported that 67% reduction during the chiller peak-time operation could be achieved by implementing the PCM tank with free-cooling (B. P. Walsh et al., 2013). In the application of PCM into the air supply side of the HVAC systems, three different operation modes (i.e., charging, ordinary and discharging operations) are respectively presented based on the specific requirement (M. Yamaha & S. Misaki, 2006). It is worth mentioning that the indoor air

temperature and the phase change temperature are the major variables for the charging/discharging control of the building integrated PCM.

2.3 Demand limiting control under uncertainty

The operation/control processes of building energy systems for demand/load management are irrevocably affected by uncertainty, with the stochastic nature of climate conditions and human behavior. The definition of uncertainty is regarded as “any deviation from the unachievable ideal of completely deterministic knowledge of the relevant system” by Walker et al.(W. E. Walker et al., 2003).

In a computational model, the uncertainties can be categorized into two locations: model-inherent uncertainty and parameter uncertainty. Models are an abstraction of reality in the form of a simplified mathematical representation. Any insufficient knowledge about the specific physical processes presented in a model could contribute to the model-inherent uncertainty (L. Uusitalo et al., 2015). In terms of the model-inherent uncertainty, there is no generic methodology to deal with such uncertainty due to the model-specific nature (E. Rajabally et al., 2002). It is even more difficult to deal with the model uncertainty for energy system models since energy models are claimed to be non-validatable by several authors (S. Pfenninger et al., 2014; J. M. F. Rager & F. Maréchal, 2015). Due to these facts, this thesis will not consider model-inherent uncertainty. In terms of model parameter uncertainty, it corresponds to the process of assigning values to the model’s input parameters and might be derived due to lack of knowledge, unreasonable assumptions, etc. with regards to the parameters’ real values. This type of

uncertainty has been the focus of most studies related to the domain of optimal building energy system controls (e.g., for demand management or peak demand limiting). This thesis will also focus on this type of uncertainty. However, quite few existing studies on demand limiting consider the uncertainty in the operation/control action.

Based on the uncertainty quantification techniques, such as uncertainty analysis and sensitivity analysis, modelers can better comprehend the behavior of the model under uncertain conditions. Instead of making a single operation/design decision for energy systems, these techniques provide more information for modelers to make decisions themselves. Therefore, demand limiting under load uncertainty is based on the optimization principles and techniques for optimization under uncertainty. There are two main representatives for optimization under uncertainty, i.e., stochastic programming (SP) and robust optimization (RO), which are presented as follows. A general review for the optimization methods under uncertainty is presented in (N. V. Sahinidis, 2004). In addition, reviews on the application of optimization methods under uncertainty into the energy systems can be found in (M. Aien et al., 2016; A. Soroudi & T. Amraee, 2013; Y. Zeng et al., 2011).

Stochastic programming

Generally, stochastic programming (SP) is a commonly-used method of optimization under uncertainty. Stochastic programs are mathematical programs, in which some of the parameters suffer uncertainty. The basic assumption in SP is that uncertainty is probabilistic, and the

probability distributions of the parameter are known or can be estimated. With such probability distributions, the optimization for a measure of performance can be conducted using different criteria from the Decision Theory as follows (J. R. Birge & F. Louveaux, 2011).

Expectation criterion is the most common criterion in stochastic programming, which would appeal to risk-neutral decision-makers (G. Mavromatidis et al., 2018). The expectation value is represented as the weighted average of the possible values of the parameter.

Maximum criterion is very conservative and risk-averse and would appeal to the pessimistic decision-maker, which uses the maximum possible value of the parameter.

Minimum criterion, in full contrast to *Maximum criterion*, presents the point of an extremely optimistic and risk-seeking decision-maker, who seeks to minimize the adjusted threshold in the best situation and ignores the possibility of the extremely worst situation.

Hurwicz criterion seeks a compromise between the extremely pessimistic criterion and the extremely optimistic criterion, which is applicable for neither too optimistic nor too pessimistic decision-makers. The Hurwicz criterion weighs the Maximum criterion and the Minimum criterion using w and $(1-w)$ as weights. Where, w represents the decision-maker's optimism level. $(1-w)$ represents the decision-maker's pessimistic level.

Value-at-Risk (VaR) criterion is also a risk-averse decision-making criterion. Compared to the aforementioned Maximum criterion, the *VaR* criterion is less conservative and considers the probability of the worst situation for the hourly threshold adjustment. The VaR_α is defined as the

adjusted threshold, which corresponds to the α quantile and will be exceeded with a probability of (1-α) %. Where α is a given value in the range of [0,1]. Figure 2.6(A) shows the VaR_α value for the hourly adjusted threshold ($\triangle PD_{set,adj}$) distribution. When α equals to 0, the *VaR* criterion is equal to the Minimum criterion, while when α equals to 1, the *VaR* criterion is equal to the Maximum criterion.

Conditional Value-at-Risk (CVaR) criterion is an additional risk measure for risk-averse decision-making (R. T. Rockafellar & S. Uryasev, 2000), which takes an average of the extreme values in the tail of the distribution of the hourly adjusted threshold, beyond the *VaR* value. Given a value α ($0 \leqq \alpha \leqq 1$), the $CVaR_\alpha$ is defined as the expected value of the hourly possible adjusted thresholds that are larger than the VaR_α. Figure 2.6(B) shows the $CVaR_\alpha$ value for the hourly adjusted threshold ($\triangle PD_{set,adj}$) distribution. It can be seen that the decision-maker use the $CVaR_\alpha$ value for hourly threshold adjustment according to the average effect of the (1-α)•100% worst situations at the tail of the $\triangle PD_{set,adj}$ distribution, instead of the VaR_α value at the α quantile.

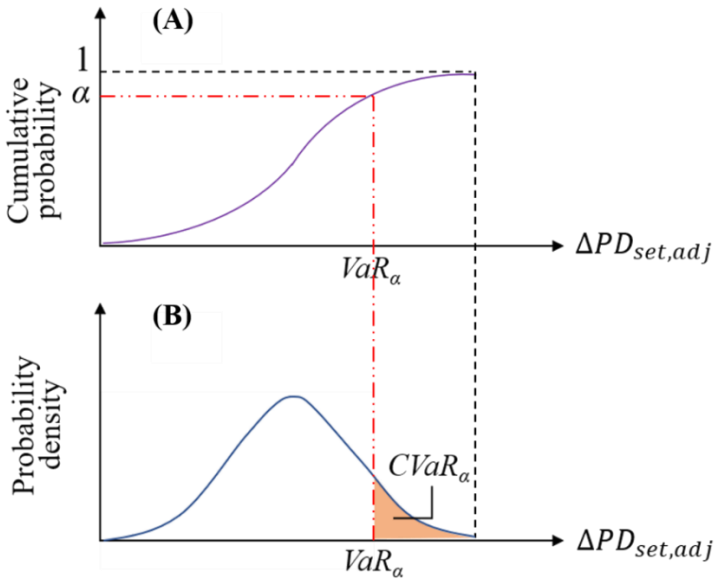

Figure 2.6. Definitions of (A). $CVaR_\alpha$ and (B). VaR_α for the hourly adjusted threshold ($\triangle PD_{set,adj}$) distribution.

The main disadvantage of the stochastic programming is that it requires the probabilistic information for each uncertain parameter in the form of either scenario with associated probabilities or a probability distribution. However, such information might be difficult or even impossible to obtain.

Robust optimization

Robust optimization is a relatively new approach for optimization under uncertainty, which is an alternative to stochastic programming and can address the main drawback associated with stochastic programming. Instead of probabilistic information, robust optimization only requires a set-based representation of uncertainty, usually in the form of an interval around the nominal value. An overview of robust optimization can be referred to (A. Ben-Tal et al., 2009; D.

Bertsimas & A. Thiele, 2006). It aims to optimize the objective function against worst-case realizations of the unknown-but-bounded uncertain parameters (A. Thiele et al., 2009). The drawback of this approach could lead to overly conservative solutions (D. Bertsimas & M. Sim, 2004).

2.4 Summary

This chapter presents a review on building load prediction methods, building demand limiting studies and methods, and demand limiting control under uncertainty. From the above review, the following research gaps are identified:

i. Research studies on probabilistic load forecasting for individual buildings considering real-time weather forecasting uncertainty and uncertain peak loads and monthly peak building demand limiting control considering load uncertainty over the billing period of a month are seriously insufficient and need more efforts.

ii. Most existing studies on the probabilistic load forecasting for buildings implement temperature scenarios generated from historical climate data, instead of the real probabilistic temperature forecasts, which do not make use of updated online information on future weather condition and cannot provide the best prediction of the building load. There are limited studies on probabilistic load forecasting for individual building load profiles, but they are only applicable for short-term probabilistic load forecasting or a residential building. In terms of uncertain building peak loads (vital to peak demand limiting), no existing study

considers them in developing probabilistic forecasting models over the billing cycle of a month.

iii. Most existing studies on building demand limiting control strategies are conducted over a short period, e.g., one day rather than an entire billing cycle. These control strategies might not achieve the maximum cost saving when the peak demand charge is a major factor over the billing cycle, due to the fact that the partial/complete offset is not considered between the peak demand cost reduction and the costs of associated limiting efforts over a billing period. Moreover, no existing study has considered the building load uncertainty in peak building demand limiting over the billing cycle of a month.

iv. In the real-time building demand limiting control over a period, a small limiting capacity (e.g., using small-scale storages) is preferred but could lead to the shortage of backup energy supply for peak demand limiting when the actual peak demands are much larger than the predicted peak demands. In the situation of very limited capacity, proactive-adaptive control is needed for peak demand limiting before using up the storage capacity. No existing study has considered the peak building demand limiting under the situation of demand limiting duration of a billing cycle (e.g., a month), load uncertainty and small-scale thermal storages simultaneously.

CHAPTER 3 FRAMEWORK OF ADAPTIVE OPTIMAL MONTHLY PEAK BUILDING DEMAND LIMITING STRATEGY AND BUILDING DATA ACQUISITION

This chapter presents the overall framework of the proposed adaptive optimal monthly peak building demand limiting strategy together with building data acquisition. Section 3.1 introduces the overall framework. Section 3.2 describes the building and data acquisition concerned in model training and validation case studies of the models and strategies developed.

3.1 Framework of adaptive optimal monthly peak building demand limiting strategy

The overall framework of the developed adaptive optimal peak building demand limiting strategy is illustrated in Figure 3.1. It comprises three major components: the building load forecasting model, the optimal threshold resetting scheme and the proactive-adaptive demand limiting control scheme. The building load forecasting model is developed to forecast the probabilistic loads based on the weather forecast and calendar information, which includes two basic functions: the probabilistic normal load forecasting and the probabilistic uncertain peak load (or abnormal peak load) forecasting. The optimal threshold resetting scheme is developed to identify the optimal limiting threshold based on the forecasted probabilistic demand profiles, which includes the quantification of uncertain economic benefits (i.e., cost savings) of implementing a demand limiting control and the monthly demand limiting threshold optimization. The proactive-adaptive

demand limiting control scheme is developed to online update the limiting threshold for online demand limiting control, which includes the online update of the demand profile prediction, the online demand limiting threshold reset and the online demand limiting control. The adaptive optimal monthly peak demand limiting strategy works in an adaptive manner over the billing cycle of a month and starts again at a new billing cycle.

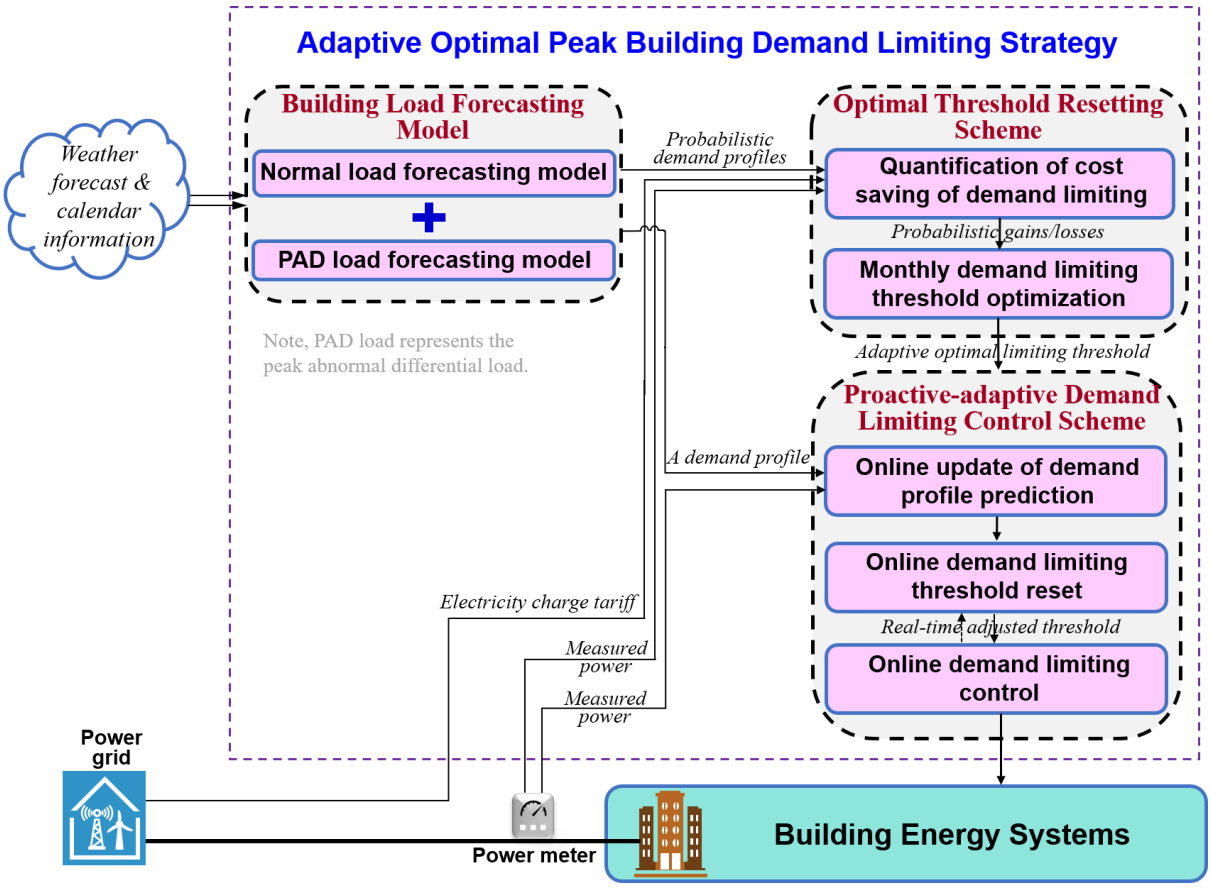

Figure 3.1. The overall framework of the adaptive optimal peak demand limiting strategy.

3.2 Description of the building and data acquisition

Description of the building

An educational building, i.e., Phase 7, on the campus of The Hong Kong Polytechnic University (in Hong Kong within the sub-tropic climate zone), is selected in the study and shown in Figure 3.2. It is equipped with different research facilities, laboratories, classrooms, lecture theaters and staff offices. The gross floor area is 26,264 m^2.

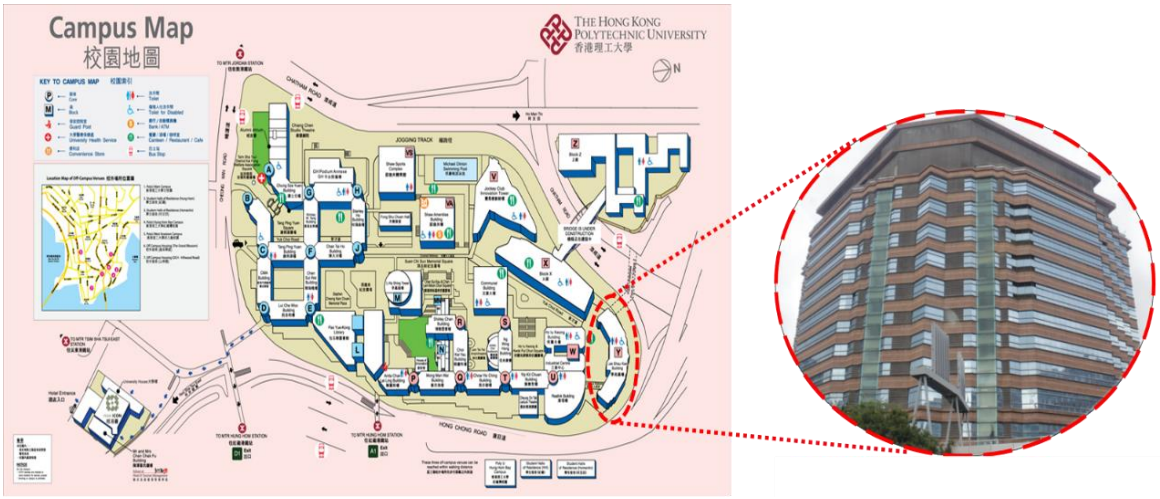

Figure 3.2. An educational building (named Phase 7) on the campus of The Hong Kong Polytechnic University.

Data acquisition

The facility management office (FMO) of the campus uses the BMS (building management system) to monitor and control building energy systems. The electricity consumption of a campus building can be recorded at the 1-minute interval based on a particular communication protocol,

e.g., the BACnet. The electricity demand is measured via the power metering system in the 30-minute interval, which is the average weighted value of power demands in 30 minutes and also used to charge the monthly peak demand by the CLP company in Hong Kong.

In Hong Kong, the peak load (demand) of commercial buildings usually occurs during the on-peak time (i.e., from 9:00 AM to 21:00 PM, excluding Sundays and public holidays), which results in a critical issue for peak demand limiting and contributes to the high monthly electricity cost. For simplicity and forecast precision, the historical datasets only during the on-peak time (i.e., office hour) are used for model training and validation tests, and the load spikes from chillers' starting in the morning before 8:00 AM are not considered in this study. There are two reasons for this choice. Firstly, these spikes occur during the off-peak time, during which the demand charge price is much lower than that during the on-peak time in Hong Kong. Secondly, these load spikes are not the effective causes of actual monthly peak loads based on analyzing the practical load profiles of many buildings. The electrical load profile of the Phase 7 building shows a seasonal variation and uncertain peak loads in each month, as shown in Figure 3.3. Moreover, the daily electrical demand/load profiles of the Phase 7 building in both 1-min and 30-min intervals show daily variation and abnormal peak loads during office hours on different workdays, as shown in Figure 3.4. In Hong Kong, the monthly peak billing demand is based on 30-min average demand. Once the 1-min peak demands are well controlled, the monthly peak billing demand will be well limited.

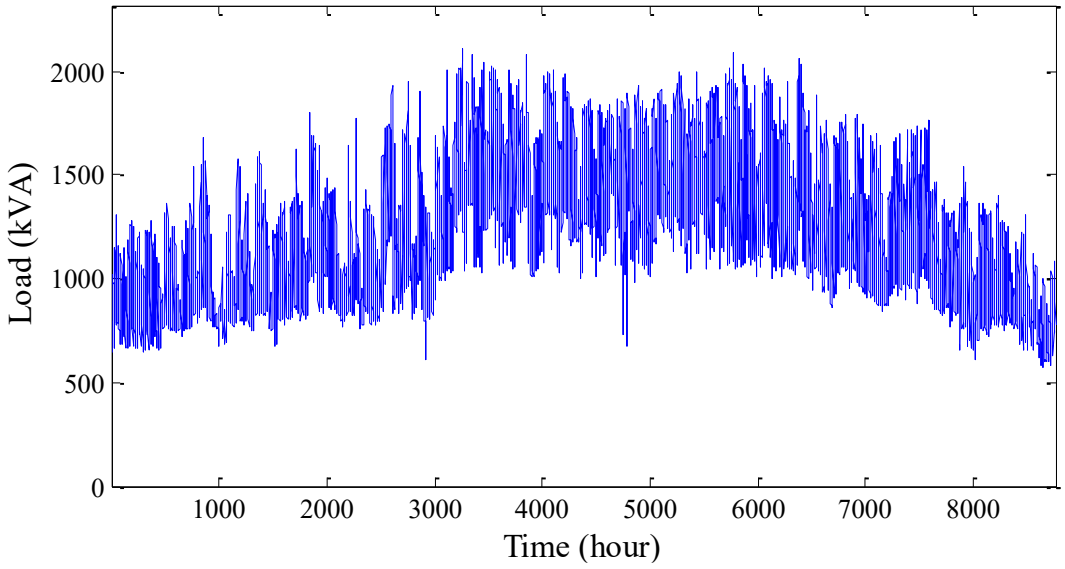

Figure 3.3. The electrical load profile of the Phase 7 building in the year 2013.

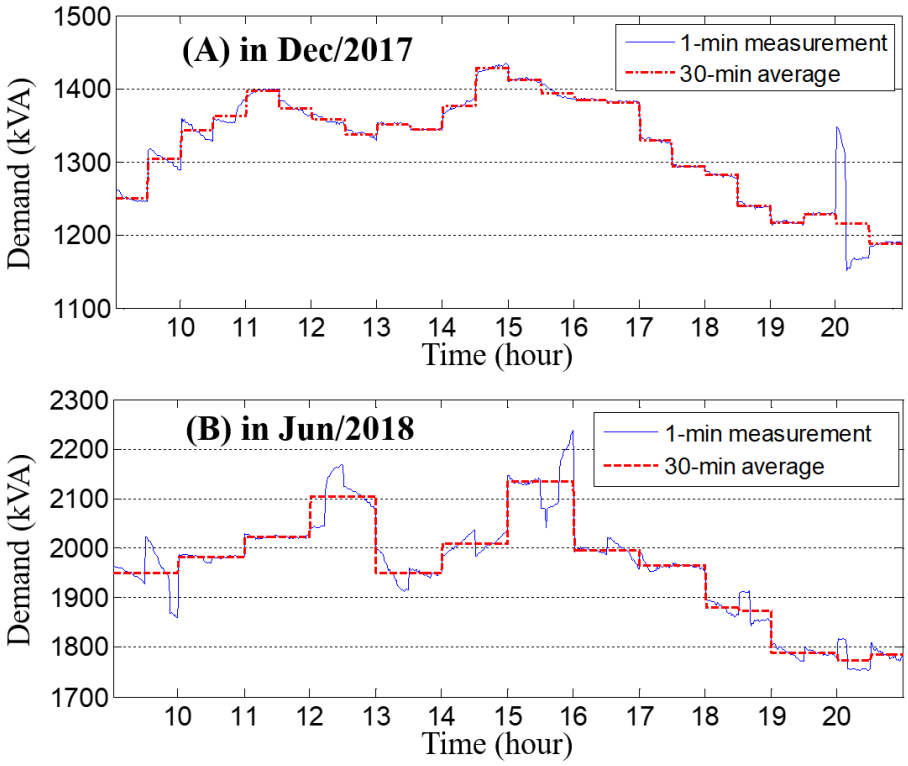

Figure 3.4. 1-min and 30-min average electrical demand profiles of the Phase 7 building during office hours on typical workdays.

The weather forecast from the Hong Kong Observatory (HKO) includes the deterministic outdoor dry-bulb temperature and relative humidity forecasts at the 1-hour interval and the probabilistic daily maximum and minimum temperature forecasts in the 1-day interval. The forecast horizon for these deterministic forecasts is 9 days, while that for these probabilistic forecasts is 14 days. In each month, the 9-day weather forecast data reported daily by the HKO are recorded daily. These 1-hour interval weather forecasts are used to forecast building loads at the 1-hour time interval. As outdoor temperature and relative humidity during the on-peak time are much stable at each hour, the forecasted peak load at the 1-hour time interval is assumed to equal that at 30-min time interval.

3.3 Summary

This chapter introduces the framework of the adaptive optimal monthly peak building demand limiting strategy and the building data acquisition. The developed strategy includes three major functions: the probabilistic building load forecasting, the optimal threshold resetting scheme and the proactive-adaptive demand limiting control scheme.

CHAPTER 4 DEVELOPMENT OF PROBABILISTIC LOAD FORECASTING MODEL

This chapter presents the development of a probabilistic load forecasting model for buildings. This model is capable of quantifying load uncertainties derived from weather forecasting uncertainty and abnormal peak load. Section 4.1 introduces the data preprocessing for model building. Section 4.2 introduces the modeling approach for probabilistic load forecasting. In Section 4.3, a probabilistic normal load forecasting model is built using the artificial neural network (ANN), which uses the probabilistic weather forecast and the calendar information. In Section 4.4, a probabilistic peak abnormal differential load forecasting model is built using statistical methods to quantify two major parameters: occurrence and magnitude. Section 4.5 introduces the model parameter identification approaches.

4.1 Data preprocessing-load dataset decomposition method

To train a building load model with satisfactory prediction accuracy, it is necessary to preprocess the raw data to fulfill the needs in the model training process. In this study, the original load dataset needs to be decomposed into the normal load dataset and the abnormal load dataset for model training. The normal load is mainly affected by outdoor weather conditions and general space usage schedule, which would not experience much change in magnitude comparing its neighboring loads. The abnormal load is affected by not only outdoor weather conditions and space usage schedule but some unpredictable extreme events. Two commonly-used methods (i.e.,

the linear regression (LR) and the local outlier factor (LOF)) are first introduced. The LR method can decompose the abnormal loads which have little correlation with the outdoor weather conditions among the whole load dataset, but it has weakness in detecting the abnormal loads in the local time series load dataset (such as load data in a day). The LOF method can well detect the discontinuous abnormal load from its neighboring loads, but it might fail when a group of abnormal loads occurs continuously. Therefore, taking the advantages of both methods, a hybrid method integrating the LR and the LOF is proposed to decompose the original load dataset.

4.1.1 Linear regression

In the decomposition of the load dataset using the LR method, the sensitivity analysis is firstly conducted using the Pearson correlation (J. Benesty et al., 2009) between the load and each weather variable (dry-bulb temperature, relative humidity, and enthalpy). Next, the datasets of the load together with the selected sensitive weather variable are clustered according to the hour of the day, and then the linear regression model is built between the two variables in each cluster. Clustering the load data by time period is to consider the fact that the dominating factors on the load are not only the weather but also the pattern of activities which are regarded to be time dependent. Finally, the Kernel density estimation (KDE) function is used to analyze the residuals between the actual loads and the estimated loads in each cluster and decompose the abnormal loads.

The enthalpy represents the combined weather effects of the outdoor dry-bulb temperature and humidity. It is worth noticing that the sensitivity analysis was conducted between the load and

each weather variable (i.e., *T*, *RH,* and *h*) in *k*th order based on the Pearson correlation coefficient, which is widely used in the measure of the linear relationship between two variables (J. Cohen et al., 2013). The enthalpy is found to be the best representative weather variable, as shown in Table 3.1, when only one is to be selected. Table 3.1 shows that the enthalpy in the second order is the most sensitive to the load, with the largest Pearson coefficient of 0.914. Hence, the linear regression model is built between the load and the enthalpy in the second order in each cluster.

Table 4.1. Computed Pearson correlation coefficients between load and each weather variable

	T	T^2	T^3	RH	RH^2	RH^3	h	h^2	h^3
Pearson coefficient	0.876	0.880	0.870	0.246	0.211	0.177	0.910	**0.914**	0.902

To obtain the estimates of the loads which are highly correlated to the outdoor weather conditions, a linear regression model in each cluster is established as expressed by Eq. (3.1). Then, the residual ε_t between the actual load and the estimated load is calculated using Eq. (3.2).

$$L'_t = \mathrm{a}_0 + \mathrm{a}_1 {h_t}^2 + \mathrm{a}_2 h_t \tag{4.1}$$

$$\varepsilon_t = L_t - L'_t \tag{4.2}$$

where, L'_t represents the estimated hourly load at the time *t* using the linear regression model. a_0, a_1, and a_2 are the constant coefficients, which can be identified by the least square method using the historical data. L_t is the hourly actual load at the time *t*.

To decompose the abnormal loads from normal loads, the actual loads with a large discrepancy with the estimated loads are separated by analyzing the residuals using the Kernel density estimation function. The Kernel density estimation function is a non-parametric estimate of the distribution shape (B. J. Worton, 1989), as expressed by Eq. (3.3). Where the bandwidth h_{bw} is optimized and identified using Eq. (3.4) (B. W. Silverman, 1986).

$$\hat{f}_{h_{bw}}(\varepsilon) = \frac{1}{n h_{bw}} \sum_{i=1}^{n} K\left(\frac{\varepsilon - \varepsilon_i}{h_{bw}}\right) \tag{4.3}$$

$$h_{bw} = \left(\frac{4\hat{\sigma}^5}{3n}\right)^{\frac{1}{5}} \tag{4.4}$$

where, ε_1, ε_2, …, and ε_n are the random residual samples. n is the sample size. $K(\bullet)$ is the Kernel smoothing function. h_{bw} is the bandwidth. $\hat{\sigma}$ is the standard deviation of the residual samples. The actual loads, with their corresponding residuals out of the 95% confidence interval of the KDE function, are decomposed as the abnormal loads in each cluster. Finally, the decomposed abnormal loads of all clusters are united as the total abnormal load dataset.

4.1.2 Local outlier factor

In the decomposition of load dataset using the local outlier factor (LOF) method, the *LOF* value of each time series load is firstly calculated. Then all *LOF* values of loads are analyzed using the empirical cumulative distribution function (ECDF) to decompose the abnormal loads.

The LOF method is a classic outlier detection strategy (M. M. Breunig et al., 2000). With the LOF method, the anomaly degree of the load L_t in the dataset is measured with the *LOF* value

(J. Wang & X. Su, 2011), as given by Eq. (3.5).

$$LOF(L_t) = \frac{\sum_{i \in N_k(L_t)} lrd_k(i)/lrd_k(L_t)}{|N_k(L_t)|} \tag{4.5}$$

where, $lrd_k(i)$ is the local density the object i from its neighbors. $lrd_k(L_t)$ is the local density of the load L_t in its k-distance neighborhood $N_k(p)$. $|N_k(p)|$ is the size of $N_k(p)$. k is the number of the minimum points in the neighborhood, typically set to be not less than 10 (M. M. Breunig et al., 2000). $LOF(L_t)$ reflects the degree of the load L_t as a local outlier. A value of approximately 1 indicates that the load at the time t is very close to its neighbors and thus not an abnormal load, while values significantly larger than 1 indicate abnormal loads.

To decompose the abnormal loads with the larger *LOF* values, all loads' *LOF* values are analyzed with the empirical cumulative distribution function (S. Coles et al., 2001). Let (x_1, …, x_n) be the random values (i.e., loads in this study) with the common cumulative distribution function $F(l)$. Then the empirical cumulative distribution function is defined by Eq. (3.6).

$$\hat{F}_n(l) = \frac{\text{number of elements in the sample} \leq l}{n} \tag{4.6}$$

where, n is the number of all the random values (loads). l is a particular value of the random values (loads). When n approaches ∞, $\hat{F}_n(l)$ approaches $F(l)$. The *LOF* value significantly larger than 1 corresponds to the larger cumulative probability, which means that the abnormal loads with the larger *LOF* values have larger cumulative probabilities. Hence, the actual loads with their *LOF* values' cumulative probability over 95% are decomposed as the abnormal load dataset.

4.1.3 Hybrid method developed

Assuming that Set $\boldsymbol{A}$ is the abnormal load dataset decomposed using the LR method and Set $\boldsymbol{B}$ is the abnormal load dataset decomposed using the LOF method, the combined abnormal load dataset is the union of the two sets, as expressed by Eq. (3.7). After the combined abnormal load dataset is decomposed from the original load dataset, the gaps in the original time series load dataset are filled by the "recovered normal loads" using the linear interpolation method, as expressed by Eq. (3.8), for the convenience of using the dataset.

$$\boldsymbol{A} \cup \boldsymbol{B} = \{x: x \in \boldsymbol{A} \text{ or } x \in \boldsymbol{B}\} \tag{4.7}$$

$$\frac{L_{gap,t} - L_{t-i}}{i} = \frac{L_{t+j} - L_{gap,t}}{j} \tag{4.8}$$

where, $L_{gap,t}$ is the gap in the original time series load dataset at the time t after load dataset decomposition. L_{t-i} and L_{t+j} are the two nearest neighboring time series loads from the $L_{gap,t}$. The original time series load dataset with the abnormal loads replaced by their recovered normal loads is regarded and used as the updated normal load dataset.

After the decomposition of the load dataset, the abnormal differential load is defined as the deviation between the abnormal load and the updated normal load at the same time. Then, the dataset of the abnormal differential load with a positive value is regarded as the peak abnormal differential load dataset. The decomposed datasets of normal load and peak abnormal differential load are used to train and validate the normal load forecasting model and peak abnormal load forecasting model, respectively.

After the decomposition of the original load dataset, the datasets for model training are normalized using Eq. (3.9), which helps reduce data redundancy and improve data integrity. Where $\boldsymbol{y}$ is a variable. y_i is a random value of the variable $\boldsymbol{y}$. $y_{noz,i}$ is the normalized value. max($\boldsymbol{y}$) and min($\boldsymbol{y}$) are the maximum and minimum values in the dataset, respectively.

$$y_{noz,i} = \frac{y_i - \min(\boldsymbol{y})}{\max(\boldsymbol{y}) - \min(\boldsymbol{y})} \tag{4.9}$$

4.2 The modeling approach for probabilistic load forecasting

The approach of the proposed probabilistic load forecasting model is illustrated in Figure 4.1. It comprises two basic components for two major functions: the probabilistic normal load forecasting and the probabilistic peak abnormal differential (PAD) load forecasting. For the probabilistic normal load forecasting, a model is built using the artificial neural network (ANN), which uses the probabilistic weather forecasts (e.g., T_{min} and T_{max}) from the Hong Kong Observatory and the calendar information. For the probabilistic PAD load forecasting, statistical methods are used to quantify two major probabilistic characteristic parameters, i.e., the probability of the occurrence and the probability distribution of magnitude. The probabilistic forecasts of the occurrence and magnitude of the PAD load are generated based on the calendar information.

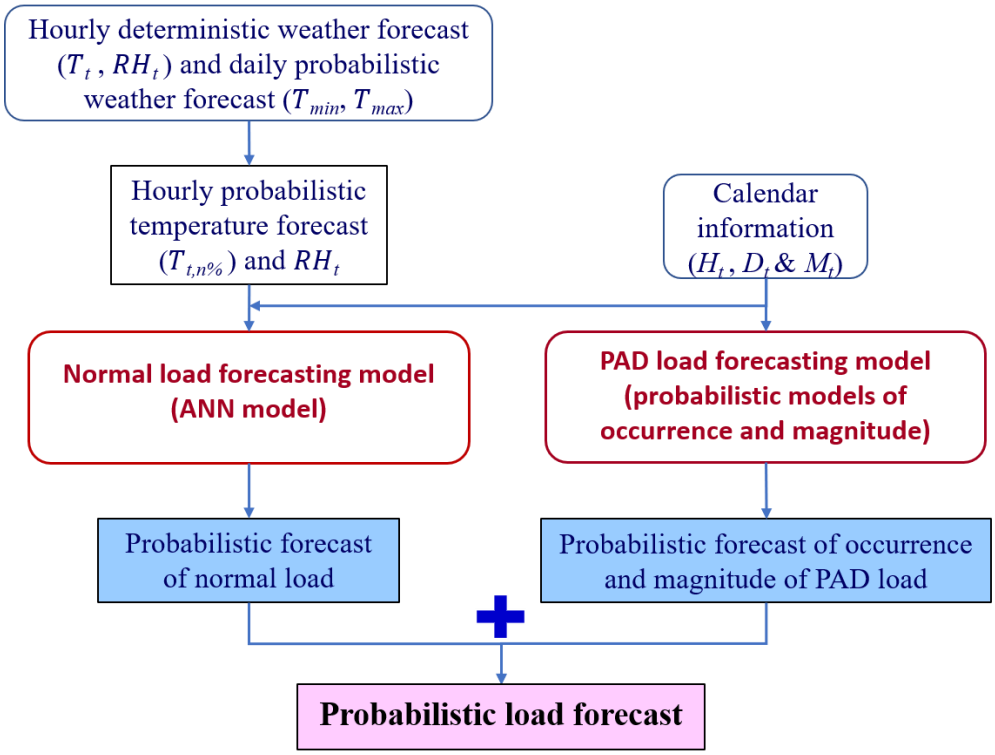

Figure 4.1. Components and steps of the proposed probabilistic load forecasting model.

This model considers the weather forecasting uncertainty and uncertain peak load, which are the major factors for uncertainties in individual buildings. Two basic load forecasts can be obtained using this model: the hourly probabilistic normal load forecast and the hourly probabilistic peak abnormal differential load forecast. They are regarded independent with each other, due to the fact that the normal load is mainly affected by outdoor weather conditions while the peak abnormal differential (PAD) load is usually the result of extreme and random events In this study, the probabilistic load forecast concerns the probabilistic forecasts of the normal load and the peak abnormal differential load, as only the abnormal peak load is involved in peak demand management. In an actual load simulation of a particular moment, the probabilistic load forecast might equal to the normal load forecast (absence of abnormal load) or the normal load forecast

plus the peak abnormal differential load forecast.

In this thesis, the term ‘load’ represents the building electric load. The term ‘normal load’ represents the load which has no significant deviation from its neighboring loads in magnitude. The term ‘abnormal load’ represents the load, which has a significant deviation from its neighboring loads in magnitude. The term ‘abnormal peak load’ represents the load has a significant and positive deviation from its neighboring loads in magnitude. The term ‘peak abnormal differential load’ is defined as the differential between the abnormal peak load and the normal load at a time step.

4.3 Probabilistic normal load forecasting model

The electricity consumption in commercial buildings is dominantly affected by outdoor weather conditions and space usage. The relationship between the load and the outdoor weather variables can be described using various models, e.g., the linear regression model. But the influence of space usage on the electric load is difficult to quantify as space usage needs to be described by many variables. When only the data of building electricity use and weather variables are accessible, it is difficult to construct white (physical) models concerning space usage schedule. However, the calendar information potentially reflects space usage schedule, e.g., the operation schedule of a building and schedule of uses/occupants. Hence, the ANN, a data-driven method, is adopted to model the relationship between the load and the outdoor weather variables together with calendar variables.

4.3.1 ANN model

The ANN is a self-adaptive machine learning method with few priori assumptions, which is also a universal functional approximator (G. Zhang et al., 1998). Compared to other computational techniques, the ANN shows superior performance due to its better capability of mapping the relationship between the inputs and output(s) without making complex mathematical formulations(L. V. Fausett, 1994). ANN model extracts the non-linear relationship among the model inputs by different network learning mechanisms using training data (M. Q. Raza & A. Khosravi, 2015). ANN modeling carries out the required output starting the input vectors without considering the assumption of any determinate relationship between the inputs and the output (A. N. Celik & T. Muneer, 2013). Hence, ANNs work as "black box" employing distinct features such as input, hidden and out layers of neurons, training functions for the learning process form a set of past data, transfer functions between layers that allow information flow (C. Renno et al., 2016). There are different types of ANNs, among which the back-propagation (BP) neural network is the most popular one (M. Cilimkovic, 2015) and used in this study. BP neural network uses the gradient method to change the weight values and bias values quickly to reduce errors. The typical BP neural network contains three layers, the input layer, the hidden layer, and the output layer. This section describes the process to build the deterministic normal load forecasting model using the three-layer BP neural network. The BP neural network contains many learning algorithms, and it is difficult to select an optimal one for a certain problem. In this study, the Levenberg-Marquardt (LM) learning algorithm is selected due to its higher computational speed

in the convergence of the network training compared with other optimization algorithms. Like other optimization algorithms, it is difficult to distinguish whether the LM reaches the global minimum or not. The LM method is selected in this study due to facts that it offers a better learning process and is one of the most widely applied algorithms (M. Benedetti et al., 2016). In fact, if the test accuracy of the ANN model using LM is acceptable, the difference between the local minimum and global minimum would be minimal and can be ignored.

The selected ANN structure and algorithm are used for the predictive ANN model to forecast the hourly deterministic normal load. This ANN structure contains three layers, the input layer, the hidden layer and the output layer. The detailed ANN model settings are described as follows.

Input layer: In the ANN model, inputs are the outdoor dry-bulb temperature (T_t), relative humidity (RH_t), and the calendar variables (i.e., hour of the day (H_t), day of the week (D_t), and month of the year (M_t)). In this study, only the on-peak time is considered. Therefore each calendar variable has certain ranges (H_t (9, 10, …, 20), D_t (1, 2, …, 6) and M_t (1, 2, …, 12)).

Hidden layer: In the BP network, the number of hidden neurons determines how well a problem can be learned. The trial and error approach is usually used to obtain the right number of hidden neurons since there is no science to this issue. In general, the number of hidden neurons might be evaluated using the following empirical formula (S. A. Kalogirou, 2001):

$$m = \frac{1}{2}(\text{inputs} + \text{outputs}) + \sqrt{\text{number of training patterns}} \tag{4.10}$$

Output layer: The output of the ANN model is the normal load (L_t) at the same time series as

set in the inputs.

Learning algorithm: The Levenberg-Marquardt (LM) learning algorithm is chosen, which is known as *trainlm* in the MATLAB toolbox.

Training and testing samples: The historical datasets of the input and output variables are used as the training and testing samples with 7/8 and 1/8 of the datasets, respectively. In the simulation tests of this study, the proposed ANN model is built in the MATLAB environment using the Neural Network Toolbox.

When the ANN deterministic load forecasting model is available, the probabilistic normal load forecast is generated by importing the probabilistic forecast of the input variables into the model. As the outdoor dry-bulb temperature is one of the most dominant contributors to the variability and quantity of electricity consumption in commercial/ non-residential buildings among all the input variables and its probabilistic forecast is available from the weather forecast, the probabilistic forecast of the temperature is chosen to quantify the probability distribution of the normal load forecast in this study.

4.3.2 Hourly probabilistic temperature forecast

Currently, there is no available hourly probabilistic temperature forecast for application. In this study, it is generated based on the accessible daily probabilistic maximum/minimum temperature forecasts and the accessible hourly deterministic temperature forecast. The Hong Kong Observatory (HKO) provides the probabilistic forecasts of the daily minimum and maximum

temperatures in the web plot format respectively (as shown in Figure 4.2), which are digitized into time series data, in this study, using WebPlotDigitizer (A. Rohatgi). The probabilistic forecast of the daily minimum (or maximum) temperature with a particular value (i.e., T_{min}=T_i) represents the probability (in percentage) of the daily minimum (or maximum) temperature to occur in the range of plus/minus one degree around that temperature value (i.e. [T_i-1, T_i+1]).

$$F_{T_{min}}(T_i) = P(T_{min} \leq T_i + 1) - P(T_{min} \leq T_i - 1) \tag{4.11}$$

where, F_{Tmin} is the forecasted probability of the daily minimum temperature with a particular value from the HKO weather forecast. P is the probability of a variable. T_{min} represents the probabilistic forecast of the daily minimum temperature, and T_i is a particular value of T_{min}. Meanwhile, the probabilistic forecast of the daily maximum temperature from the HKO weather forecast is expressed in the same way as Eq. (4.2).

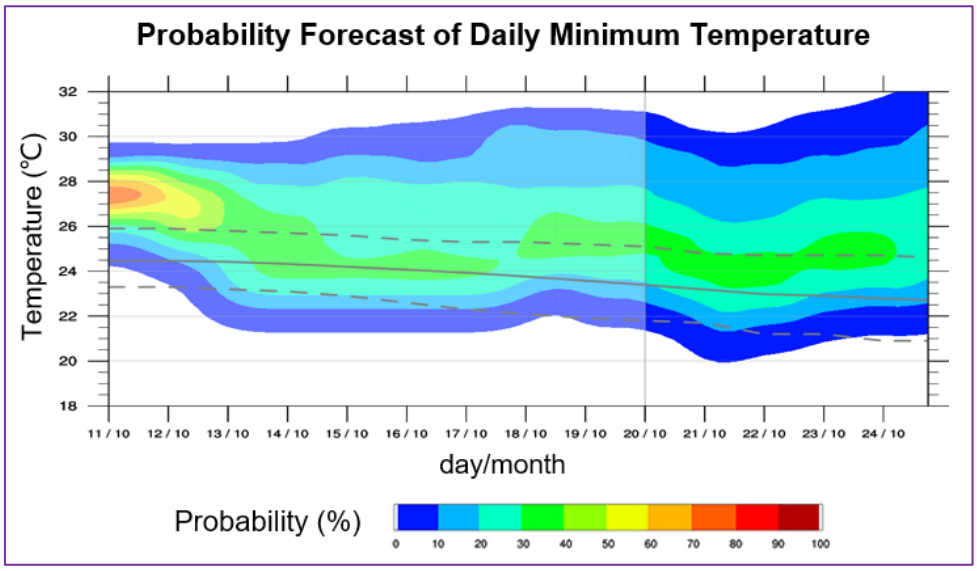

Figure 4.2. An example (web image) of the probabilistic forecast of the daily minimum temperature - HKO weather forecast.

The aforementioned probabilistic forecast of the daily minimum temperature from the HKO weather forecast is different from the commonly used cumulative probability. Hence, the probabilistic forecast of the daily minimum temperature is firstly transferred into the cumulative distribution function (CDF) of the daily minimum temperature forecast with a one-degree temperature interval. Then both the 1-99% quantile CDFs of the daily probabilistic minimum temperature forecast, and the daily probabilistic maximum temperature forecast are generated using the linear interpolation among the previously transferred CDF (with one-degree temperature interval). Afterward, the hourly probabilistic temperature forecast at the n% quantile at the hour h ($T_{h,n\%}$) is generated using the linear interpolation on the basis of the estimated 1-99% quantile CDFs of the daily minimum and maximum temperature forecasts ($T_{min,n\%}$ and $T_{max,n\%}$), the daily deterministic minimum and maximum temperature forecasts (T^{min} and T^{max}) and the hourly deterministic temperature forecast at the hour h (T_h).

With the estimated hourly probabilistic temperature forecast among all the quantiles (i.e., $n\% \in$ (1%, …, 99%)) at the hour h, the hourly probabilistic normal load forecast is generated at each quantile accordingly. To be specific, for each predicted quantile $T_{h,n\%}$ of the temperature, the ANN load forecasting model is performed by replacing the deterministic value T_h with the estimated probabilistic value $T_{h,n\%}$, and a probabilistic normal load $L_{h,n\%}$ is obtained accordingly. Based on the Hong Kong weather forecast duration, the 9-day ahead probabilistic temperature forecasts can be estimated and then inputted into the ANN model for 9-day ahead probabilistic load forecasts.

4.4 Probabilistic peak abnormal differential load forecasting model

The peak abnormal differential (PAD) load is insensitive to the outdoor weather conditions but partially related to the calendar information. In addition, the PAD load usually occurs with a small probability, which means that the historical data of the PAD load are quite limited. Hence, a few years' data of the PAD load are required to model the relationship of the PAD load characteristics (occurrence and magnitude) with calendar information. In this section, the probability distribution of the PAD load occurrence is firstly modeled using statistical analysis. Secondly, the probability distribution of the PAD load magnitude is modeled using one of the four commonly-used probability density functions (PDF) as listed later in this section, which is selected based on their fitness.

4.4.1 Probabilistic model of occurrence

The PAD load occurrence is highly related to the hour of the day, and the month of the year. Hence, the probabilistic model of the PAD load occurrence is used to forecast the probability of the PAD load occurrence ($P_{PAD,pre}^{m,h}$) based on the empirical probability of the PAD load occurrence ($P_{PAD}^{m,h}$), as given by Eq. (4.3). Where, $P_{PAD,pre}^{m,h}$ represents the predicted probability of the PAD load occurrence at a specific time in a period. $P_{PAD}^{m,h}$ represents the empirical probability of the PAD load occurrence based on the historical data. The superscript m and h represent the month and the hour, respectively. In this study, the model covers the office hours (12 hours a day) of an entire year (i.e., M=12，H=12).

$$P_{PAD,pre}^{m,h} = P_{PAD}^{m,h} \ (month: m = 1 \dots M, hour: h = 1 \dots H) \tag{4.12}$$

This probabilistic model of occurrence is built based on the assumptions that the PAD load occurs with the same probability at certain office hour of all workdays in a month. Here, a "relative PAD load occurrence frequency" is defined as the percentage of PAD load occurrence times at certain office hour in workdays among the total times of PAD load occurrence in the period of training (or historical) data. A "monthly PAD load occurrence probability" is defined as the ratio of the total times of PAD load occurrence to the total number of office hours in a month. Therefore, the PAD load occurrence probability at a certain hour *h* in a month *m* is calculated by multiplying the relative PAD load occurrence frequency and the monthly PAD load occurrence probability.

4.4.2 Probabilistic model of magnitude

Table 4.2. Detailed descriptions of the four commonly-used probability distribution functions

Function	Formula	Coefficient description
Normal distribution	$f(x;\mu,\sigma^2) = \frac{1}{\sqrt{2\pi\sigma^2}} e^{-\frac{(x-\mu)^2}{2\sigma^2}}$	μ is the mean parameter, and σ is the standard deviation parameter.
Gamma distribution	$f(x;\alpha,\beta) = \frac{x^{\alpha-1}e^{(-\frac{x}{\beta})}}{\beta^{\alpha}\Gamma(\alpha)}$	α is a shape parameter, β is an inverse scale parameter, and $\Gamma(\alpha)$ is a complete Gamma function.
Weibull distribution	$f(x;k,\lambda) = \frac{k}{\lambda}(\frac{x}{\lambda})^{k-1} e^{-(x/\lambda)^k}$	λ is the scale parameter, and k is the shape parameter.

Lognormal distribution	$f(x;\emptyset,\gamma)=\frac{1}{x\sqrt{2\pi\emptyset^2}}e^{-\frac{(\ln(x)-\gamma)^2}{2\emptyset^2}}$	$\emptyset$ is the mean parameter of ln(x), and γ is the standard deviation parameter of ln(x).

The probability distribution of the PAD load magnitude is firstly fitted using four commonly-used PDFs: i.e., Normal distribution, Gamma distribution, Weibull distribution and Lognormal distribution (M. Evans et al., 2000). To be specific, the training data of the PAD load magnitude (x) are used to fit its probability distribution ($f(x)$) using the four PDFs. The PDF offering the best fitness is selected as the probability distribution forecast model of the PAD load magnitude. Detailed descriptions of the four PDFs are presented in Table 4.1.

4.5. Model parameter identification

The parameters of the deterministic ANN load forecasting model and the probabilistic PAD load magnitude model are identified based on the model identification approaches and the preprocessed training datasets. These model identification approaches are presented in this section, while the preprocessing of the raw training data is presented in the next section.

When training the ANN model, the weights and biases of the network are tuned to optimize the network performance (i.e., minimize the mean square error between the network outputs and the target outputs) using the steepest descent training algorithm (D. E. Rumelhart et al., 1985) by adopting the Neural Network Toolbox in MATLAB. The mean square error *mse* is calculated by Eq. (4.4). Where, z^a is the actual target output vector. z is the network output vector.

$$mse = \frac{1}{N}\sum_{i=1}^{N}(\boldsymbol{z}_i^a - \boldsymbol{z}_i)^2 \quad (4.13)$$

In the training (fitting) of the probabilistic PAD load magnitude model, the parameters defining each PDF of the PAD load magnitude are calculated using the maximum likelihood method as presented in Table 4.2.

Table 4.3. Detailed descriptions of the maximum likelihood method for parameter identification of each probability distribution function

Function	Identified parameter	Description
Normal distribution	$\mu = \frac{1}{n}\sum_{i=1}^{n} x_i$ $\sigma^2 = \frac{1}{n}\sum_{i=1}^{N}(x_i - \mu)^2$	Normal distribution parameters are evaluated using the maximum likelihood method.
Gamma distribution	$LL = \ln\prod\prod_{i-1}^{n}\{h(x_i;\alpha,\beta)\}$ $= \sum_{i-1}^{n}\ln\{h(x_i;\alpha,\beta)\}$	Gamma distribution parameters are evaluated using the maximum likelihood method which maximizes the logarithm of the likelihood function.
Weibull distribution	$k = \left[\frac{\sum_{i=1}^{n} {x_i}^k \ln(x_i)}{\sum_{i=1}^{n} {x_i}^k} - \frac{\sum_{i=1}^{n}\ln(x_i)}{n}\right]^{-1}$ $\lambda = \left[\frac{1}{n}\sum_{i=1}^{n} {x_i}^k\right]^{1/k}$	Weibull shape and scale parameters are calculated using the maximum likelihood method (D. Kececioglu, 2002).
Lognormal distribution	$\gamma = \frac{1}{N}\sum_{i=1}^{N}\ln(x_i)$ $\emptyset^2 = \frac{1}{N}\sum_{i=1}^{N}[\ln(x_i) - \gamma]^2$	Lognormal parameters are estimated using the maximum likelihood method without an iterative procedure.

After the parameters of the four fitted PDFs are identified, the Kolmogorov-Smirnov (K-S) test is introduced as the error metric to evaluate the fitness of each PDF (A. Clauset et al., 2009). The K-S error is based on the largest vertical difference between the *C(l)* and *O(l)*, as expressed by Eq. (4.5).

$$K - S\ error = \max|C(l) - O(l)| \tag{4.14}$$

where, *C* is the calculated cumulative distribution function for the PAD load below a particular value, based on the fitted PDF. *O* is the cumulative distribution function for the PAD load below the same value, based on the observed PAD load data. *l* is the concerned value of the PAD load. The smaller the K-S error is, the better the fitness of the PDF is.

4.6 Summary

i. This chapter introduces the development of the probabilistic load forecasting model for individual buildings. The major contents presented in this chapter are as follows. The building data preprocessing is presented, including the description of the building and data acquisition, the decomposition of load dataset and the data normalization. In the decomposition of load dataset, two commonly-used methods (i.e., the LR and LOF methods) are introduced and the hybridization of these two methods is adopted to decompose the original load dataset in this study.

ii. A probabilistic normal load forecasting model is proposed for forecasting the uncertain normal loads in a building or buildings with a billing account, mainly affected by the

uncertain outdoor temperature forecast. This model is built using the artificial neural network (ANN), which uses the probabilistic weather (i.e., temperature) forecast and the calendar information. The hourly probabilistic temperature forecast is estimated based on the weather forecasts from the observatory.

iii. A probabilistic peak abnormal differential (PAD) load forecasting model is proposed for forecasting uncertain peak loads in a building, mainly caused by extreme events. Two probabilistic models for the occurrence and magnitude of the PAD load are built using statistical methods. Four commonly-used PDFs are used to fit/train the probabilistic PAD load magnitude model.

iv. The parameters of the ANN load forecasting model and the PAD load magnitude model are identified based on the model identification approaches and the preprocessed training datasets.

CHAPTER 5 DEVELOPMENT OF OPTIMAL THRESHOLD RESETTING SCHEME

This chapter presents the optimal threshold resetting scheme for monthly peak building demand limiting considering load uncertainty, which involves two major functions as follows. The uncertain economic benefits (i.e., gains and losses) of a demand limiting control are quantified on the basis of probabilistic load forecasts. The optimal monthly limiting threshold is identified using the expectation metric based on the quantified economic benefits. The scheme optimizes the monthly limiting threshold, which is updated according to the ever-changing weather forecast and actual peak power use.

Section 5.1 introduces the needs and functions of the optimal monthly demand limiting threshold. Section 5.2 presents an outline of the optimal threshold resetting scheme. In section 5.3, a commonly-used expectation metric is used to identify the optimal monthly demand limiting threshold, among a set of potential thresholds with corresponding quantified economic benefit. In Section 5.4, the conditional probability theory is adopted to combine the probabilistic normal load forecast and the probabilistic peak abnormal differential load forecast. In Section 5.5, the quantification of economic benefit and the probability of success of implementing a demand limiting control in a month is introduced. Moreover, the probabilities of nonactivation and failure of a demand limiting control in a month are quantified as well.

5.1 Needs and functions of adaptive optimal monthly demand limiting threshold

There have been many studies on the control strategies using the HVAC systems with/without thermal storages, and one of the important and challenging issues is the identification of the optimal or practically effective and doable demand limiting threshold considering various constraints and uncertainties in a particular period, e.g., a billing cycle. Additionally, as the major factors (e.g., weather forecasts affecting the optimal achievable threshold) change from time to time (e.g., each day), the optimal limiting threshold needs to be adaptive to achieve the near-maximum (or maximum) monthly cost saving. Therefore, this chapter focuses on how to identify an optimal limiting threshold for individual buildings considering load uncertainty over a month using an adaptive mechanism.

Why adaptive optimal limiting threshold is needed and the typical scenarios

As we all know, an uncertain gambling outcome (i.e., win, loss or draw) has to be faced when making a gambling decision. Similarly, an uncertain cost saving of demand limiting has to be faced when selecting a threshold for the demand limiting control over a billing cycle, largely due to load uncertainties. Hence, it is necessary to obtain an optimal or practically effective and doable limiting threshold to achieve the maximum or near-maximum cost saving. Moreover, as the major factors (such as the latest weather forecasts and the actual peak power use up to the current moment), which affect the optimal achievable threshold, change from time to time, the optimal or proper limiting threshold needs to be reset to achieve maximum or near-maximum

monthly cost saving.

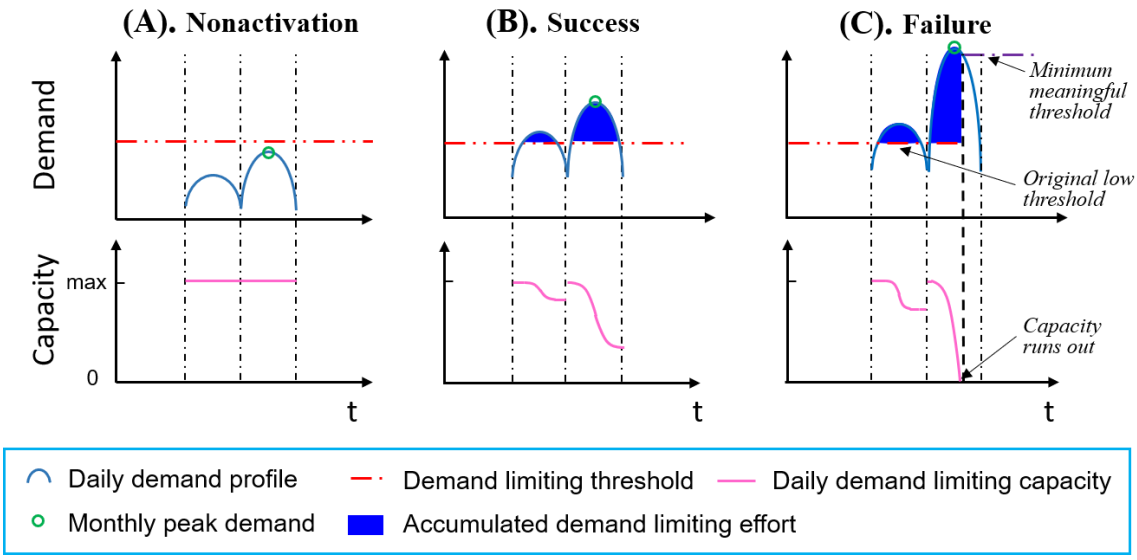

Figure 5.1. Demand, remaining limiting capacity and accumulated limiting efforts of *vs* limiting threshold in three typical scenarios when implementing monthly demand limiting.

In this study, three typical scenarios of a monthly demand limiting control using active storage facilities considering uncertainty in a month are categorized and considered, i.e., nonactivation, success or failure, which are similar and corresponding to draw, win or loss in gambling respectively, as shown in Figure 5.1. Detailed descriptions of these scenarios are given as follows.

The "*nonactivation scenario*" represents the case when a relatively high threshold is used and the peak demand limiting control is not activated over the billing cycle. In this case, the monthly peak demand remains below the limiting threshold, as shown in Figure 5.1(A). It achieves no peak demand reduction and requires no demand limiting effort, which is comparable to the "*draw scenario*" in gambling.

The "s*uccess scenario*" represents the case when a moderate threshold is used and the peak demand limiting control is activated and successful. In this case, the limiting capacity is sufficient for demand limiting control over the billing cycle. The monthly peak demand is higher than the limiting threshold and the corresponding accumulated limiting effort does not exceed the limiting capacity, as shown in Figure 5.1(B). It achieves peak demand reduction successfully as expected, which is comparable to the "*win scenario*" in gambling.

The "*failure scenario*" represents that case when a relatively low threshold is used and the peak demand limiting control is activated but fails. In this case, the limiting capacity is not sufficient for the need of demand limiting control in some days over the billing cycle. In these days, the monthly peak demand is much higher than the limiting threshold and the corresponding accumulated demand limiting effort exceeds the limiting capacity, as shown in Figure 5.1(C). It wastes all or most of the previous demand limiting efforts, which is comparable to the "*loss scenario*" in gambling. Moreover, at the moment of failure, the original low threshold is not meaningful anymore and the minimum meaningful/doable threshold is forced to the actual peak power use up to this moment.

5.2 Outline of optimal threshold resetting scheme

In this study, an optimal threshold resetting scheme is developed to determine and continuously update the optimal limiting threshold under load uncertainty, as presented in the earlier framework and shown in Figure 3.1. The optimal threshold resetting scheme includes the quantification of economic benefit (cost saving) and the probability of success of a demand

limiting control, and the monthly demand limiting threshold optimization. The probabilistic economic benefits can be quantified based on the forecasted probabilistic demand profiles (in Chapter 4). Then the optimal monthly limiting threshold is identified based on the quantified probabilistic economic benefits of different thresholds. The optimal threshold resetting scheme works in an adaptive manner each day (e.g., before office hour, 9:00), according to the updating frequency of weather forecasts in Hong Kong, over the billing cycle of a month. This adaptive manner (with receding time window) will take increasing confidence of identifying optimal monthly limiting threshold, for that load prediction uncertainty for the remaining days of the month becomes smaller when the number of remaining days becomes fewer. The monthly demand limiting threshold optimization is introduced in Section 5.3. The detailed quantification methods of cost-benefit and the probability of success are presented in Section 5.4. As there are many studies and methods on the use of HVAC systems and/or thermal storages for reducing building peak demands, the system and actual control are not the focus of this study.

In this thesis, the term ‘monthly limiting threshold’ represents the threshold determined for peak demand limiting control, which is updated from time to time. The term ‘demand limiting effort’ represents the cost paid to achieve a certain demand reduction, which might be the auxiliary energy (e.g., thermal storage) and weighted cost due to the sacrifice of service quality (e.g., thermal comfort).

5.3 Monthly demand limiting threshold optimization

Load uncertainty results in uncertain results of cost saving when conducting demand limiting

control using a particular threshold in a month. To quantify the uncertain monthly cost saving, the expectation metric is used, which is the most common criterion in the stochastic programming and a commonly-used criterion appealing to many decision-makers (G. Mavromatidis et al., 2018). With the expectation metric, the optimal monthly limiting threshold is identified, which has the maximum expected value of the monthly cost saving among all potential thresholds, as given by Eq. (5.1). In addition, the expected value of monthly cost saving of demand limiting control using a particular threshold is estimated on the basis of the expected gain and loss in the success and failure scenarios respectively, as given by Eq. (5.2).

$$PD_{set,opt} = \max_{\forall\, j\in[1,J]}{}^{-1}\left(\mathbb{E}\left[CS_j\right]\right) \tag{5.1}$$

$$\mathbb{E}\left[CS_j\right] = \mathbb{E}\left[G_j\right] \times P_{suc}\left(PD_{\mathrm{set},j}\right) - \mathbb{E}\left[L_j\right] \times P_{fail}\left(PD_{set,j}\right), PD_{set,low} \leqq PD_{\mathrm{set},j} \leqq PD_{set,up} \tag{5.2}$$

where, $PD_{set,opt}$ represents the optimal monthly limiting threshold for demand limiting control in the remaining days of a month, which should be not less than the actual peak power use up to the moment of decision-making. max^{-1} is the inverse function for computing the maximum value among a set of data. $\mathbb{E}$ is the expected value of a variable. $PD_{set,j}$ is a particular threshold among a set of potential thresholds. $PD_{set,low}$ and $PD_{set,up}$ are the lower and upper boundaries of the potential threshold respectively. In this study, these two boundaries are selected simply as the mean values of the forecasted probabilistic demand profiles at the 50% and 97.5% quantiles, respectively. CS_j represents the cost saving of demand limiting using $PD_{set,j}$ in the remaining days of a month. G_j represents the gain of demand limiting using $PD_{set,j}$ in the success scenario in the

remaining days of a month. L_j represents the loss of demand limiting using $PD_{set,j}$ in the failure scenario in the remaining days of a month. P_{suc} is the probability of success of implementing demand limiting using a particular threshold in the remaining days of a month. P_{fail} is the probability of failure of implementing demand limiting using a particular threshold in the remaining days of a month. J is the total number of potential thresholds. The expected gain ($\mathbb{E}[G_j]$) and loss ($\mathbb{E}[L_j]$) can be obtained as the weighted averages of the gains and losses (weighted using their corresponding probabilities) of all possible monthly peak demands when a particular threshold is used.

5.4 Probabilistic load forecasting

To determine the optimal monthly limiting threshold, the probabilistic forecast of uncertain building load is essentially needed. The previously developed probabilistic building load forecasting model in Chapter 4 is adopted to forecast the probabilistic demand profiles.

Figure 5.2 shows how to combine these two load forecasts into the hourly load forecast. It can be seen that, at each hour, the normal load occurs with a particular magnitude, while the PAD load might occur with a particular magnitude or not occur. Based on the conditional probability theory, the probability of the hourly load with a particular value ($D_i(t)$) is obtained, as given by Eq. (5.3). The probability of the normal load with a particular value ($D_{norm,i}(t)$) is defined as the cumulative probability of that load ($D_{norm,i}(t)$) to occur within a range of 1.0 kVA (i.e., ±0.5 kVA), as given by Eq. (5.4). Similarly, the probability of the PAD load with a particular value ($D_{PAD,j}(t)$) is defined as the cumulative probability of that load ($D_{PAD,j}(t)$) to occur within a range of 1.0 kVA

(i.e., ±0.5 kVA), as given by Eq. (5.5).

$$P(D_i(t)) = \begin{cases} P(D_{norm,i}(t)) \times P(D_{PAD,j}(t)) \times P_{PAD,oc}(t), & D_i(t) = D_{norm,i}(t) + D_{PAD,j}(t) \\ P(D_{norm,i}(t)) \times (1 - P_{PAD,oc}(t)), & D_i(t) = D_{norm,i}(t) \end{cases} \quad (5.3)$$

$$P(D_{norm,i}(t)) = P(D_{norm,i}(t) - 0.5 \leq D_{norm}(t) \leq D_{norm,i}(t) + 0.5) \quad (5.4)$$

$$P(D_{PAD,j}(t)) = P(D_{PAD,j}(t) - 0.5 \leq D_{PAD}(t) \leq D_{PAD,j}(t) + 0.5) \quad (5.5)$$

where, $D_i(t)$ is a particular value of the hourly probabilistic load forecast for time (hour) t. $D_{norm,i}(t)$ is a particular value of the hourly probabilistic normal load forecast for time t. $D_{PAD,j}(t)$ is a particular value of the hourly peak abnormal differential load forecast for time t. $P_{PAD,oc}(t)$ is the occurrence probability of the hourly PAD load for time t. $D_{norm}(t)$ is the hourly probabilistic normal load forecast for time t. $D_{PAD}(t)$ is the hourly peak abnormal differential load forecast for time t.

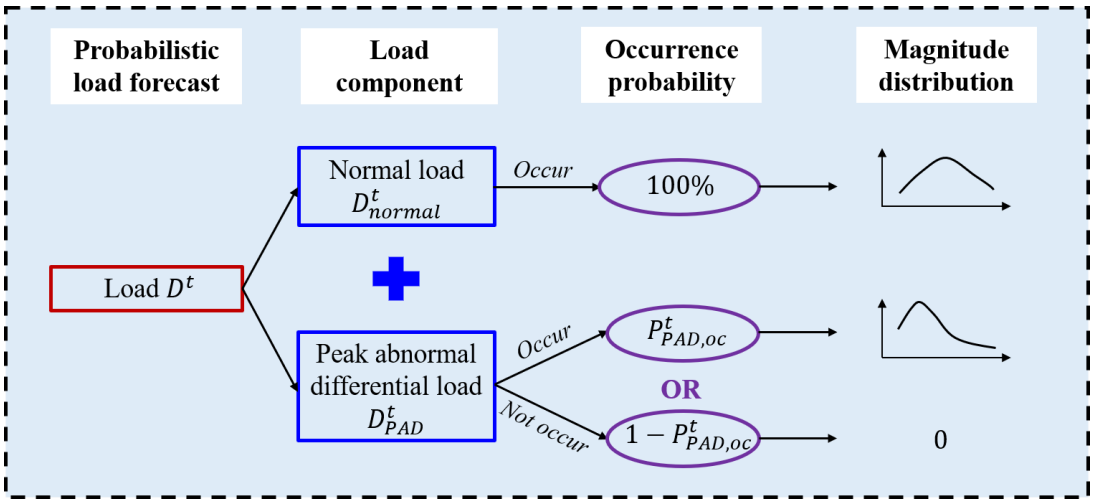

Figure 5.2. Load combination schematic for the hourly probabilistic load forecast.

5.5 Quantification of economic benefit and probability of success of a demand limiting control

Based on the forecasted probabilistic demand profiles, the economic benefit and the probability of success of implementing a demand limiting control using a particular threshold in a month can be quantified. Moreover, the probabilities of nonactivation and failure of implementing a demand limiting control should also be quantified. This is because these two possible scenarios affect the expected monthly cost saving together with the success scenario. Specifically, the expected cost benefit and the probability of each scenario are quantified.

5.5.1 Nonactivation scenario

Monthly nonactivation probability

In the nonactivation scenario, all daily peak demands remain below the limiting threshold in the remaining days of a month. Therefore, the monthly nonactivation probability is regarded as the product of the daily nonactivation probability of all the remaining days, as given by Eq. (5.6). Here, the daily nonactivation probability represents the probability that the daily peak demand remains below the limiting threshold, as shown in Figure 5.3 and given by Eq. (5.7). Figure 5.3(A) illustrates the forecasted daily probabilistic demand profiles at different quantiles. Figure 5.3(B) illustrates the probability density of the daily peak demand and the daily nonactivation probability.

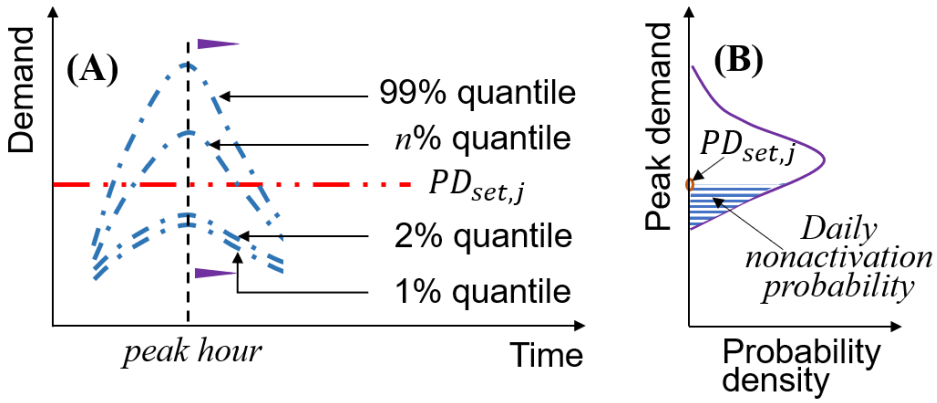

Figure 5.3. The mechanism for determining the daily nonactivation probability: (A) Forecasted probabilistic daily building demand profiles; (B) Probability density of the daily peak demand and daily nonactivation probability.

$$P_{non}(PD_{set,j}) = \prod_{d=1}^{N} P_{non}^{d}\left(PD_{set,j}\right) \tag{5.6}$$

$$P_{non}^{d}\left(PD_{set,j}\right) = P\left(PD^{d} \leq PD_{set,j}\right), 1 \leqq d \leqq N \tag{5.7}$$

where, P_{non} is the monthly nonactivation probability of implementing demand limiting using $PD_{set,j}$ in the remaining days of a month. N is the number of the remaining days of a month, including the current day. P is the probability of an event. P_{non}^{d} is the daily nonactivation probability of implementing demand limiting using $PD_{set,j}$ on the dth day. PD^{d} is the daily probabilistic peak demand forecast on the dth day, which is regarded as the probabilistic demand/load forecast at the peak hour on the dth day. Here, the peak hour is simply taken as the hour that has the maximum expected value of the hourly probabilistic demand forecasts on one day. This simplification is mainly due to the fact that the monthly peak demand (at the 30-min time interval) is one of all the daily peak demands, which occur in a particular hour each day.

The superscript d represents a future day of a month. d=1 represents the current day. d=N represents the last future day of the month.

As the probabilistic demand profiles account for K days ahead due to the limitation of the K-day weather forecast duration, the identified optimal limiting threshold based on the probabilistic demand profiles is effective in the future K days (K=9 in this study for current applications in Hong Kong). Actually, the number of remaining days (N) might be larger than the number of days for the weather forecast, K. In this case, the nonactivation probability in the remaining N days is assumed to equal that in the future K days. The identified optimal limiting threshold based on K-day ahead load forecast is preferable for monthly peak demand limiting, compared to the traditional threshold based on 1-day ahead load forecast. Because this traditional threshold is identified without considering the offset between overall limiting efforts and the peak demand reduction in K days and might result in significant ineffective limiting efforts.

5.5.2 Success scenario

Monthly success probability

In the success scenario, all daily demand limiting efforts needed are not over the limiting capacity. The daily limiting effort using active thermal storages is assumed proportional to building electrical energy reduction during demand limiting, which can then be quantified based on the forecasted demand profile. Here, a critical quantile of daily demand profile is defined as the specific quantile, at which the daily demand limiting effort needed is equal to the limiting

capacity for demand limiting control using a particular limiting threshold, $PD_{set,j}$. The peak demand of this critical quantile of daily demand profile is then the upper limit of the limiting threshold for success scenario. The corresponding value of this critical quantile is therefore chosen as the daily probability of both success and nonactivation scenarios ($P^{d}_{suc+non}(PD_{set,j})$) under a limiting threshold $PD_{set,j}$. The monthly success probability can be therefore calculated on the basis of this combined probability and the daily nonactivation probability, as given by Eq. (5.8). Where, P_{suc} is the monthly success probability of implementing demand limiting using $PD_{set,j}$ in the remaining days of a month.

$$P_{suc}\left(PD_{set,j}\right) = \prod_{d=1}^{N} P^{d}_{suc+non}\left(PD_{set,j}\right) - \prod_{d=1}^{N} P^{d}_{non}\left(PD_{set,j}\right) \tag{5.8}$$

Quantification of monthly gain

In a particular success case, the monthly gain of a limiting control is determined by the difference between the reduction of peak demand cost and the extra total cost of accumulated limiting efforts in a month, as given by Eq. (5.9). The reduced electrical energy consumption during the demand limiting period is assumed as 0, for that there is an offset between the reduced energy consumption and the rebound effect after the demand limiting period. A peak demand (x_i) is regarded as the demand of the same quantile at the peak hour in the remaining days. The corresponding accumulated limiting efforts are regarded as the sum of all the possible maximum daily limiting efforts needed. The probability of this particular monthly gain ($G_j(x_i)$) is considered having the same probability of x_i in the success scenario at that peak hour.

$$G_j(x_i) = a \times \left(x_i - PD_{set,j}\right) - b \times \sum_{d=1}^{N} \Delta E^d(x_i, PD_{set,j}) \quad (5.9)$$

where, a is the unit price of the electricity demand. b is the unit price of the demand limiting effort using the active thermal storage. x_i is a particular value of the monthly peak demand in the success scenario. ΔE^d is the possible maximum daily demand limiting effort under x_i and $PD_{set,j}$ in the success scenario, which is assumed proportional (with the coefficient λ) to the corresponding daily electrical energy consumption reduction during the demand limiting period. In this study, the loss of storage is ignored, and then λ is assumed as 2.5 since the overall COP of the air-conditioning system assumed to be 2.5 (C. Yan et al., 2017). The daily electrical energy consumption can be calculated on the basis of the demand profile at a particular quantile.

When the number (N) of remaining days is larger than the number of days for the weather forecast, K, the peak demand reduction in the remaining N days is assumed to equal that in the future K days. Moreover, the accumulated limiting efforts needed in the remaining N days are assumed to equal N/K times of those in the future K days.

5.5.3 Failure scenario

Monthly failure probability

In the failure scenario, the monthly failure probability is complementary to the sum of the monthly nonactivation and success probabilities, as given by Eq. (5.10). Where P_{fail} is the monthly failure probability of implementing demand limiting using $P_{set,j}$ in the remaining days of a month.

$$P_{fail}(PD_{set,j}) = 1 - P_{suc}(PD_{set,j}) - P_{non}(PD_{set,j}) \quad (5.10)$$

Quantification of monthly loss

In a failure case, proactive control may simply force the limiting threshold to the minimum meaningful threshold after the limiting capacity runs out, as shown in Figure 5.4(A). However, such proactive adjustment of the limiting threshold might not be the choice for the most effective limiting control and result in less reduction of monthly peak demand when the possible maximum daily limiting effort in the remaining days is not considered. Therefore, a perfect adjustment of the limiting threshold is assumed and adopted to guarantee the future possible maximum daily limiting effort equal to the limiting capacity, as shown in Figure 5.4(B).

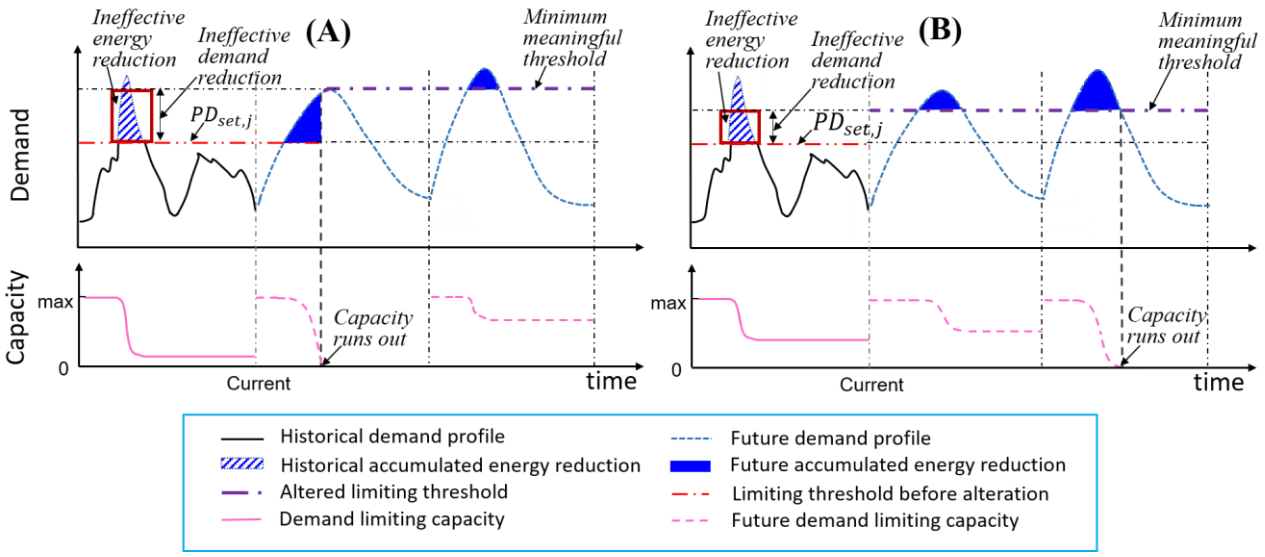

Figure 5.4. Demand, remaining limiting capacity and accumulated limiting effort *vs.* limiting threshold in a failure case: (A) An imperfect proactive adjustment of limiting threshold; (B) A perfect proactive adjustment of limiting threshold.

The monthly loss is equivalent to the total cost of the accumulated previous limiting efforts below the new adjusted threshold, i.e., the ineffective energy reduction multiplied by the factor λ, as shown in Figure 5.4. A building model (S. Wang & X. Xu, 2006) is used to estimate the original hourly power use without implementing demand limiting control, based on the actual hourly power use in the condition with the implementation of the demand limiting control.

5.6 Summary

This chapter presents an adaptive optimal threshold resetting scheme for peak demand limiting under load uncertainty over the billing cycle of a month. As the load uncertainty is inevitable, the monthly peak demand limiting control using a deterministic limiting threshold has a high risk of nonactivation or even failure, which would result in no net cost saving or even negative one. In this situation, the developed scheme is very useful and can identify the optimal monthly limiting threshold in an adaptive manner. The major contents presented in this chapter are as follows.

i. An expectation metric in the stochastic programming is used to identify the optimal limiting threshold among a set of potential thresholds based on the quantified probabilistic economic benefits of implementing demand limiting control using these thresholds.

ii. The hourly probabilistic load forecast is obtained by combining the probabilistic normal load forecast and the probabilistic PAD load forecast according to the conditional probability theory.

iii. The probabilities of the three typical scenarios (i.e., nonactivation, success and failure) of

demand limiting and the corresponding probabilistic gains and losses are quantified when a particular limiting threshold is used. Then, the effective decision for selecting a proper demand limiting threshold can be made on the basis of the operator's preference on risks (i.e., the quantified probabilities).

CHAPTER 6 DEVELOPMENT OF PROACTIVE-ADAPTIVE DEMAND LIMITING CONTROL SCHEME

This chapter presents the development of proactive-adaptive demand limiting control scheme for the real-time implementation of demand limiting under load uncertainty, which is based on the aforementioned optimal threshold resetting scheme. This scheme is capable of proactively resetting the limiting threshold online before using up the storage capacity when only small-scale storages are available. Section 6.1 presents the needs of proactive-adaptive demand limiting control scheme. Section 6.2 presents the proactive-adaptive demand control scheme, which includes three major functions. Section 6.3 presents the online update of daily demand profile prediction based on a moving average prediction error. Section 6.4 presents the online demand limiting threshold reset based on the updated remaining storage capacity and daily demand profile prediction. Section 6.5 presents the online demand limiting control using a small-scale active thermal storage.

6.1 Needs of proactive-adaptive demand limiting control

In the building demand limiting, small-scale storages are usually preferred, as a cost-effective option, due to the low initial investment cost and space cost. However, in practical real-time demand limiting control applications, small-scale storages could lead to the shortage of backup energy supply for peak demand limiting when the actual peak demands are much larger than the predicted peak demands. In the situation of limited storage capacity, proactive-adaptive control

is needed for peak demand limiting before using up the storage capacity, which can proactively reset the limiting threshold online based on the remaining storage capacity.

6.2 Proactive-adaptive demand limiting control scheme

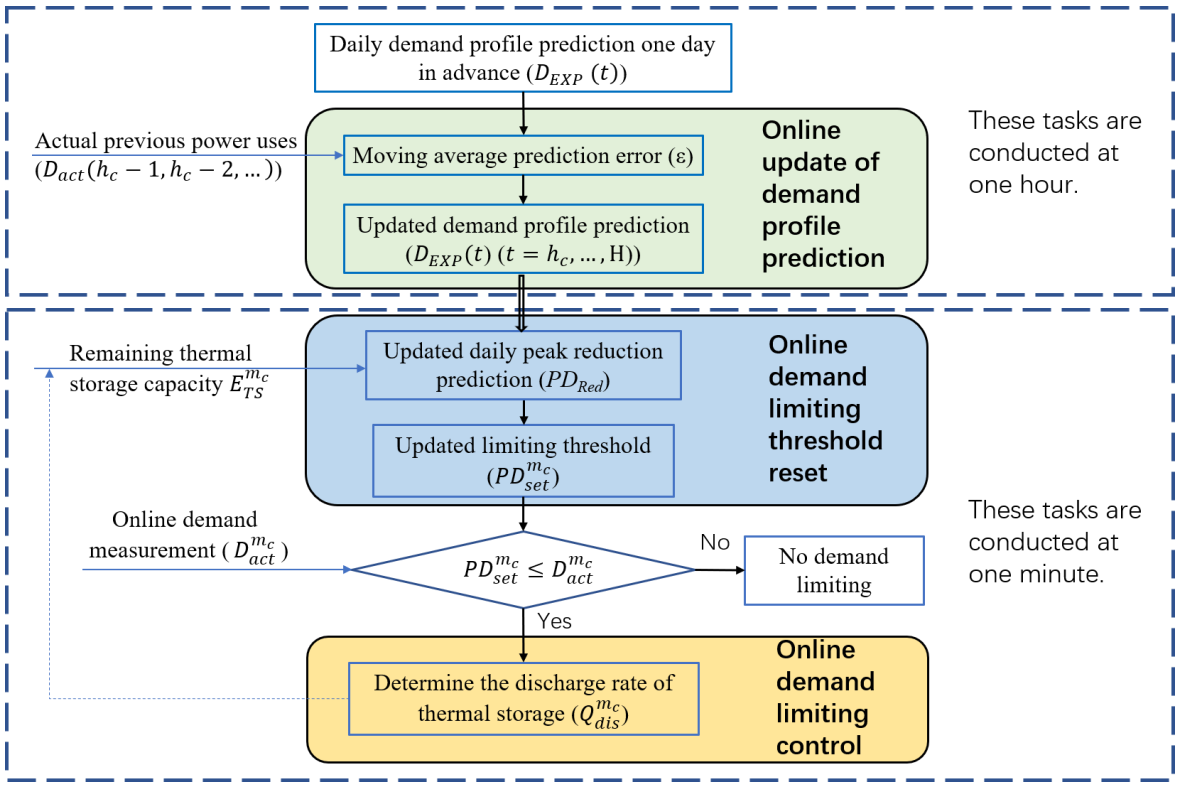

Figure 6.1. Flowchart of the proactive-adaptive demand limiting control scheme.

The proactive-adaptive demand limiting control scheme includes three major functions: the update of demand profile prediction, the online demand limiting threshold resetting and the online demand limiting control, as shown in Figure 6.1. The online update of demand profile prediction updates the daily demand profile prediction at the 1-hour interval, based on the moving average prediction error (ε). The online demand limiting threshold resetting updates the limiting threshold at the 1-minute interval, based on the remaining storage capacity ($E_{TS}^{m_c}$) and

the updated daily demand profile prediction. The online demand limiting control is activated to discharge the active thermal storage (with the rate ($Q_{dis}^{m_c}$)) when the online measured demand ($D_{act}^{m_c}$) is over the current limiting threshold ($PD_{set}^{m_c}$). This proactive-adaptive scheme works each day (e.g., during office hours, 9:00 - 21:00) based on the daily-updated optimal monthly limiting threshold from the developed optimal threshold resetting scheme in Chapter 5.

6.3 Online update of daily demand profile prediction

The probabilistic load forecasts can be obtained using the previous developed building load forecasting model. In this study, the expected hourly load/demand forecasts in an entire day are regarded to constitute the predicted deterministic daily demand profile. This is mainly because the expectation metric is a risk-neutral criterion for decision-making and is commonly-used in the decision-making area (G. Mavromatidis et al., 2018). The expected hourly load forecasts in the remaining hours of the day are updated on the basis of the moving average prediction error, as given by Eq. (6.1). The moving average prediction error is calculated at each hour of the day as the average difference between the actual power uses and the expected hourly demand forecasts in the previous three hours, as given by Eq. (6.2). The accuracy of the demand profile prediction for the remaining hours of one day significantly affects the estimated limiting effort needed for the day. This moving average difference method will help update the demand profile prediction each hour according to the real-time forecasting performance.

$$D_{EXP}(t) = \sum D_i(t) * P(D_i(t)) + \varepsilon, (t = h_c, \dots, \mathrm{H}) \tag{6.1}$$

$$\varepsilon = \left(\sum_{t=h_c-3}^{h_c-1} D_{act}(t) - \sum_{t=h_c-3}^{h_c-1} D_{EXP}(t)\right)/3 \tag{6.2}$$

where, $D_{EXP}(t)$ represents the expected hourly load forecast for time (hour) t. $D_i(t)$ represents a particular value of the hourly probabilistic load forecast for time t. P is the probability of an event. ε represents the moving average prediction error for updating the daily demand profile. h_c represents the current hour. H represents the last hour of the demand limiting period. $D_{act}(t)$ is the actual power use for time t.

6.4 Online demand limiting threshold reset

Based on the updated daily demand profile prediction, the demand limiting threshold is updated (or reset) online on the basis of the possible daily peak demand reduction, as given by Eq. (6.3). The possible daily peak demand reduction for the remaining time of a day can be estimated according to the updated daily demand profile prediction and the remaining storage capacity at the current step (i.e., minute), as given by Eq. (6.4). The remaining storage capacity at the current step can be obtained based on the recordings of the discharged thermal storage.

$$PD_{set}^{m_c} = \max_{t \in [h_c, \mathrm{H}]} (D_{EXP}(t)) - PD_{Red} \tag{6.3}$$

$$PD_{Red} = f\left(D_{EXP}(t), E_{TS}^{m_c}\right),\ t = h_c, \dots, \mathrm{H} \tag{6.4}$$

where, $PD_{set}^{m_c}$ is the online limiting threshold at the current step, m_c, which should be no less than the peak power use up to the current step. The superscript m_c represents the current step.

PD_{Red} is the estimated peak demand reduction when the remaining storage capacity equals the daily limiting effort for the remaining time of a day. $E_{TS}^{m_c}$ is the remaining storage capacity at the current step, m_c.

6.5 Online demand limiting control

Based on the current threshold updated at the 1-min interval, the online demand limiting action is activated when the online measured demand ($D_{act}^{m_c}$) is over the online threshold ($PD_{set}^{m_c}$). In such a case, a certain amount of the thermal energy is discharged in the rate of $Q_{dis}^{m_c}$ to reduce the cooling load of the air-conditioning system (e.g., the chiller plant and the primary air unit). This discharged thermal energy is assumed proportional (assuming a constant overall COP of the air-conditioning system, λ) to the corresponding power use reduction of the air-conditioning system during the demand limiting period. Therefore, the actual building power use reduction ($\Delta Pow_{act}^{m_c}$) is estimated, as given by Eq (6.5).

$$\Delta D_{act}^{m_c} = \Delta Pow_{act}^{m_c} = \begin{cases} \frac{Q_{dis}^{m_c}}{\lambda}, & D_{act}^{m_c} > PD_{set}^{m_c} \\ 0, & D_{act}^{m_c} \leq PD_{set}^{m_c} \end{cases} \quad (6.5)$$

where, $D_{act}^{m_c}$ is the actual building power use at the current step, m_c. $\Delta D_{act}^{m_c}$ is the actual building power use reduction at the current step, m_c. $Q_{dis}^{m_c}$ represents the discharge rate of the active thermal storage at the current step, m_c. $\Delta Pow_{act}^{m_c}$ is the actual power use reduction of the air-conditioning system at the current step, m_c, which is regarded to equal the actual building power use reduction during the demand limiting period. λ is the coefficient between the used active thermal energy and the corresponding electrical energy consumption reduction from air-

conditioning systems during the demand limiting period. In this study, the loss of storage is ignored, and λ is assumed as 2.5 since the overall COP of the air-conditioning system is assumed to be 2.5 (C. Yan et al., 2017).

6.6 Summary

This chapter presents a proactive-adaptive demand limiting control scheme for monthly peak demand limiting under load uncertainty. The major contents presented in this chapter are as follows.

i. A proactive-adaptive demand limiting control scheme is proposed to update the limiting threshold online and conduct online demand limiting control. This scheme consists of three major components: the online update of daily demand profile prediction, the online demand limiting threshold reset and the online demand limiting control.

ii. The predicted daily demand profile is updated online on the basis of the moving average prediction error, which can reduce the short-term fluctuation response of the prediction errors.

iii. The demand limiting threshold is reset online on the basis of the possible daily peak demand reduction, which can be estimated according to the predicted daily demand profile and remaining storage capacity. When the storage is not sufficient for demand limiting in the remaining hours of a day, the threshold is proactively reset.

CHAPTER 7 VALIDATION OF PROBABILISTIC LOAD FORECASTING MODEL, OPTIMAL THRESHOLD RESETTING SCHEME AND PROACTIVE-ADAPTIVE DEMAND LIMITING CONTROL SCHEME

This chapter presents the validation tests and test results for the developed adaptive optimal monthly peak building demand limiting strategy concerning three aspects: the developed probabilistic load forecasting model, the optimal threshold resetting scheme and the proactive-adaptive demand limiting control scheme. All these three validation tests are conducted on the Matlab platform. Section 7.1 presents the training and validation of the probabilistic load forecasting model. Section 7.2 presents the validation of the optimal threshold resetting scheme for monthly peak demand limiting in different seasons. Section 7.3 presents the validation of the proactive-adaptive demand limiting control scheme for monthly peak demand limiting in different seasons.

7.1 Training and validation of probabilistic load forecasting model

In the training and validation of the probabilistic load forecasting model, the historical electrical load data of the Phase 7 building and historical weather data from the HKO from Jan/2009 to Dec/2016 are collected and used. Moreover, in the real-time test of the probabilistic normal load forecasting model, the 9-day interval weather forecasts reported daily by the HKO are recorded daily in both Oct and Dec/2017. And the measured load data in these two months are also used

to benchmark the real-time forecasting accuracy.

7.1.1 Model training and results

7.1.1.1 Decomposition of load dataset

In the decomposition of load dataset using the LR method, the historical data of load and enthalpy from Jan/2009 to Dec/2016 were classified into 12 clusters (based on office hour of working days) and then the coefficients of the LR model in each cluster were identified, as listed in Table 7.1.

Table 7.1. Identified coefficients of the linear regression model in each cluster

Coefficient	Cl_1	Cl_2	Cl_3	Cl_4	Cl_5	Cl_6	Cl_7	Cl_8	Cl_9	Cl_{10}	Cl_{11}	Cl_{12}
a_0	874	842	868	846	846	850	804	803	821	828	798	778
a_1	0.12	0.09	0.09	0.09	0.09	0.08	0.07	0.07	0.09	0.12	0.12	0.11
a_2	1.91	5.33	5.14	5.21	4.90	6.00	8.08	7.89	5.96	3.14	2.89	2.93

Note: Cl_1 represents the cluster of datasets at 9:00 and Cl_{12} represents the cluster at 20:00.

The residuals between the actual loads and the estimated loads in each cluster were analyzed using the Kernel density estimation function. The optimized bandwidth of the KDE function in each cluster was set as 25 according to the optimization formula. All the actual loads with their corresponding residuals out of the 95% confidence interval of the KDE function were selected as the abnormal loads (Set ***A***). Figure 7.1 shows the histograms and KDE functions of residuals

between the actual loads and the estimated loads at selected hours (i.e., 9:00 and 14:00). It can be seen that the estimated KDE functions well matched the histograms of the load residuals in both of the two clusters.

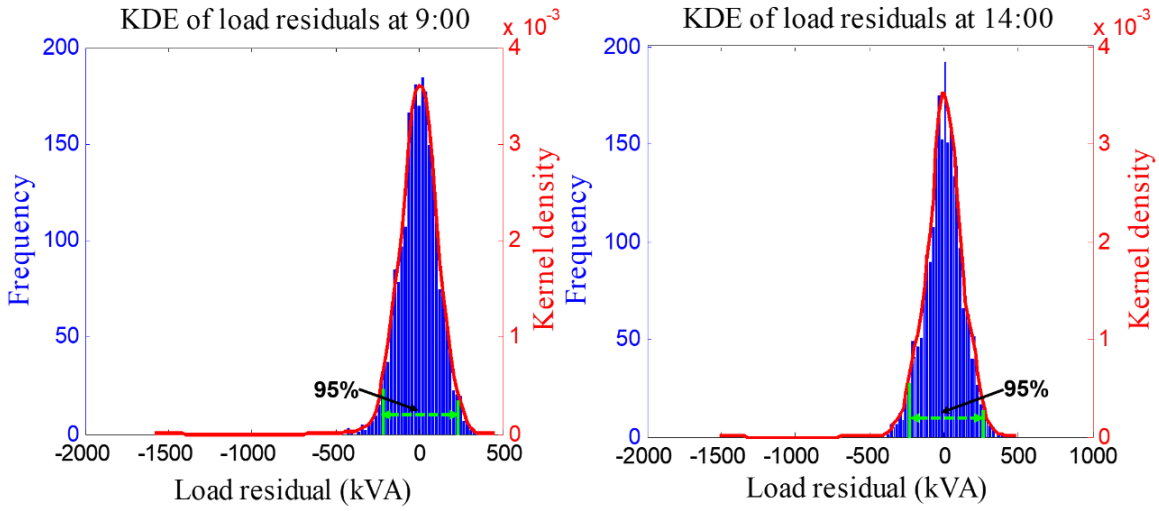

Figure 7.1. Histograms and Kernel density estimation functions of load residuals at 9:00 and 14:00.

The historical load data from Jan/2009 to Dec/2016 were also used in the decomposition of load dataset using the LOF method. The *LOF* value of each hourly load was calculated with the parameter k (set as the recommended value 10). Then all *LOF* values were analyzed with the empirical cumulative distribution function, and the actual loads with their *LOF* value's empirical cumulative probability over 95% were regarded as the abnormal loads (Set ***B***). Figure 7.2 shows the histograms and empirical cumulative distribution functions of the *LOF* values of all loads in selected years (i.e., 2009 and 2013). It can be seen that most of the *LOF* values of loads were close to 1.

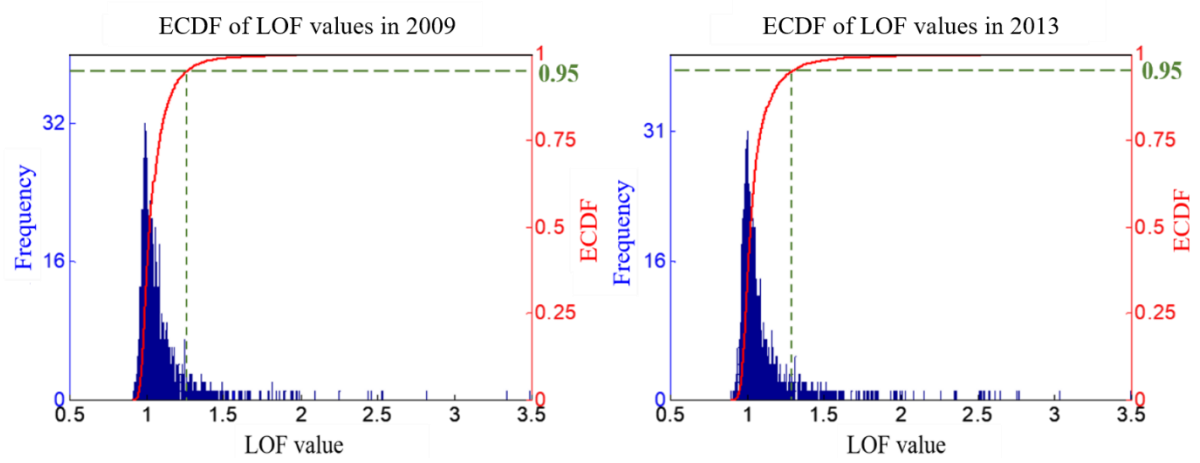

Figure 7.2. Histograms and empirical cumulative distribution functions of the *LOF* values of the loads in 2009 and 2013.

After load dataset decomposition using each of the LR, LOF and hybrid methods, the ratios of the number of the decomposed abnormal loads to the number of all the loads using these methods are listed in Table 7.2. It can be seen that the ratio from using the hybrid method integrating LR and LOF was 0.068, much larger than that from using either method, which indicates the hybrid method is more sensitive and robust.

Table 7.2. The ratios of the number of decomposed abnormal loads to the number of all the loads using the three methods

	LR	LOF	Hybrid
Ratio	0.036	0.035	0.068

The results of the load datasets decomposition during the office hour in 2013 are shown in Figure 7.3 for illustration. It can be seen that most extremely large and small loads were decomposed as

abnormal loads by both the LR and the LOF methods.

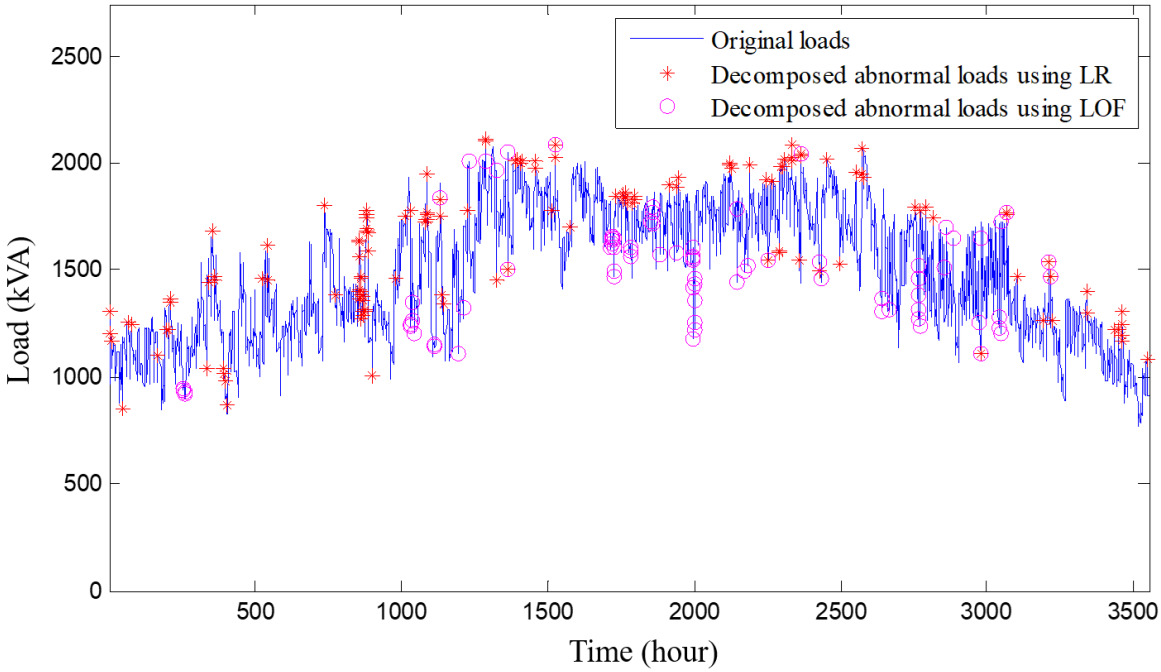

Figure 7.3. Load dataset decomposition results during office hours in 2013.

7.1.1.2 Training of ANN model

To train the ANN model, the historical datasets of the normal load, weather variables, and calendar variables from Jan/2009 to Dec/2015 were used. The number of hidden neurons in the hidden layer was set as 12 according to Eq. (4.1) and the trial and error. Besides, the mean square error was set as 0.001, the learning rate was set as 0.5, and the iteration times were set as 1000.

7.1.1.3 Training of probabilistic magnitude model

In the training of the probabilistic model of the peak abnormal differential (PAD) load magnitude, the PAD load data from Jan/2009 to Dec/2015 were used to train/fit the probability distribution of the magnitude using the four alternative PDFs. The identified parameter values of the fitted

PDFs of the PAD load magnitude are listed in Table 7.3.

Table 7.3. Parameter values for the fitted probability density functions of the peak abnormal differential load magnitude

	Normal		Gamma		Weibull		Lognormal	
Parameter	μ	σ	α	β	λ	k	ϕ	γ
Value	109.8	75.5	2.3	47.7	122.9	1.6	4.5	0.7

Table 7.4 shows the statistical errors of the trained PDFs of the PAD load magnitude data. The Lognormal distribution fit the observed data best among the four PDFs, with the smallest K-S error of 0.0398. Therefore, the Lognormal distribution (ϕ=4.5, γ=0.7) was selected for the forecasted probability distribution of the magnitude in the later years.

Table 7.4. Statistical errors for the proposed probability density functions

	Normal	Gamma	Weibull	Lognormal
K-S error	0.1379	0.0573	0.0680	0.0398

7.1.2 Model validation and results

7.1.2.1 Performance evaluation criteria

To evaluate the deterministic normal load forecasting model, the commonly-used mean absolute percentage error (MAPE) indicator, mean absolute error (MAE) indicator and root mean squared

error (RMSE) are adopted, as given by equations (7.1-7.3). Where, L_i is the measured load (kVA). $\hat{L}_i$ is the forecasted load (kVA). *i* is a certain number. *n* is the length of the test time series.

$$\text{MAPE} = \frac{1}{n}\sum_{i=1}^{n}\left|\frac{L_i-\hat{L}_i}{L_i}\right| \tag{7.1}$$

$$\text{MAE} = \frac{1}{n}\sum_{i=1}^{n}\left|L_i-\hat{L}_i\right| \tag{7.2}$$

$$RMSE = \sqrt{\frac{1}{n}\sum_{i=1}^{n}\left(L_i-\hat{L}_i\right)^2} \tag{7.3}$$

To evaluate the PAD load magnitude model, the deviations between the observed data and their forecasts are assessed using the K-S error as shown earlier in Eq. (4.5).

7.1.2.2 Validation of ANN deterministic load forecasting model

In the validation test of the ANN deterministic load forecasting model, the historical datasets of the normal load, weather variables, and calendar variables in 2016 were used. The calculated monthly MAPEs, MAEs and RMSEs of the test results are listed in Table 7.5. The average MAPE was 5.0%, the average MAE was 77.8 kVA, and the average RMSE was 108 kVA in the year. The minimum MAPE was 2.9%, which occurred in July, the minimum MAE was 46 kVA, which occurred in January, and the minimum RMSE was 54 kVA, which occurred in January. This shows the forecast accuracy of the deterministic load forecasting model is satisfactory.

Table 7.5. MAPEs, MAEs and RMSEs of test results of the ANN model in 2016

	Jan	Feb	Mar	Apr	May	Jun	Jul	Aug	Sept	Oct	Nov	Dec
MAPE (%)	4.0	4.8	5.4	5.8	6.2	7.0	2.9	3.1	5.0	3.9	6.5	7.0
MAE (kVA)	46	55	70	94	114	142	55	58	80	61	77	82
RMSE (kVA)	54	90	98	144	148	171	79	87	116	101	109	106

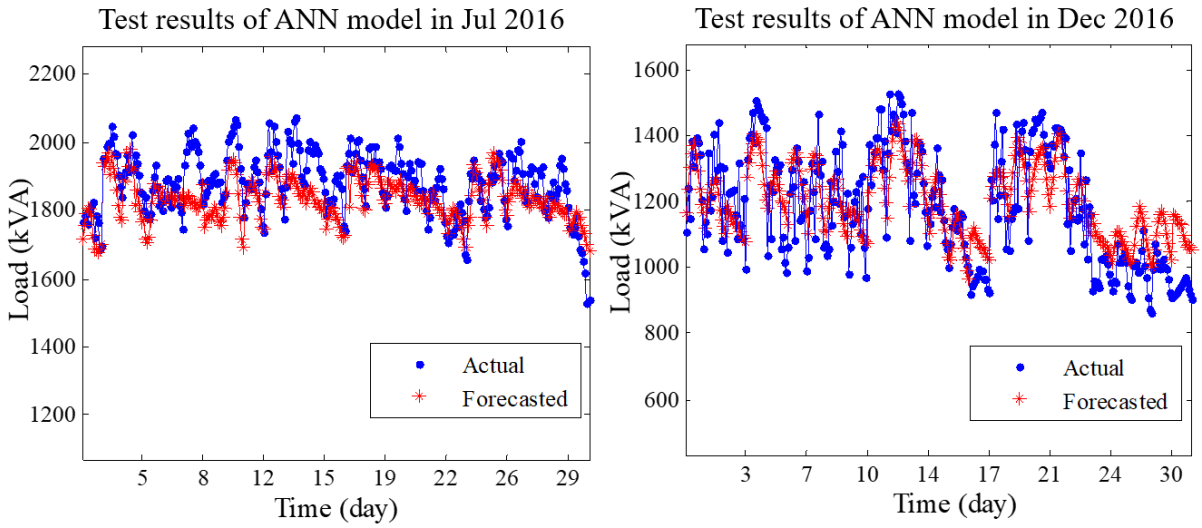

Figure 7.4. Load forecast using the deterministic load forecasting model compared with actual measurements during office hours (Jul and Dec/2016).

The detailed load forecast in Jul and Dec/2016 and the comparison with actual measurements are shown in Figure 7.4, which are the best and the worst results, respectively. It can be seen that load forecasts in both months matched the actual loads with the satisfactory agreement, while the agreement in July was better than that in December. It is because that in Hong Kong

December is in the transition season and the weather condition fluctuates significantly.

7.1.2.3 Validation of probabilistic models of occurrence and magnitude

To validate the probabilistic model of the peak abnormal differential (PAD) load occurrence, the PAD load data in 2016 were used. The forecasts of the relative PAD load frequencies (i.e., percentages) at different office hours of work days in 2016 are shown and compared with the actual data in Figure 7.5. It can be seen that the forecasts of the relative frequencies matched the actual data very well during most hours while the forecasts at 9:00, 19:00 and 20:00 have relatively larger deviations. With more PAD load data, the forecast accuracy of the relative frequency can be improved.

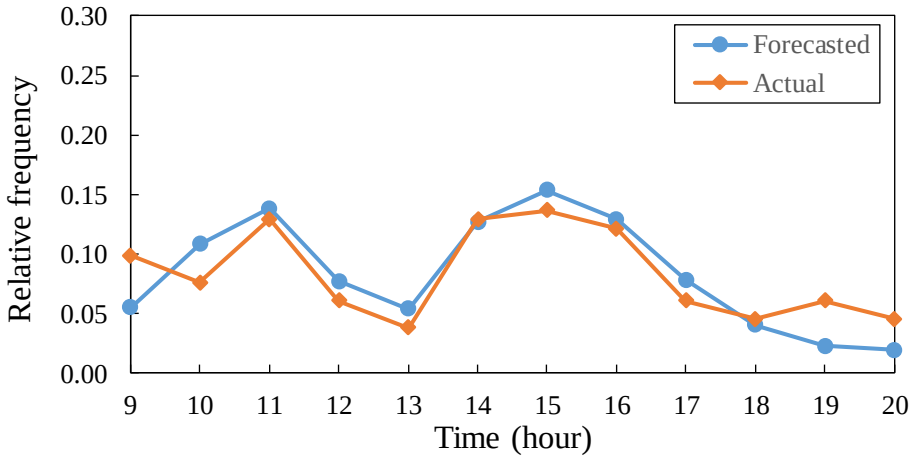

Figure 7.5. Forecasted and actual relative frequencies of the peak abnormal differential load at different office hours (2016).

To validate the probabilistic model of the PAD load magnitude, the PAD load data in 2016 were also used. The K-S error between the forecasted distribution and the observed distribution of the

PAD load in 2016 was 0.09, showing a very satisfactory accuracy. The forecasted and observed probability densities of the PAD load magnitude are shown in Figure 7.6. It can be seen that most of the forecasted probability densities of the PAD load magnitude matched well the observed ones.

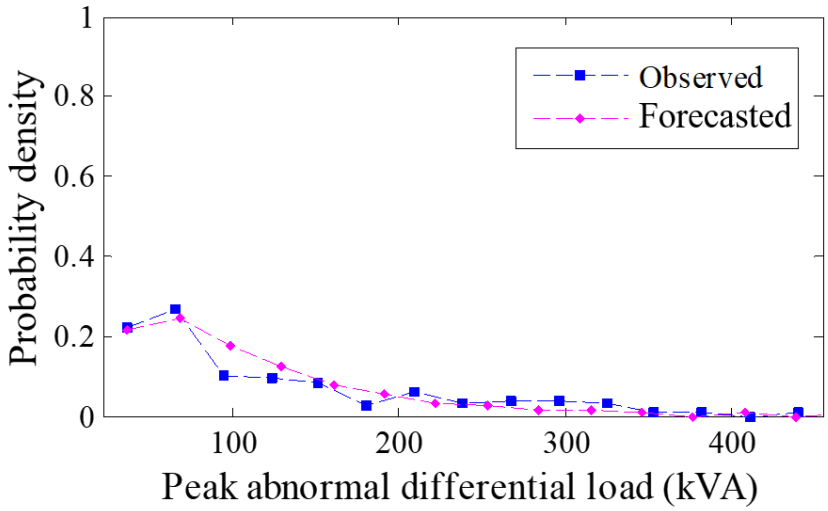

Figure 7.6. Comparison between forecasted and observed probability densities of the peak abnormal differential load magnitude (2016).

7.1.2.4 Real-time application case studies

In the real-time application case studies, the 9-day interval probabilistic normal load forecasts were generated using 9-day interval weather forecast, which is provided and updated daily by the Hong Kong Observatory (HKO).

To evaluate the probabilistic forecast models, the sharpness, resolution and reliability of forecasts are usually considered (T. Hong & S. Fan, 2016), which are also considered in this study to

evaluate the probabilistic forecast model of the normal load. The pinball loss function (T. Hong et al., 2016) is used to calculate the quantile scores of the probabilistic load forecast results. The pinball loss for the load at each quantile and each hour is calculated using Eq. (7.4).

$$Pinball\left(L_{t,q\%},\ L_t,\ q\%\right) = \begin{cases} q\%\left(L_t - L_{t,q\%}\right) & L_t \geq L_{t,q\%} \\ (1-q\%)\left(L_{t,q\%} - L_t\right) & L_t < L_{t,q\%} \end{cases} \tag{7.4}$$

where, $q\%$ is the target quantile of the quantile load forecast. The mean of the pinball losses across all the quantiles and all the forecasted hours in a month is regarded as the pinball score for the probabilistic load forecast. A lower pinball score indicates a better probabilistic forecast.

Case 1 - October (using weather forecasts on four days)

The 9-day weather forecast data in Oct/2017 reported by the HKO in four days (i.e., 30/Sept, 9/Oct, 18/Oct and 27/Oct) were used to compose the probabilistic weather forecasts of all days in the month. The weather forecast reported by the HKO includes the probabilistic forecasts of the daily maximum/minimum temperatures and the deterministic forecasts of the hourly temperature and relative humidity. The hourly probabilistic temperature forecasts, as shown in Figure 7.7, were obtained by processing these available temperature forecast data using the proposed method in Section 4.2.2. Figure 7.7 shows the 90% prediction interval of the hourly probabilistic temperature forecasts and the actual reported temperatures in Oct/2017. The boundaries of the 90% prediction interval are the 5% quantile and 95% quantile, respectively.

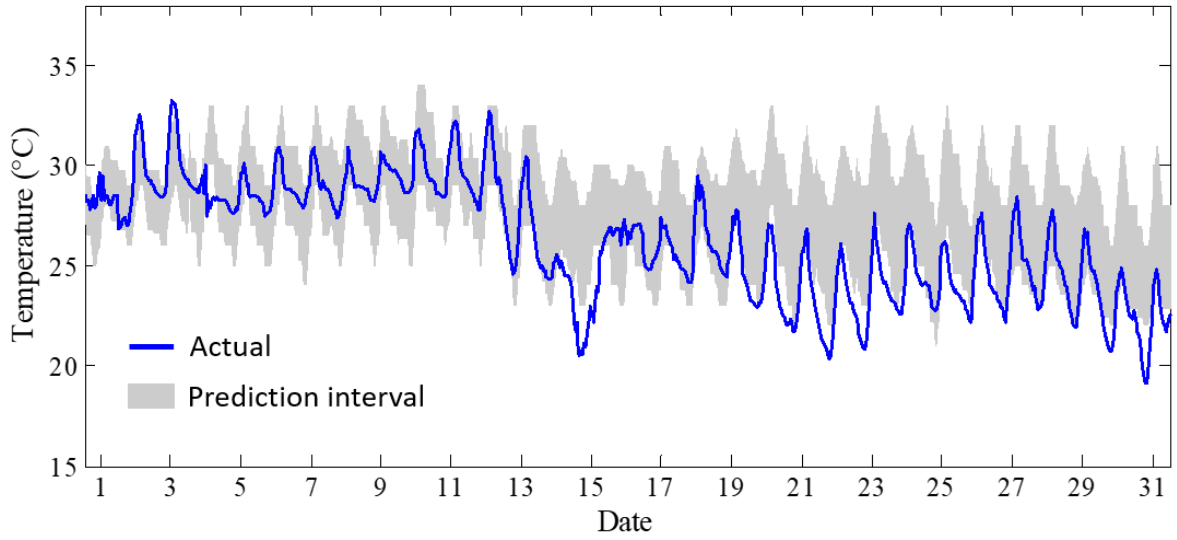

Figure 7.7. Generated hourly probabilistic temperature forecasts of Oct/2017. The shading represents the boundaries of the 90% prediction interval.

These hourly probabilistic temperature forecasts and the hourly deterministic relative humidity forecasts during office hours in October were used by the ANN model as the inputs to generate the probabilistic normal load forecasts and the results are shown in Figure 7.8. It shows the actual loads, the mean probabilistic normal load forecasts and the 90% prediction intervals in October and the probability density of normal load at an hour. It can be seen that most of the actual loads fell in the 90% prediction intervals. The small figure in the right illustrates the probability distribution of the forecasted normal load at 14:00 on 16/Oct. The MAPE, MAE and RMSE between the mean probabilistic normal load forecasts and the actual loads in Oct/2017 were 0.084, 147 kVA and 170 kVA respectively (listed in Table 7.6), showing an acceptable forecast accuracy.

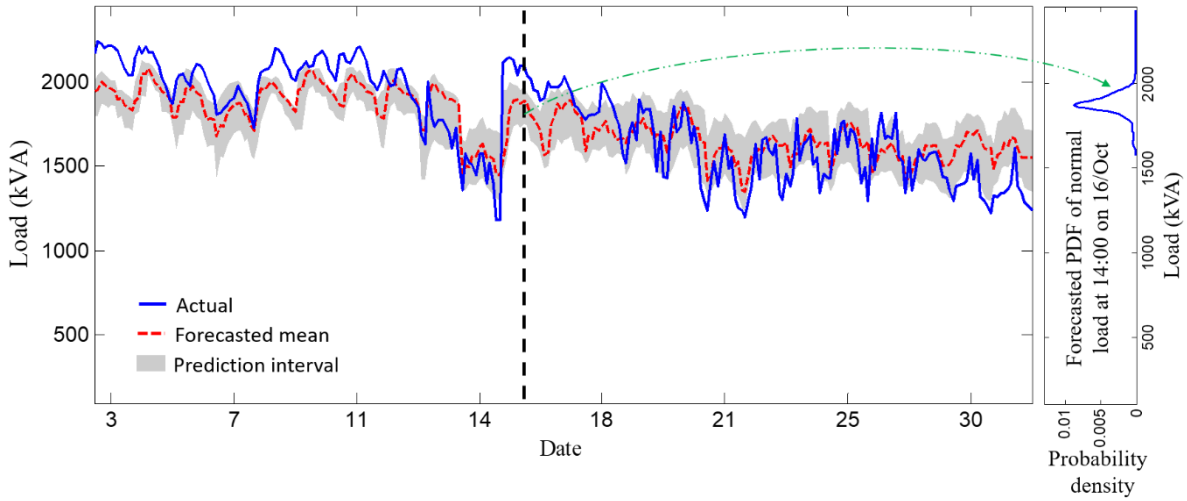

Figure 7.8. Probabilistic normal load forecasts of Oct/2017 and the probability density of normal load at one hour. The shading represents the boundaries of the 90% prediction interval.

Case 2 - December (using one-day-ahead weather forecasts)

The 9-day weather forecast data reported by the HKO in Dec/2017 were recorded daily and used to compose the probabilistic weather forecasts of all days in the month. Different from Case 1, the one-day-ahead weather forecasts updated daily were used for load forecasts of every day in the month. It means that the normal load forecasts of a day are obtained using the weather forecasts of that day reported in the previous day. The hourly probabilistic temperature forecasts using the one-day-ahead weather forecasts in December were generated in the same way as that in Case 1, as shown in Figure 7.9. It shows the 90% prediction interval of the hourly probabilistic temperature forecasts using one-day-ahead weather forecasts and the actual reported temperatures in December. It can be seen that most of the actual temperatures were in the middle of the prediction interval.

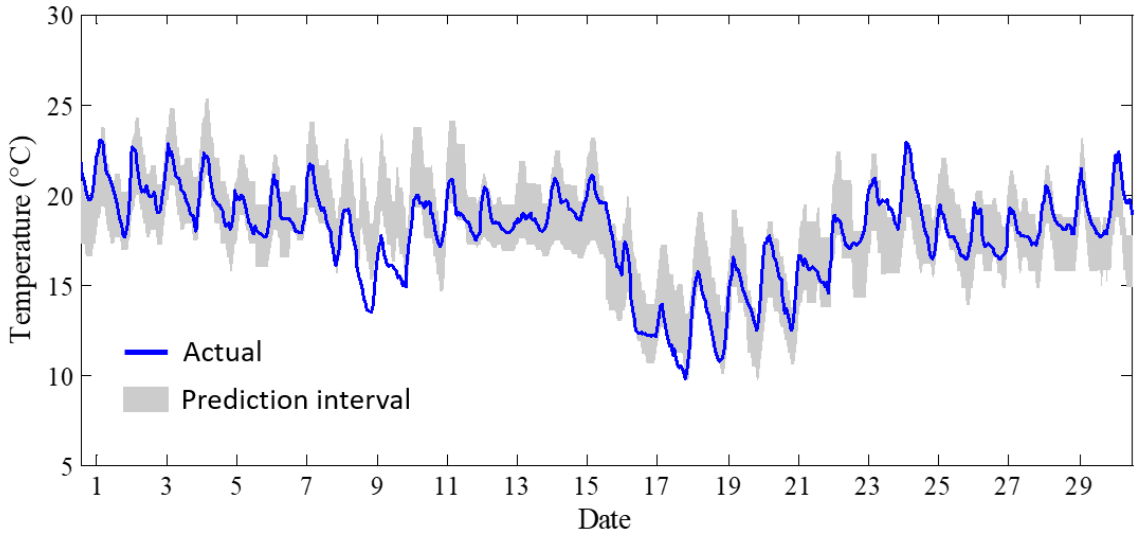

Figure 7.9. Generated hourly probabilistic temperature forecasts of Dec/2017 using one-day-ahead weather forecasts. The shading represents the boundaries of the 90% prediction interval.

These hourly probabilistic temperature forecasts and the hourly deterministic relative humidity forecasts during office hours in Dec/2017 were used by the ANN model to generate the probabilistic normal load forecasts, and the results are shown in Figure 7.10. It shows the actual loads, the mean probabilistic normal load forecasts and the 90% prediction intervals using one-day-ahead weather forecasts in Dec and the probability density of normal load at an hour. It can be seen that most of the mean probabilistic normal load forecasts were close to the actual loads, which was better than the forecast results in Case 1. The small figure in the right illustrates the probability distribution of the forecasted normal load at 14:00 on 15/Dec. In this case, the MAPE, MAE and RMSE between the mean probabilistic normal load forecasts and the actual loads in December were 0.047, 64 kVA and 80 kVA respectively (listed in Table 7.6), showing a satisfactory forecast accuracy.

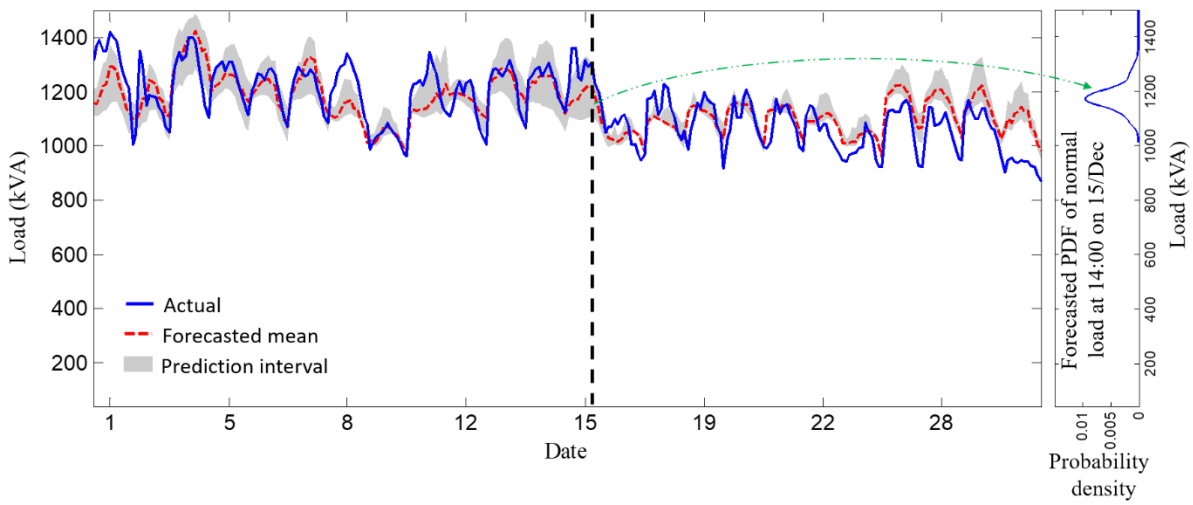

Figure 7.10. Probabilistic normal load forecasts of Dec/2017 using one-day-ahead weather forecasts and the probability density of normal load at one hour. The shading represents the boundaries of the 90% prediction interval.

Case 3 - December (using nine-day-ahead weather forecasts)

Different from Case 2, the nine-day-ahead weather forecasts updated daily were used for normal load forecasts of each day in the month. It means that the normal load forecasts of each day are obtained using the weather forecasts of that day made nine days ago. The hourly probabilistic temperature forecasts using the nine-day-ahead weather forecasts in Dec/2017 were generated in the same way as that in Case 1, as shown in Figure 7.11. It shows the 90% prediction interval of the hourly probabilistic temperature forecasts using nine-day-ahead weather forecasts and the actual reported temperatures in Dec. It can be seen that most of the actual temperatures were also in the middle of the prediction interval, but the average bandwidth of the prediction interval was larger than that in Figure 7.9.

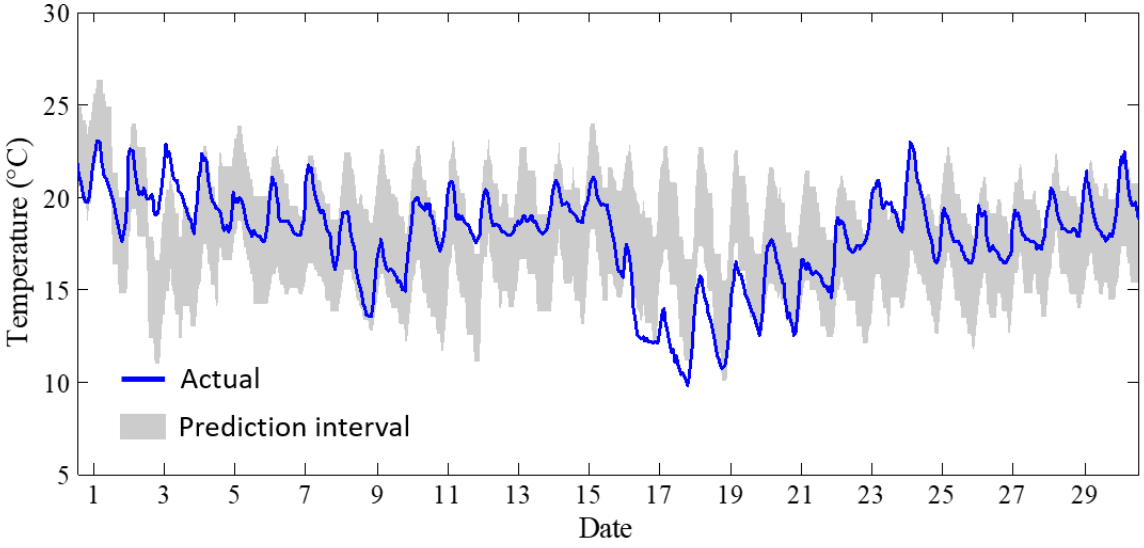

Figure 7.11. Generated hourly probabilistic temperature forecasts of Dec/2017 using nine-day-ahead weather forecasts. The shading represents the boundaries of the 90% prediction interval.

These hourly probabilistic temperature forecasts and the hourly deterministic relative humidity forecasts during office hours in December were used by the ANN model to generate the probabilistic normal load forecasts, and the results are shown in Figure 7.12. It shows the actual loads, the mean probabilistic normal load forecasts and the 90% prediction intervals using nine-day-ahead weather forecasts in December and the probability density of normal load at an hour. It can be seen that most of the mean probabilistic normal load forecasts were close to the actual loads, which was better than the forecast results in Case 1 but not as good as those in Case 2. The small figure in the right illustrates the probability distribution of the forecasted normal load at 14:00 on 15/Dec. In this case, the MAPE, MAE and RMSE between the mean probabilistic normal load forecasts and the actual loads in December were 0.067, 65 kVA and 82 kVA respectively (listed in Table 7.6), showing an acceptable forecast accuracy.

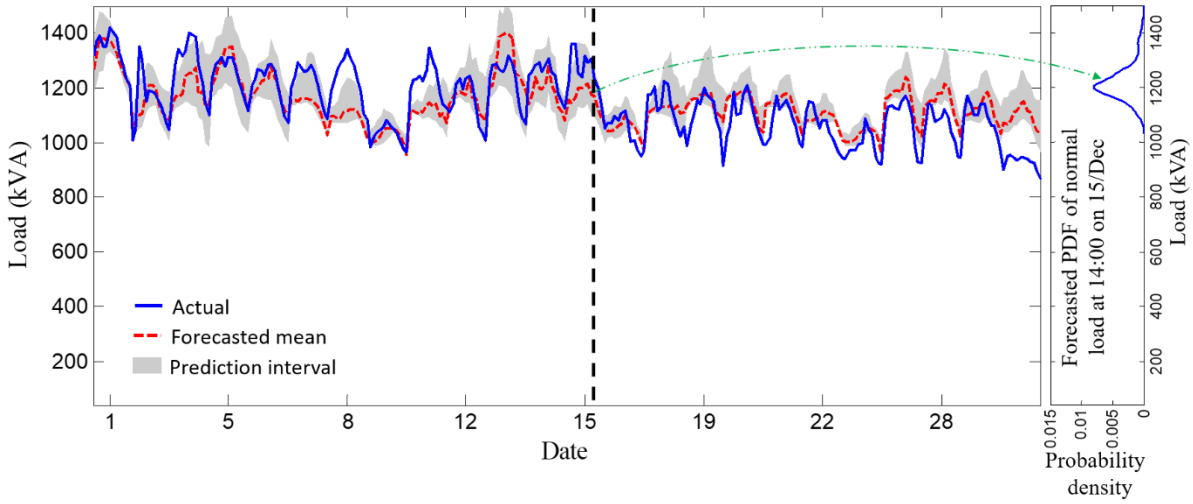

Figure 7.12. Probabilistic normal load forecasts of December using nine-day-ahead weather forecasts and the probability density of normal load at one hour. The shading represents the boundaries of the 90% prediction interval.

Comparison of forecast accuracies in three cases

To evaluate the probabilistic normal load forecasts in the above three cases, the mean probabilistic normal load forecasts are compared with the actual loads using the MAE, MAPE and RMSE. Besides, the pinball scores of the three cases are calculated and compared. Table 7.6 presents the detailed performance evaluation metrics for the probabilistic normal load forecasts of the three cases. The smaller the performance evaluation metric is, the more accurate the probabilistic normal load forecasts are. The probabilistic load forecasts in Case 2 shows the best performance with the smallest value in each individual performance evaluation metric.

Table 7.6. Performance evaluation metrics for the probabilistic normal load forecasts in the three cases

	Case 1	Case 2	Case 3
MAE_{prob} (kVA)	143	64	65
$MAPE_{prob}$ (%)	8.4	4.7	6.7
$RMSE_{prob}$ (kVA)	170	80	82
Pinball score	58.9	27.6	27.8

Remark: MAE_{prob} is the mean absolute error between the mean probabilistic normal load forecasts and the actual loads, $MAPE_{prob}$ is the mean absolute percentage error between the mean probabilistic normal load forecasts and the actual loads, and $RMSE_{prob}$ is the root mean square error between the mean probabilistic normal load forecasts and the actual loads.

Figure 7.13 shows the percentage of the actual loads falling within the predicted quantile of the probabilistic normal load forecasts in a month period in three cases. It can be seen that the overall predicted quantile bandwidth (1%-99%) in Case 2 was the smallest, which indicates the performance of the probabilistic normal load forecasts in Case 2 was the most accurate.

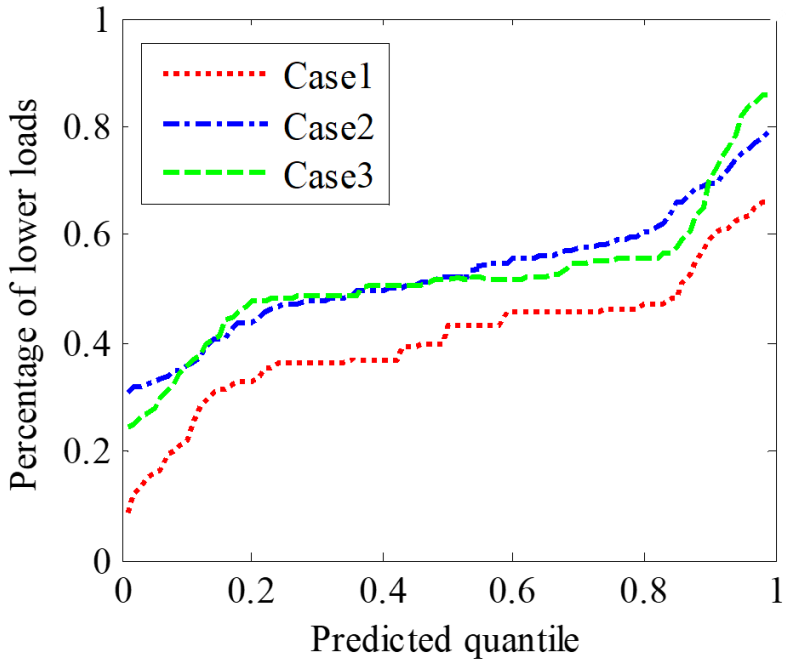

Figure 7.13. Comparison of the percentages of observed actual load values falling in the predicted quantile of the probabilistic normal load forecasts in three cases.

Comparing Case 1 with Case 2, the five probabilistic normal load forecasting accuracy indicators (i.e., MAE_{prob}, $MAPE_{prob}$, $RMSE_{prob}$, the pinball score and the overall predicted quantile bandwidth (1%-99%)) of Case 2 were smaller than that of Case 1. It indicates that the probabilistic load forecasts of Case 2 were superior to that of Case 1, and the probabilistic load model can offer better forecasts using the most updated (i.e., one-day-ahead) weather forecasts compared with the case using the nine-day weather forecasts without daily updating.

Comparing Case 2 with Case 3, the five probabilistic normal load forecasting accuracy indicators of Case 2 were smaller than that of Case 3. It indicates that the probabilistic load forecasts of Case 2 were superior to that of Case 3. It means that the shorter the period of the weather forecast is the better accuracy the probabilistic normal load forecasts can achieve.

Comparing Case 1 with Case 3, the first three probabilistic normal load forecasting accuracy indicators (i.e., MAE_{prob}, $MAPE_{prob}$ and $RMSE_{prob}$) of Case 1 were larger than that of Case 3, due to the fact that the (deterministic) weather forecasts in December were more accurate than that in October. But the last indicator (i.e., the overall predicted quantile bandwidth (1%-99%)) of Case 1 was smaller than that of Case 3, indicating that bandwidth of load forecasts was smaller in Case 1.

In general, the probabilistic normal load forecasting accuracy is affected by the probabilistic weather forecasting accuracy from the HKO. Comparison studies for the proposed probabilistic load forecasting approach are expectable and could be conducted in the near future when studies using standard datasets of compatible format (i.e., the probabilistic weather forecast is included) are available.

7.2 Validation of optimal threshold resetting scheme

In the validation of the optimal threshold resetting scheme for adaptive monthly peak demand limiting, active thermal storages with ideal control are adopted. The historical electrical load data of the Phase 7 building in winter and summer (i.e., Dec/2017 and June/2018) are collected and used at the 1-hour time interval. And in each month, the 9-day weather forecast data reported daily by the Hong Kong Observatory (HKO) are recorded daily. Moreover, sensitivity analysis of the cost benefits of the developed scheme using different means of demand limiting and different electricity demand tariffs is conducted.

7.2.1 Identification of parameters in quantification formulae

To quantify the optimal threshold resetting scheme, some parameters in quantification formulae are identified. The unit price of the electricity demand (i.e., *a* in Eq. (5.9)) is set as 120 HKD/kVA and the unit price of the electricity consumption is 0.6 HKD/kWh, according to a real tariff (Large Power Tariff) from the Hong Kong CLP power company. The unit price of the demand limiting effort using the ideal thermal storage (i.e., *b* in Eq. (5.9)) is calculated as 0.24 HKD/kWh, when assuming that the overall COP of the air-conditioning system is 2.5 earlier (C. Yan et al., 2017). A simplified cold active storage model (B. Cui et al., 2014) is used to quantify the demand limiting capacity for the Phase 7 building and an active storage with the limiting capacity (*Cap*) of 4763 kWh is adopted.

7.2.2 Winter case study and test results

In the winter case study, the datasets during the office hours in Dec/2017 were used for the validation test. The 9-day weather forecast data reported/updated daily by the HKO in December are recorded each day. They are used to forecast/update the 9-day probabilistic demand profiles each day, which are then used to identify/update the optimal monthly limiting threshold. In the following subsections, the first workday in December is selected to illustrate the identification procedure of the optimal monthly limiting threshold. Afterward, the procedure is conducted repeatedly to obtain/update the monthly limiting threshold in an adaptive manner for demand limiting control in the following days of the month.

7.2.2.1 Optimal monthly limiting threshold identification on the first workday of December

On the first workday of December (before office hour, e.g., 9:00 AM), the probabilistic demand profiles during office hours in the following 9 days were forecasted in advance, as shown in Figure 7.14. Different confidence intervals of the probabilistic demand profiles are shown in the figure, such as 20%, 40%, 60% and 99%. In addition, the range of the tested thresholds was identified as [1149 kVA, 1287 kVA].

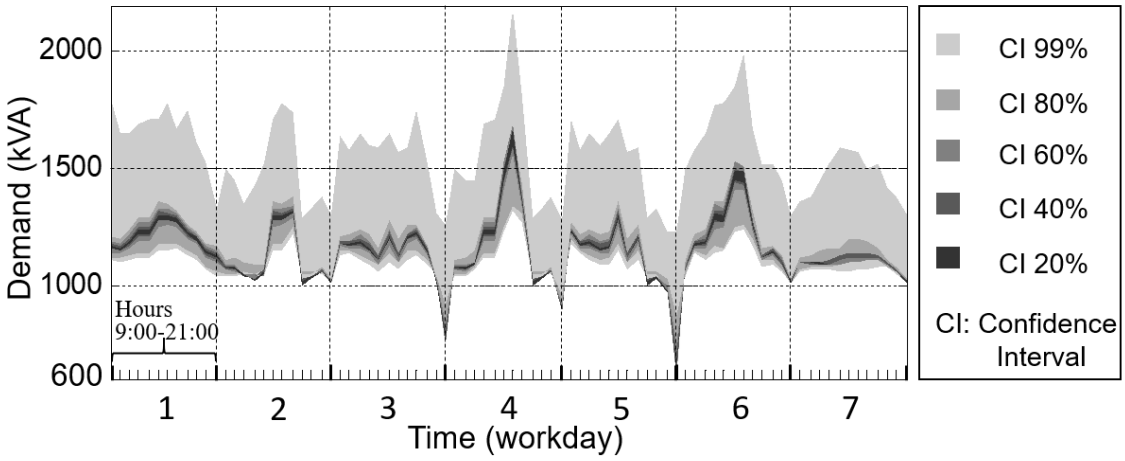

Figure 7.14. Probabilistic demand profiles during office hours between 01/Dec and 09/Dec/2017 forecasted in the early morning of 01/Dec.

Based on the forecasted probabilistic demand profiles, the probability density distributions (PDF) of the daily peak demand in workdays between 01/Dec and 09/Dec were obtained, as shown in Figure 7.15.

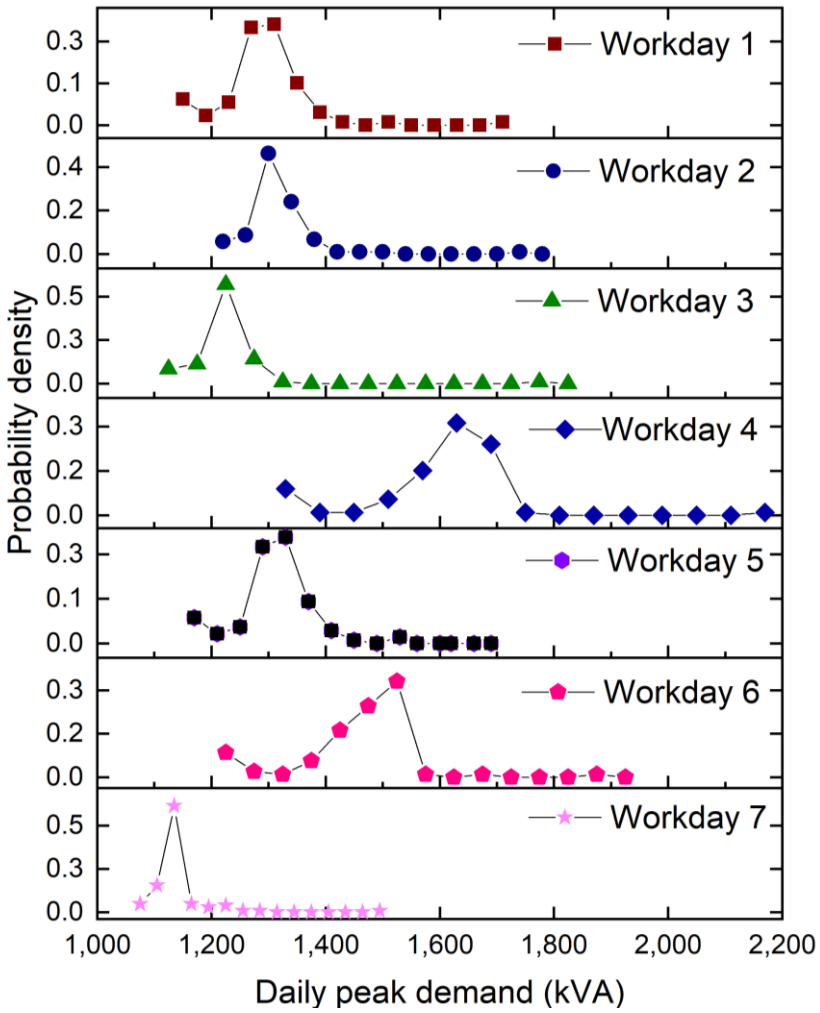

Figure 7.15. Probability density of the daily peak demand in workdays between 01/Dec and 09/Dec/2017 forecasted in the early morning of 01/Dec.

With these PDFs of the daily peak demand, the probability of each scenario (nonactivation, success and failure) was quantified when a particular threshold was used on one day. Based on these quantified daily probabilities, the monthly probability of each scenario using that threshold was estimated, as shown in Figure 7.16. It can be seen that all the monthly success probabilities accounted for over 85%, all the monthly failure probabilities were less than 16%, and all the monthly nonactivation probabilities were 0%.

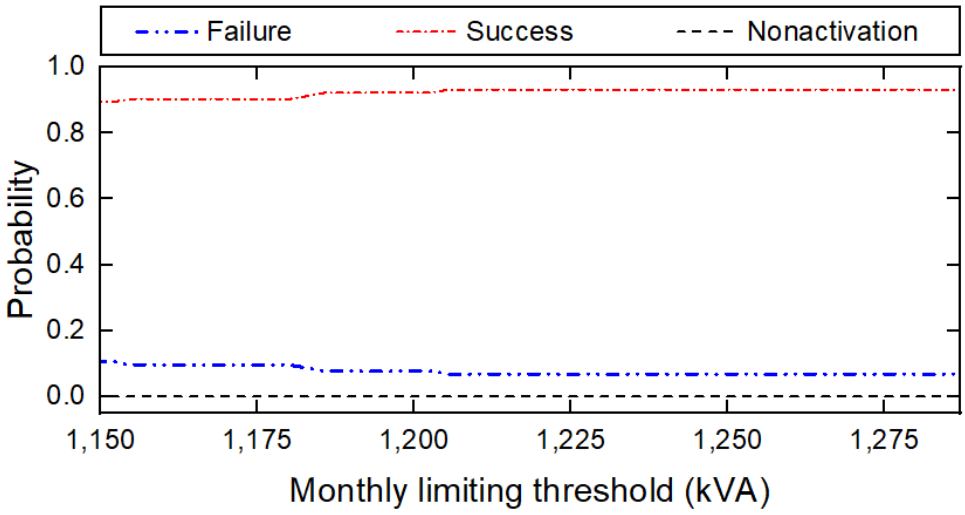

Figure 7.16. Quantified monthly probabilities of three scenarios when implementing demand limiting using different thresholds on the first workday of Dec/2017.

Based on the quantified monthly probabilities at different thresholds, the expected monthly cost savings and the expected monthly gains were quantified, as shown in Figure 7.17. It can be seen that they changed in the same trend along with the increase of the limiting threshold. After the quantification of the expected monthly cost savings among different thresholds, the optimal monthly limiting threshold was identified of 1287 kVA, and the corresponding cost saving was 14,592 HKD.

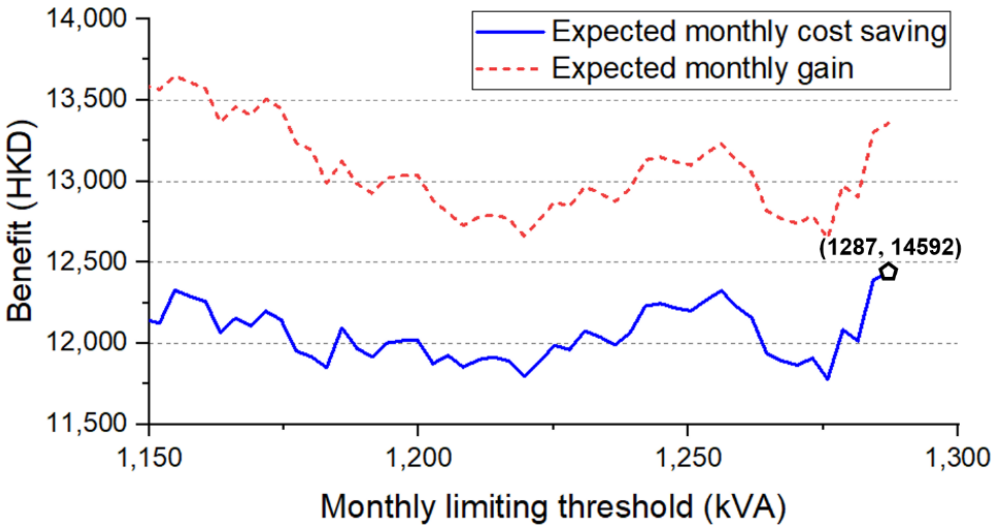

Figure 7.17. Expected monthly cost savings and expected monthly gains when implementing demand limiting using different thresholds on the first workday of Dec/2017.

7.2.2.2 Validation of the developed scheme for monthly peak demand limiting in December

Similarly, on each of the following workdays, the identification procedure using the optimal threshold resetting scheme is conducted repeatedly to obtain and update the optimal limiting threshold. In addition, the ideal demand limiting control is conducted on the basis of the identified adaptive optimal limiting threshold. The difference lies in that the actual peak power use was considered in updating the optimal limiting threshold. Figure 7.18 shows the validation results of demand limiting using the adaptive optimal threshold resetting scheme in Dec/2017.

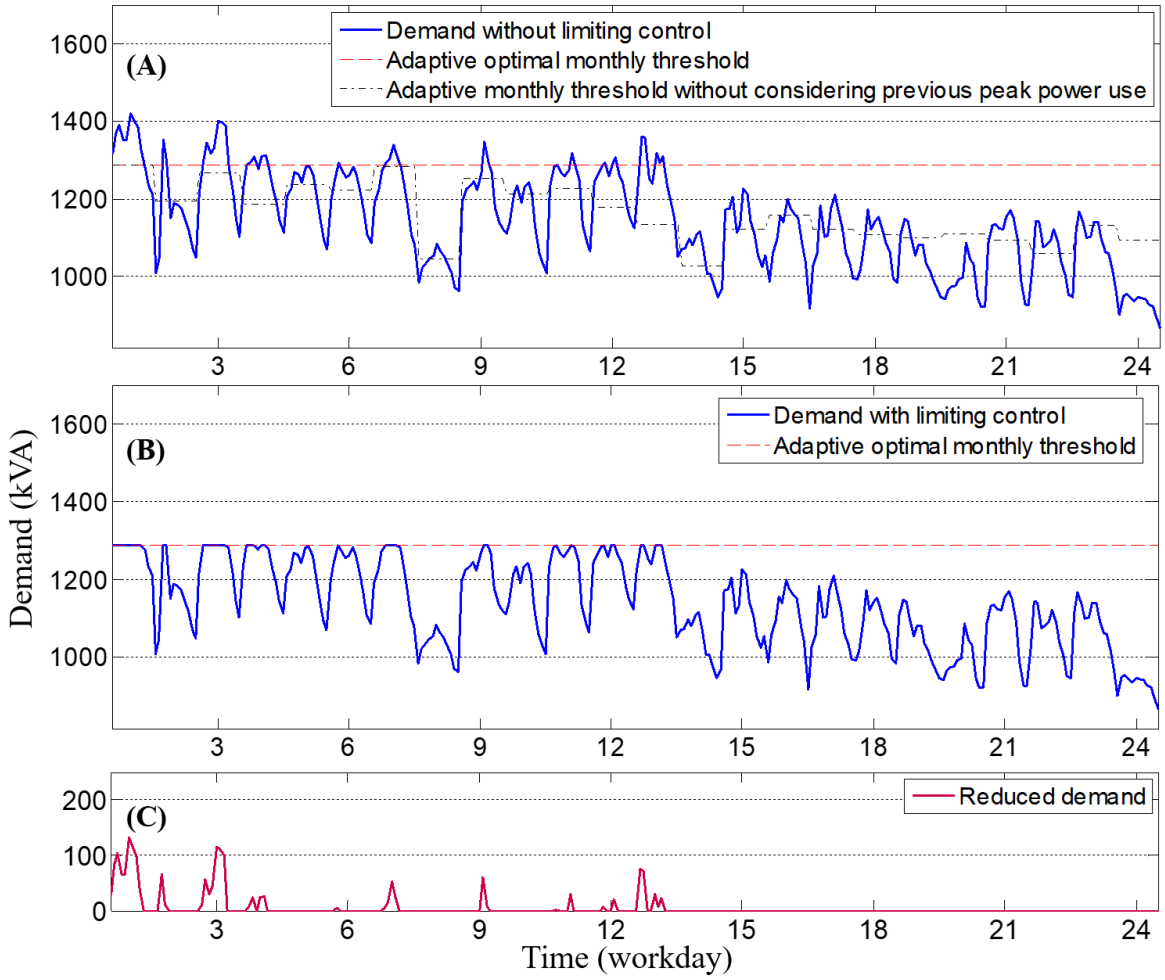

Figure 7.18. Building demand profiles in Dec/2017 under different situations: (A) no demand limiting; (B) demand limiting using the developed scheme. (C) Actual demand reduction using the developed scheme.

Figure 7.18(A) shows the power demand profile of the Phase 7 building, without implementing demand limiting, measured in Dec/2017. It can be seen that the monthly peak demand occurred on the first workday. The actual demand in the second half of the month was smaller. Two adaptive thresholds are also included. One is the adaptive optimal monthly limiting threshold, and the other is the adaptive monthly limiting threshold without considering the actual peak of

previous power use. The second threshold fluctuated due to the changes of the updated load forecast and could be even lower than the actual peak of previous power use. In contrast, the adaptive optimal monthly limiting threshold remained stable for the whole month. This is because the peak power use occurred on the first workday and the adaptive optimal limiting threshold was not allowed to be less than the actual peak power use.

Figure 7.18(B) shows the power demand profile when implementing demand limiting using the developed adaptive optimal threshold resetting scheme. Figure 7.18(C) shows the demand reduction when implementing the developed scheme for monthly peak demand limiting. During the demand limiting periods, the active thermal storage was discharged to restrict peak demands over the adaptive optimal monthly limiting threshold. After implementing demand limiting using the developed scheme in Dec/2017, the achieved monthly peak demand reduction was 132 kVA, 9.3% of the actual monthly peak demand (1419 kVA). That contributed to the actual monthly net cost saving of 14,769 HKD (3.07% of the actual electricity charge of that month).

7.2.3 Summer case study and test results

In the summer case study, the datasets during the office hours in Jun/2018 are used for the validation test. Similar to the winter case, the 9-day weather forecast data reported/updated daily by the HKO in June are recorded each day. They are used to forecast/update probabilistic demand profiles to further identify/update the optimal monthly limiting threshold. In the following subsections, the first workday in June is selected to illustrate the identification procedure of the optimal monthly limiting threshold. This procedure is conducted repeatedly to obtain/update the

monthly limiting threshold in an adaptive manner for demand limiting control in the following days of the month.

7.2.3.1 Optimal monthly limiting threshold identification on the first workday of June

On the first workday of June (before office hour, e.g., 9:00 AM), the probabilistic demand profiles during office hours in the following 9 days were forecasted in advance, as shown in Figure 7.19. Different confidence intervals of the probabilistic demand profiles are shown in the figure, such as 20%, 40%, 60% and 99%. In addition, the range of the tested thresholds was identified as [1822 kVA, 1973 kVA].

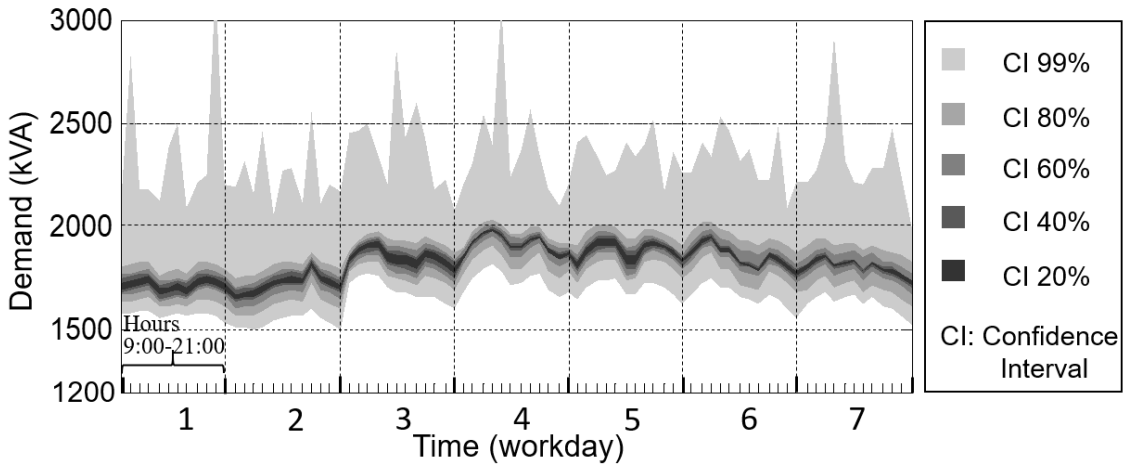

Figure 7.19. Probabilistic demand profiles during office hours between 01/Jun and 09/Jun/2018 forecasted in the early morning of 01/Jun.

Based on the forecasted probabilistic demand profiles, the monthly probabilities of each scenario using particular thresholds were estimated in the same way as that in the winter case, as shown in Figure 7.20. It can be seen that all the monthly success probabilities accounted for over 80%,

the monthly failure probabilities varied between 7% and 19%, and the monthly nonactivation probabilities varied between 0% and 12%.

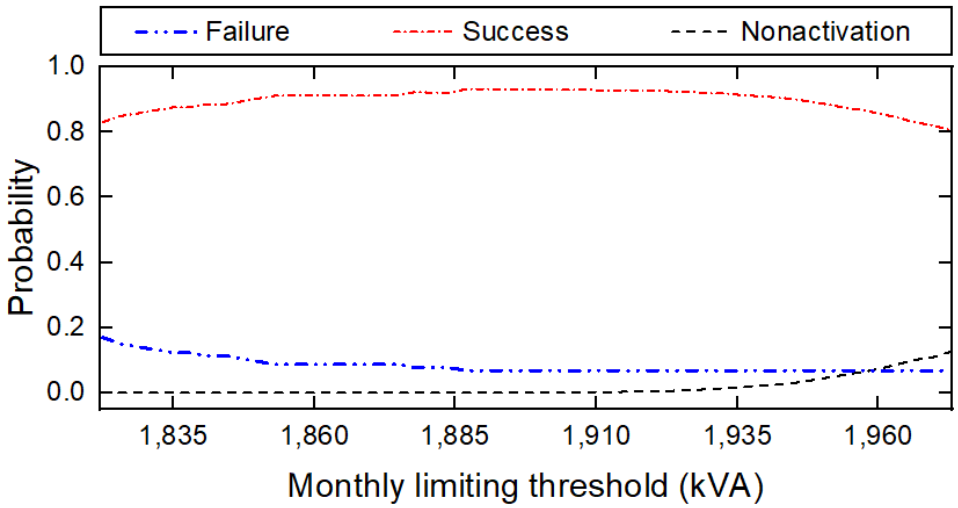

Figure 7.20. Quantified probabilities of three scenarios when implementing demand limiting using different thresholds on the first workday of Jun/2018.

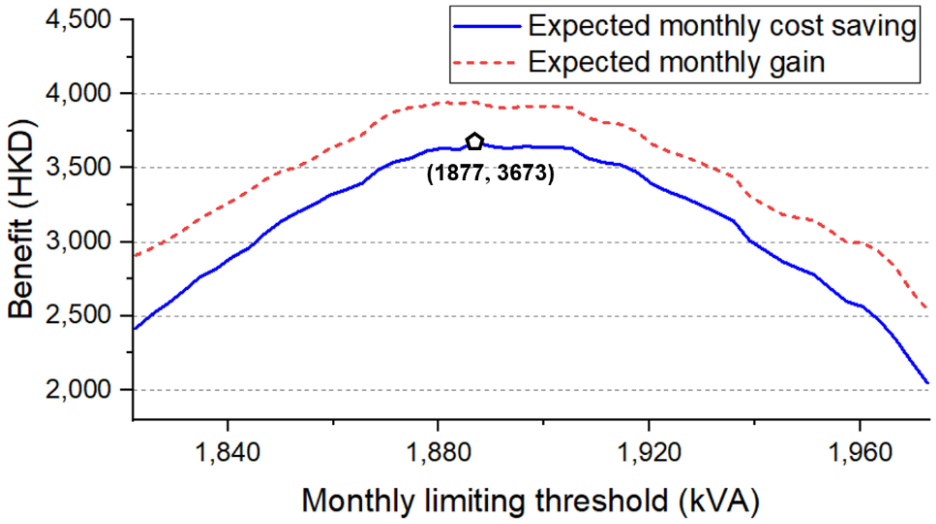

Figure 7.21. Expected monthly cost savings and expected monthly gains when implementing demand limiting using different thresholds on the first workday of Jun/2018.

Based on the quantified monthly probabilities at different thresholds, the expected monthly cost savings and the expected monthly gains were quantified, as shown in Figure 7.21. It can be seen that the optimal monthly limiting threshold was identified of 1877 kVA, and the corresponding cost saving was 3673 HKD.

7.2.3.2 Validation of the developed scheme for monthly peak demand limiting in June

Similarly, on each of the following workdays, the identification procedure using the optimal threshold resetting scheme is conducted repeatedly to obtain/update the optimal limiting threshold. In addition, the ideal demand limiting control is conducted on the basis of the identified adaptive optimal limiting threshold. Figure 7.22 shows the validation test results of demand limiting using the adaptive optimal threshold resetting scheme in Jun/2018.

Figure 7.22(A) shows the power demand profile of the Phase 7 building, without implementing demand limiting, measured in Jun/2018. It can be seen the monthly peak demand occurred on the sixteenth workday. Two adaptive thresholds are also included. One is the adaptive optimal monthly limiting threshold, and the other is the adaptive monthly limiting threshold without considering the actual peak of previous power use. On the first three workdays, both thresholds were updated in the same trend since they were determined on the predicted power demand profile only as the actual peak of previous power use was below the thresholds.

Figure 7.22(B) shows the power demand profile when implementing demand limiting using the developed adaptive optimal threshold resetting scheme. Figure 7.22(C) shows the demand

reduction when implementing the developed scheme for monthly peak demand limiting. During the demand limiting periods, the active thermal storage was discharged to restrict peak demands over the adaptive optimal monthly limiting threshold. After implementing demand limiting using the developed scheme in Jun/2018, the achieved monthly peak demand reduction was 278 kVA, 13.0% of the actual monthly peak demand (2135 kVA). That contributed to the actual monthly net cost saving of 20,686 HKD (1.99% of the actual electricity charge of that month).

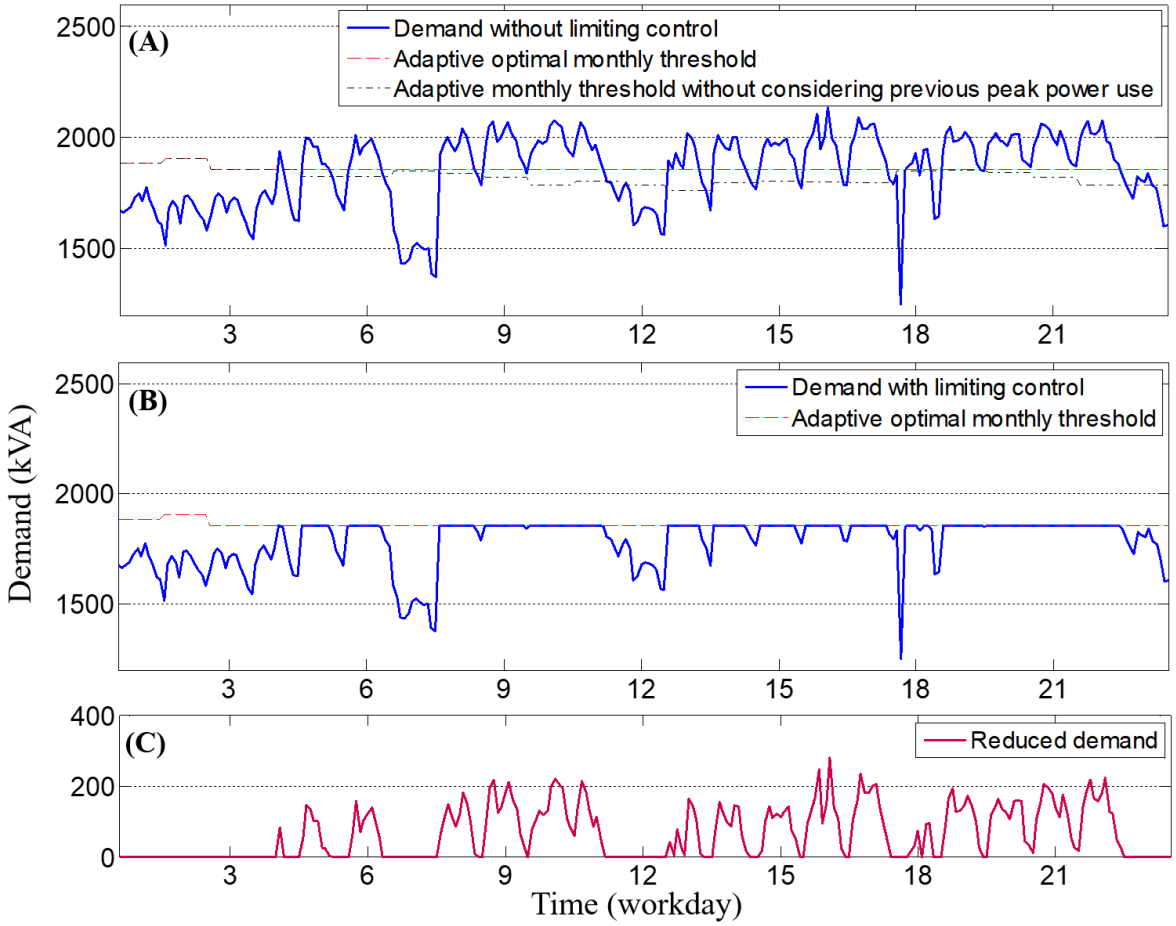

Figure 7.22. Building demand profiles in Jun/2018 under different situations: (A) no demand limiting; (B) demand limiting using the developed scheme. (C) Actual demand reduction using the developed scheme.

7.2.4 Results of sensitivity analysis

To further study the performance of demand limiting using the developed scheme, sensitivity analysis is conducted on the effects of means of demand limiting and electricity charge tariff on the monthly economic benefit. The means of demand limiting could be any of the existing building storage systems, e.g., phase change material, ice storage, etc. Their demand limiting capacity and the unit price of limiting effort are abstracted to quantify the economic benefit of demand limiting. As for the electricity charge tariff, there are different options in different regions and countries. In this section, the summer month (i.e., Jun/2018) is chosen to conduct sensitivity analysis and the parameters used in validation case studies are used as the baseline case. Tables (7.7-7.9) show the results of sensitivity analysis using the three parameters on the cost-benefit metrics of demand limiting (i.e., monthly cost saving, monthly accumulated limiting effort, peak demand reduction and percentage of peak demand reduction).

Table 7.7 shows how the unit price of limiting effort affects the cost-benefit metrics of demand limiting when the developed scheme is used. It can be seen that both the monthly cost saving and the monthly accumulated limiting effort decrease with the increase of the unit price of limiting effort. In addition, the less the unit price of limiting effort is, the more the monthly peak demand reduction will be.

Table 7.7. Effects of the unit price of limiting effort on the cost-benefit metrics of demand limiting using the developed scheme

Unit price of limiting effort (HKD/kWh)	Monthly cost saving (HKD)	Monthly accumulated limiting effort (kWh)	Peak reduction (kVA)	Percentage of peak reduction
0.24 (baseline)	20,686	45,107	278	13.0%
0.32	18,894	43,830	274	12.8%
0.4	14,718	39,149	253	11.9%
0.48	12,929	36,351	253	11.9%
0.56	11,750	25,396	216	10.1%
0.64	11,274	20,669	204	9.6%

Table 7.8 shows how the unit price of electricity demand affects the cost-benefit metrics of demand limiting when the developed scheme is used. It can be seen that the monthly cost saving decreases with the decrease of the unit price of electricity demand. In addition, the less the unit price of electricity demand is, the less the monthly accumulated limiting effort and the monthly peak demand reduction and will be.

Table 7.8. Effects of the unit price of electricity demand on the cost-benefit metrics of demand limiting using the developed scheme

Unit price of electricity demand (HKD/kVA)	Monthly cost saving (HKD)	Monthly accumulated limiting effort (kWh)	Peak reduction (kVA)	Percentage of peak reduction
120 (baseline)	20,686	45,107	278	13.0%
110	17,909	45,107	278	13.0%
100	15,203	41,322	268	12.5%
90	12,574	40,089	264	12.4%
80	9,814	37,278	253	11.9%
70	7,541	36,355	253	11.9%

Table 7.9 shows how the limiting capacity affects the cost-benefit metrics of demand limiting when the developed scheme is used. It can be seen that the monthly cost saving decreases with the decrease of the unit price of electricity demand in most cases. In addition, the less the limiting capacity was, the less the monthly accumulated limiting effort and the monthly peak demand reduction and would be. When a storage of very small limiting capacity is used for demand limiting, the limiting capacity could run out, and the limiting threshold might be forced to the actual peak power use. In this situation, little monthly cost saving and peak demand reduction

could be achieved, as the last case shown in Table 7.9 (the marked italic row).

Table 7.9. Effects of the limiting capacity on the cost-benefit metrics of demand limiting using the developed scheme

Limiting capacity (kWh)	Monthly cost saving (HKD)	Monthly accumulated limiting effort (kWh)	Peak reduction (kVA)	Percentage of peak reduction
4,763 (baseline)	20,686	45,107	278	13.0%
4,250	17,113	32,308	218	10.2%
3,750	13,079	15,860	146	6.8%
3,250	13,404	14,698	146	6.8%
2,750	11,237	10,437	118	5.5%
2,250	*6,243*	*6,845*	*68*	*3.2%*

7.3 Validation of proactive-adaptive demand limiting control scheme

In the validation of the proactive-adaptive demand limiting control scheme for monthly peak demand limiting, a small-scale active thermal storage with ideal control is adopted. The historical electrical load data of the Phase 7 building in winter and summer (i.e., Dec/2017 and June/2018) are collected and used at the 1-minute interval. And in each month, the 9-day weather forecast data reported daily by the Hong Kong Observatory (HKO) are recorded daily.

7.3.1 Identification of parameters of optimal threshold resetting scheme for proactive-adaptive demand limiting control

Based on the sensitivity analysis of the main parameters in the optimal threshold resetting scheme (i.e., *a, b, Cap*), a particular set of these three parameters are selected for testing the proactive-adaptive demand limiting control scheme, i.e., a=70 HKD/kVA, b=0.32 HKD/kWh, Cap=2250 kWh. This selection attempts to explore online optimal limiting threshold resetting when only an active storage of relatively small capacity is available, which has a high risk of failure in peak demand limiting.

7.3.2 Winter case study and test results

In the winter case study, the datasets during the office hours in Dec/2017 were used for the validation test. The 9-day weather forecast data reported/updated daily by the HKO in December were recorded each day. They were used to forecast/update the 9-day probabilistic demand profiles each day, which were then used to identify/update the optimal monthly limiting threshold. In the real-time demand limiting control, the developed proactive-adaptive monthly peak demand limiting strategy (i.e., the adaptive optimal monthly peak demand limiting strategy with both the optimal threshold resetting scheme and proactive-adaptive demand limiting control) is validated and compared with the baseline demand limiting strategy (i.e., the adaptive optimal monthly peak demand limiting strategy only with the optimal threshold resetting scheme but no proactive-adaptive demand limiting control).

7.3.2.1 Validation of the developed strategy for online demand limiting in winter

Validation tests of demand limiting using both the baseline demand limiting strategy and the developed online monthly peak demand limiting strategy were conducted, as shown in Figure 7.23. Figure 7.23(A) shows the real-time demand profile of the building, without implementing demand limiting, measured in Dec/2017. It can be seen that the effective monthly peak billing demand (i.e., maximum 30-min average demand) occurred as 1419 kVA on the 1st workday, and some real-time higher strikes of very short time occurred on the 3rd and 9th workdays. Note, in Hong Kong, the peak demand charge is based on the maximum 30-min average demand (kVA) over a month.

Figure 7.23(B) shows the power demand profile when implementing demand limiting using the baseline demand limiting strategy. During the demand limiting periods, the active thermal storage was discharged to restrict peak demands over the adaptive optimal monthly limiting threshold. It can be seen that the adaptive monthly threshold was updated twice at the end of the 2nd and 11th workdays. As the storage capacity is sufficient for demand limiting control in the winter month, no failure of demand limiting occurred.

Figure 7.23(C) shows the power demand profile when implementing demand limiting using the developed proactive-adaptive monthly peak demand limiting strategy. It can be seen that the adaptive monthly threshold appeared the same as that in Figure 7.23(B). This is because the storage capacity is sufficient for demand limiting control and the online threshold reset action is not activated in the whole month.

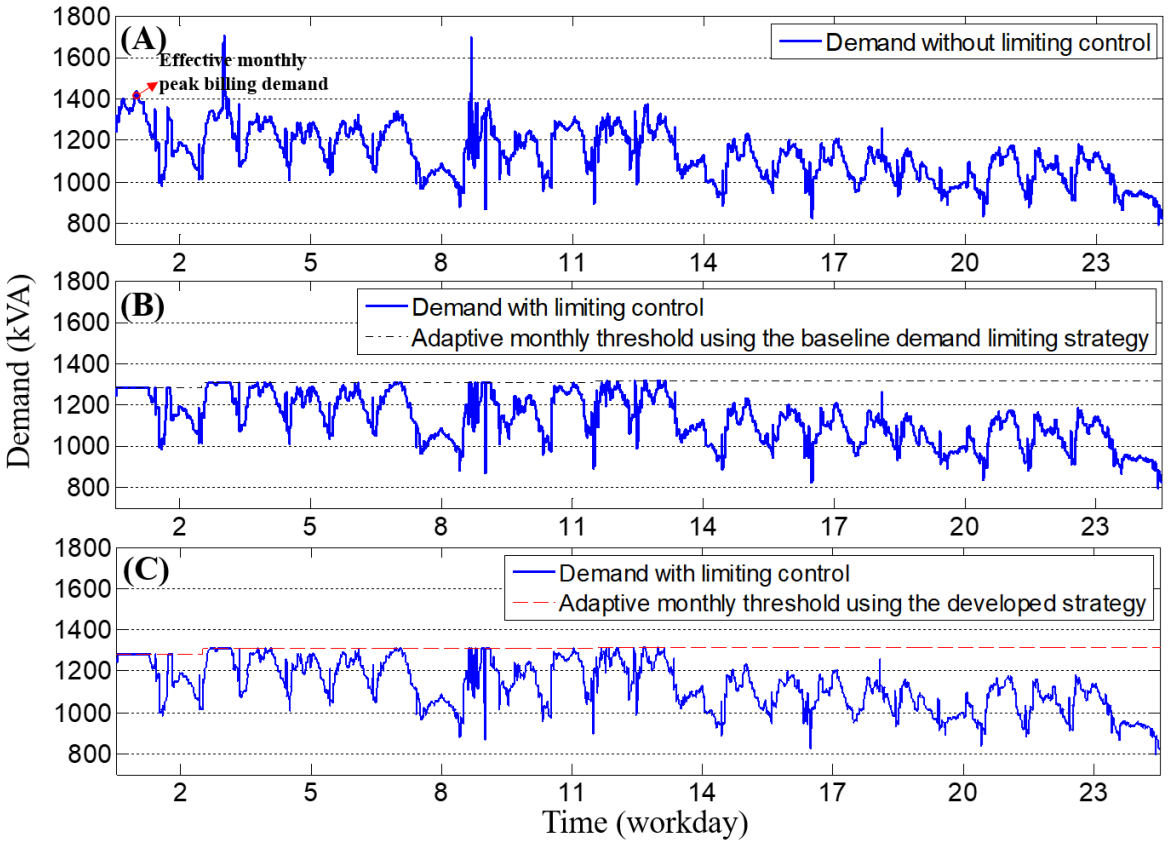

Figure 7.23. Real-time building demand profiles in Dec/2017 under different situations: (A) no demand limiting; (B) demand limiting using the baseline demand limiting strategy; (C) demand limiting using the developed strategy.

7.3.2.2 Comparison between cost-benefit metrics of the two demand limiting strategies in winter

After implementing demand limiting using the above two strategies in Dec/2017, some cost-benefit metrics of the monthly peak demand limiting are listed in Table 7.10. It can be seen that demand limiting using both strategies can achieve the same considerable monthly peak demand reduction. The achieved monthly peak reduction was 103 kVA, 7.3% of the actual monthly peak demand (1419 kVA). That contributes to the monthly net cost saving of 6203 HKD.

Table 7.10. Cost-benefit metrics of demand limiting using different strategies in Dec/2017

Demand limiting strategy	Peak demand (kVA)	Peak reduction (kVA)	Peak saving percentage	Accumulated thermal energy use (kWh)	Total cost saving (HKD)
No demand limiting	1419	0	0	0	0
Baseline strategy	1316	103	7.3%	3147	6203
Developed strategy	1316	103	7.3%	3147	6203

7.3.3 Summer case study and test results

In the summer case study, the datasets during the office hours in Jun/2018 were used for the validation test. The 9-day weather forecast data reported/updated daily by the HKO in June were recorded each day. They were used to forecast/update the 9-day probabilistic demand profiles each day, which were then used to identify/update the optimal monthly limiting threshold. In the real-time demand limiting control, the developed proactive-adaptive monthly peak demand limiting strategy is validated and compared with the baseline demand limiting strategy as well. In addition, one specific workday is selected to illustrate how the proactive-adaptive demand limiting control scheme works before using up the storage capacity.

7.3.3.1 Validation of the developed strategy for online demand limiting in summer

Validation tests of demand limiting using both the baseline demand limiting strategy and the

developed online monthly peak demand limiting strategy were conducted, as shown in Figure 7.24. Figure 7.24(A) shows the real-time demand profile of the building, without implementing demand limiting, measured in Jun/2018. It can be seen that the effective monthly peak billing demand occurred as 2135 kVA on the 16th workday, and some real-time higher strikes of very short time occurred on the 10th, 13th and 16th workdays.

Figure 7.24(B) shows the power demand profile when implementing demand limiting using the baseline demand limiting strategy. On the first three workdays, the adaptive monthly threshold using the baseline demand limiting strategy was updated and determined according to the predicted power demand profile only, as the peak of previous power use was below the thresholds. From the 4th to 8th workday, the threshold was updated not only according to the updated power demand profile but also no less than the actual peak of previous power uses. On the 9th workday, the threshold rose suddenly and straightly at about 17:00 PM due to running out of the limiting capacity. After the 9th workday, the threshold remained flat due to the sufficient storage capacity for demand limiting control under the new limiting threshold.

Figure 7.24(C) shows the power demand profile when implementing demand limiting using the developed proactive-adaptive monthly peak demand limiting strategy. It can be seen that the adaptive monthly threshold before the 9th workday appeared the same as that in Figure 7.24(B). On the 9th workday, the threshold rose gradually and slightly before using up the limiting capacity. After the 9th workday, the threshold remained flat due to the sufficient storage capacity for demand limiting control.

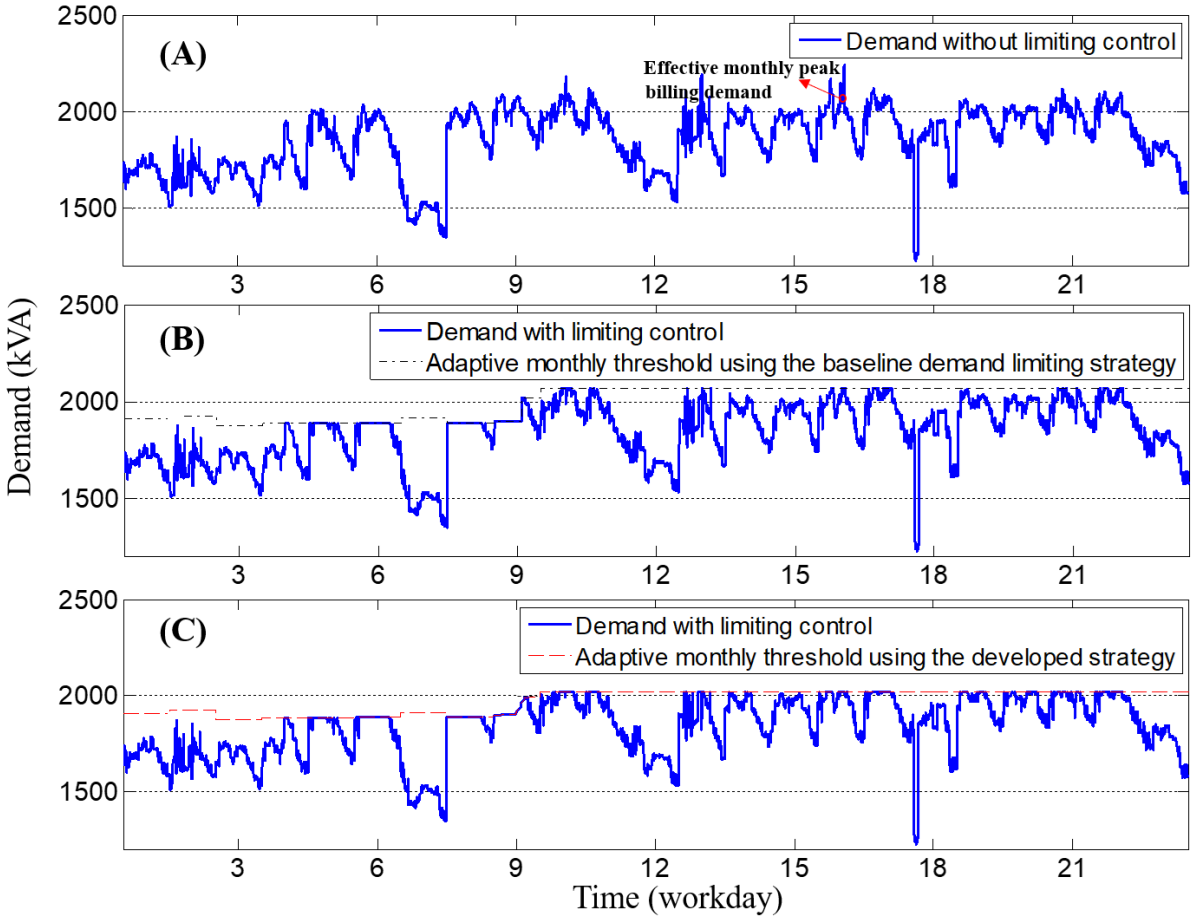

Figure 7.24. Real-time building demand profiles in Jun/2018 under different situations: (A) no demand limiting; (B) demand limiting using the baseline demand limiting strategy; (C) demand limiting using the developed strategy.

7.3.3.2 Comparison between cost-benefit metrics of the two demand limiting strategies in summer

After implementing the above two demand limiting strategies in Jun/2018, some cost-benefit metrics of the monthly peak demand limiting are listed in Table 7.11. It can be seen that demand limiting using both strategies can achieve considerable monthly peak reductions. In the validation test using the baseline demand limiting strategy, the monthly peak reduction achieved

was 146 kVA (6.8%). Moreover, considering the offset of the overall limiting effort cost using the thermal storage, the monthly net cost saving achieved was 4550 HKD. In the validation test using the developed strategy, the monthly peak reduction achieved was 184 kVA (8.6%). Similarly, when the offset of the overall limiting effort cost using the thermal storage is considered, the monthly net cost saving achieved was 7236 HKD. Comparing these two strategies, it can be seen that the proposed strategy achieved better performance, with 26% more peak demand reduction than that from the baseline demand limiting strategy.

Table 7.11. Cost-benefit metrics of demand limiting using different strategies in Jun/2018

Demand limiting strategy	Peak demand (kVA)	Peak reduction (kVA)	Peak saving percentage	Accumulated thermal energy use (kWh)	Total cost saving (HKD)
No demand limiting	2135	0	0	0	0
Baseline strategy	1989	146	6.8%	11235	4550
Developed strategy	1951	184	8.6%	17719	7236

7.3.3.3 Validation of the developed strategy for online demand limiting on a summer workday

11/Jun/2018 (i.e., the 9th workday in June) is selected to illustrate the mechanism of the developed proactive-adaptive demand limiting control scheme before using up the limiting capacity. On the 9th workday of June (before office hour, e.g., 9:00 AM), the probabilistic demand profiles during office hours in the following 9 days were forecasted in advance, as shown in Figure 7.25. Different confidence intervals of the forecasted probabilistic demand profiles are

shown in the figure, such as 20%, 40%, 60% and 99%.

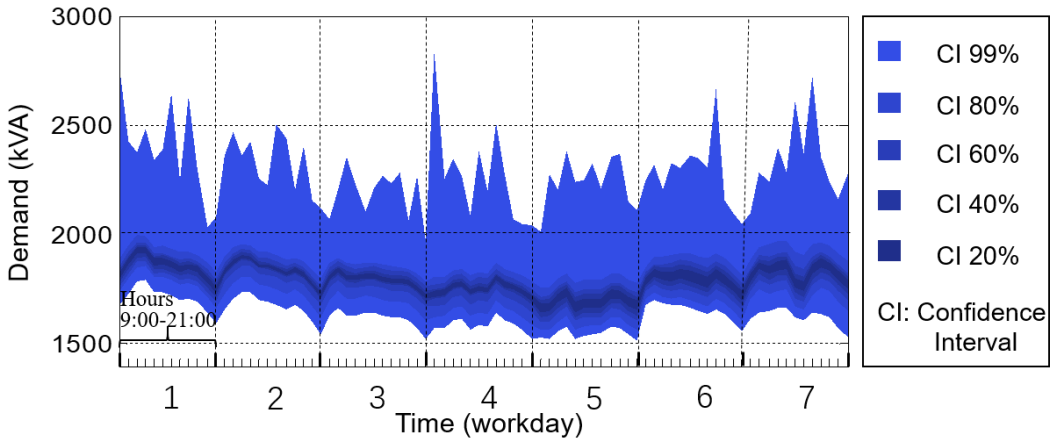

Figure 7.25. Probabilistic demand profiles during office hours between 11/June and 19/Jun/2018 forecasted in the early morning of 11/June.

Based on the forecasted demand profiles and the actual peak power use, the optimal limiting threshold was updated on the 9th workday. Then specific validation tests of demand limiting using both the developed strategy and the baseline demand limiting strategy were conducted based on this threshold, as shown in Figure 7.26.

Figure 7.26(A) shows the real-time demand profile of the building, without implementing demand limiting, measured on 11/June. It can be seen that peak demands occurred in the periods of 11:00-12:00 AM and 15:00-16:00 PM on this day.

Figure 7.26(B) shows the power demand profile when implementing demand limiting using the baseline demand limiting strategy. It can be seen that most of the peak demands from 9:10 AM to 17:00 PM were limited by discharging the active thermal storage when actual demands exceeded the adaptive monthly threshold. However, the storage capacity ran out at 17:00 PM and

the threshold was immediately forced to the actual peak power use at this moment.

Figure 7.26(C) shows the power demand profile when implementing demand limiting using the developed proactive-adaptive monthly peak demand limiting strategy. It can be seen that, before 16:00 PM, demand limiting control was conducted in the same way as that using the baseline demand limiting strategy. After 16:00 PM, the limiting threshold was gradually and slightly updated before using up the storage capacity at 18:00 PM.

After demand limiting using the baseline demand limiting strategy on 11/Jun, the daily peak reduction achieved was 86 kVA (4.1% of the daily peak demand). In contrast, after demand limiting using the developed strategy on 11/Jun, the daily peak reduction achieved was 124 kVA (6.0% of the daily peak demand). In terms of the daily accumulated limiting effort for demand limiting on this day, the entire storage capacity (i.e., 2250 kWh) was used in both strategies. It can be seen that the developed strategy is capable of achieving more peak demand reduction than the baseline demand limiting strategy in the cases when the storage capacity is insufficient.

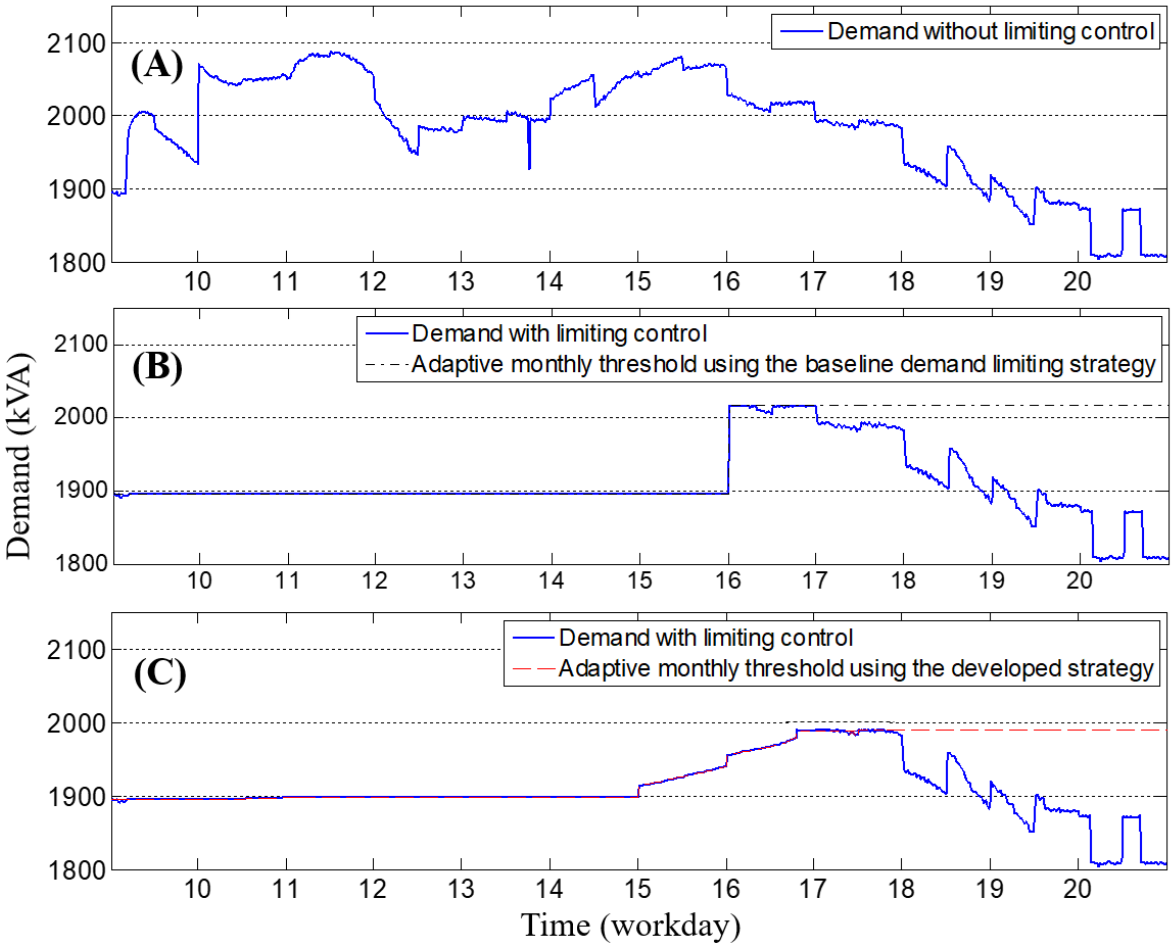

Figure 7.26. Real-time building demand profiles on 11/June under different situations: (A) no demand limiting; (B) demand limiting using the baseline demand limiting strategy; (C) demand limiting using the developed strategy.

7.4 Summary

This chapter presents the validation of the probabilistic load forecasting model, the optimal threshold resetting scheme and the proactive-adaptive demand limiting control scheme. The major conclusive remarks of the tests are as follows.

i. The ANN model for deterministic normal load forecasting was capable of obtaining results with satisfactory accuracy with the average MAPE of 5.0%, the average MAE of 77.8 kVA and the average RMSE of 108 kVA.

ii. The probabilistic occurrence model of the peak abnormal differential (PAD) load shows a good performance in forecasting the relative PAD load occurrence frequency. Moreover, the probabilistic magnitude model of the PAD load was fitted on the basis of four commonly-used probability density distributions, among which the Lognormal distribution shows the best fitness of the observed PAD load data. The probabilistic model of the magnitude well forecasted the magnitudes with the Kolmogorov-Smirnov error of 0.09.

iii. All the three real-time cases achieve acceptable accuracy, and the probabilistic normal load forecasts based on the most updated (i.e., one-day-ahead) weather forecasts were the most accurate and certain (minimum bandwidth).

iv. In a typical winter month, monthly demand limiting control using the developed optimal threshold resetting scheme achieved a considerable peak demand reduction under load uncertainty, i.e., 9.3% of the actual monthly peak demand (1419 kVA). That contributed to the monthly net cost saving of 14,769 HKD, 3.07% of the actual electricity charge of that month.

v. In a typical summer month, monthly demand limiting control using the developed optimal threshold resetting scheme also achieved a considerable peak demand reduction under load

uncertainty, i.e., 13.0% of the actual monthly peak demand (2135 kVA). That contributed to the monthly net cost saving of 20,686 HKD, 1.99% of the actual electricity charge of that month.

vi. Results of the sensitivity analysis show that the monthly cost saving decreases with the increase of the unit price of limiting effort or the decrease of the unit price of electricity demand. With the decrease of limiting capacity, the monthly cost saving decreased in most cases. It is worthwhile to identify the optimal (i.e., cost-effective) storage capacity of a building based on the actual load characteristics and the potential cost benefits.

vii. In a typical winter month, monthly demand limiting with the developed proactive-adaptive control scheme achieved a significant peak demand reduction under load uncertainty when only a small-scale storage is available, i.e., 7.3% of the actual monthly peak demand (1419 kVA).

viii. In a typical summer month, monthly demand limiting with the developed proactive-adaptive control scheme also achieved a significant peak demand reduction under load uncertainty when only a small-scale storage is available, i.e., 8.6% of the actual monthly peak demand (2135 kVA). It showed better performance (i.e., 26% more peak demand reduction) compared to demand limiting without the proactive-adaptive control scheme.

CHAPTER 8 CONCLUSIONS AND RECOMMENDATIONS

This PhD study develops an adaptive optimal monthly peak demand limiting strategy to reduce building peak demands over a month (or a billing cycle) considering load uncertainties, which includes the following three major components. The building load model forecasts the probabilistic loads of buildings, which considers weather forecasting uncertainty and uncertain peak loads. The optimal threshold resetting scheme identifies an adaptive optimal monthly limiting threshold and quantifies the uncertain economic benefits and the probability of success of implementing a demand limiting control. The proactive-adaptive demand limiting control scheme conducts online demand limiting control proactively before using up the storage capacity when small-scale thermal storages are available. An educational building in Hong Kong is selected for case studies to validate the developed adaptive optimal monthly peak demand limiting strategy.

In this chapter, the main contributions of this thesis are summarized in Section 8.1. Section 8.2 presents the conclusions based on the validation tests. Recommendations for future work are also presented in Section 8.3.

8.1 Summary of main contributions

The present study aims at developing an adaptive optimal monthly peak building demand limiting strategy considering load uncertainty. Currently, there are very few studies on peak building demand limiting over a billing cycle (typically a month), and even fewer when

considering load uncertainties. Main contributions in this study are summarized as follows:

i. A probabilistic load forecasting model is developed for real-time electric load forecasting of individual buildings considering the real-time weather forecasting uncertainty and uncertain peak load, which is vital for adaptive online decision-making and is essential for the robust control of building energy systems.

ii. Statistic models for probabilistic abnormal peak load forecasting (i.e., the occurrence and magnitude models of the abnormal peak load) are developed to forecast the uncertain peak load, which are applicable for predicting the abnormal peak loads with significant fluctuations. Furthermore, a hybrid method, integrating the linear regression method and the local outlier factor method, is developed to decompose the load measurement dataset, which shows better decomposition results than using either of them.

iii. A novel optimal threshold resetting scheme is developed for monthly peak demand limiting considering load uncertainty. This scheme is developed to identify and update the optimal demand limiting threshold under load uncertainty in short/medium period, i.e., one day to a month, which can be used for conducting adaptive peak demand limiting over a billing cycle.

iv. Uncertain economic benefits and the probability of success of implementing a demand limiting control are quantified over the billing cycle of a month. This uncertainty quantification is meaningful and very helpful for decision-makers to conduct peak demand limiting control, particularly during a median period (i.e., a week to a month) according to

their risk attitude.

v. A new proactive-adaptive demand limiting control scheme is developed for monthly peak demand limiting considering load uncertainty. This scheme is capable of online updating the limiting threshold proactively before using up the storage capacity when only small-scale storages are available.

8.2 Conclusions

The probabilistic load forecasting model

The developed probabilistic load forecasting model can successfully forecast the hourly probabilistic load, including the probabilistic normal load and the probabilistic occurrence and magnitude of the abnormal peak load, with satisfactory accuracy.

Validation results show that the ANN model for deterministic normal load forecasting was capable of obtaining results with satisfactory accuracy with the average MAPE of 5.0%, the average MAE of 77.8 kVA and the average RMSE of 108 kVA. Besides, the probabilistic occurrence model of PAD load shows a good performance in forecasting the relative PAD load occurrence frequency. The probabilistic magnitude model of the PAD load was fit on the basis of four commonly-used probability density distributions. Among them, the Lognormal distribution showed the best fitness of the observed PAD load data. The probabilistic model of the magnitude well forecasted the magnitudes with the Kolmogorov-Smirnov error of 0.09.

The optimal threshold resetting scheme

The developed optimal threshold resetting scheme is capable of identifying the optimal monthly limiting threshold in an adaptive manner. The probabilistic economic benefits and the probabilities of nonactivation/success/failure of a demand limiting control over the billing cycle are quantified. This scheme for monthly peak demand limiting can successfully reduce the monthly peak demand and achieve a considerable monthly net cost saving under load uncertainty.

Validation results show that the developed scheme for monthly peak demand limiting can achieve a considerable peak demand reduction under load uncertainty in different seasons. In a winter month, monthly demand limiting with the developed scheme achieved a 9.3% reduction of the actual monthly peak demand (1419 kVA). That contributed to the monthly net cost saving of 14,769 HKD, 3.07% of the actual electricity charge of that month. In a summer month, monthly demand limiting with the developed scheme achieved 13.0% of the actual monthly peak demand (2135 kVA). That contributed to the monthly net cost saving of 20,686 HKD, 1.99% of the actual electricity charge of that month.

The proactive-adaptive demand limiting control scheme

The developed proactive-adaptive demand limiting control scheme can successfully reduce the monthly peak demand and achieve a considerable monthly net cost saving under load uncertainty. The developed scheme is capable of proactively resetting the online limiting threshold in advance of using up the storage capacity, even when only a small active thermal storage is available.

Validation results show that the monthly demand limiting with proactive-adaptive control scheme can achieve a significant peak demand reduction under load uncertainty in different seasons. In a winter month, monthly demand limiting with the proactive-adaptive control scheme achieves 7.3% of the actual monthly peak demand (1419 kVA). In a summer month, monthly demand limiting with the proactive-adaptive control scheme achieves 8.6% of the actual monthly peak demand (2135 kVA). It shows better performance (i.e., 26% more peak demand reduction) compared to monthly demand limiting without the proactive-adaptive control scheme.

8.3 Recommendations for future work

Major efforts of this PhD study have been made on the development of probabilistic load forecasting model for buildings and adaptive monthly peak building demand limiting strategy. It would be very desirable and valuable to make further efforts on the following aspects.

i. The probabilistic normal load forecasting accuracy is affected by the probabilistic weather forecasting accuracy from the HKO. Comparison studies for the proposed probabilistic load forecasting approach are expectable and could be conducted in the near future when studies using standard datasets of compatible format (i.e., the probabilistic weather forecast is included) are available.

ii. The developed probabilistic load forecasting model is capable of quantifying the probability of building electric load larger than a certain value at a certain hour, or even on one day or one week. Besides the application of peak demand limiting under load uncertainty, there two

potential issues to be addressed. The first one is for the day-ahead forecasting of electricity price for the smart gird. The peak load forecast is essential for determining the day-ahead dynamic pricing or critical peak pricing because the peak load is a major concern of a power grid. The second one is for the optimal operation of renewable energy resources. The proposed probabilistic forecasting method can contribute to the optimization of the decisions in the operation of renewable resources under load uncertainties (e.g., the charge or discharge control of electric vehicles).

iii. In this study, only the commonly-used expectation metric is used in the optimal threshold resetting scheme considering uncertainty. Different decision-making criteria can be further explored for the adaptive monthly peak demand limiting control under load uncertainty according to the decision-makers' risk attitude.

iv. This study is validated using real site measurements. In-situ tests can be further conducted by applying the adaptive optimal monthly peak demand limiting strategy with active thermal storages into practical BMS systems.

REFERENCES

A. Ben-Tal, L. El Ghaoui, A. Nemirovski. (2009). Robust optimization (Vol. 28): Princeton University Press.

A. Celik, T. Muneer. (2013). Neural network based method for conversion of solar radiation data. Energy Conversion and Management;67:117-124.

A. Clauset, C. Shalizi, M. Newman. (2009). Power-law distributions in empirical data. SIAM review;51:661-703.

A. Gomes, C. Antunes, A. Martins. (2007). A multiple objective approach to direct load control using an interactive evolutionary algorithm. IEEE Transactions on Power Systems;22:1004-1011.

A. Hajiah, M. Krarti. (2012). Optimal control of building storage systems using both ice storage and thermal mass–Part I: Simulation environment. Energy Conversion and Management;64:499-508.

A. Rohatgi. WebPlotDigitizer. Available: https://automeris.io/WebPlotDigitizer/

A. Soroudi, T. Amraee. (2013). Decision making under uncertainty in energy systems: State of the art. Renewable and sustainable energy reviews;28:376-384.

A. Thiele, T. Terry, M. Epelman. (2009). Robust linear optimization with recourse. Rapport technique;4-37.

A. Waqas, Z. Din. (2013). Phase change material (PCM) storage for free cooling of

buildings—a review. Renewable and sustainable energy reviews;18:607-625.

B. Chen, M. Chang. (2004). Load forecasting using support vector machines: A study on EUNITE competition 2001. IEEE Transactions on Power Systems;19:1821-1830.

B. Cui, S. Wang, Y. Sun. (2014). Life-cycle cost benefit analysis and optimal design of small scale active storage system for building demand limiting. Energy;73:787-800.

B. Diaconu. (2011). Thermal energy savings in buildings with PCM-enhanced envelope: influence of occupancy pattern and ventilation. Energy and buildings;43:101-107.

B. Liu, J. Nowotarski, T. Hong, R. Weron. (2017). Probabilistic load forecasting via quantile regression averaging on sister forecasts. IEEE Transactions on Smart Grid;8:730-737.

B. Silverman. (1986). Density estimation for statistics and data analysis (Vol. 26): CRC press.

B. Walsh, S. Murray, D. O'Sullivan. (2013). Free-cooling thermal energy storage using phase change materials in an evaporative cooling system. Applied Thermal Engineering;59:618-626.

B. Worton. (1989). Kernel methods for estimating the utilization distribution in home‐range studies. Ecology;70:164-168.

C. Renno, F. Petito, A. Gatto. (2016). ANN model for predicting the direct normal irradiance and the global radiation for a solar application to a residential building. Journal of Cleaner Production;135:1298-1316.

C. Triki, A. Violi. (2009). Dynamic pricing of electricity in retail markets. 4OR: A Quarterly Journal of Operations Research;7:21-36.

C. Yan, S. Wang, C. Fan, F. Xiao. (2017). Retrofitting building fire service water tanks as chilled water storage for power demand limiting. Building Services Engineering Research and Technology;38:47-63.

C. Yan, S. Wang, F. Xiao. (2012). A simplified energy performance assessment method for existing buildings based on energy bill disaggregation. Energy and buildings;55:563-574.

D. Bertsimas, A. Thiele. (2006). Robust and data-driven optimization: modern decision making under uncertainty. Models, Methods, and Applications for Innovative Decision Making: 95-122, INFORMS.

D. Bertsimas, M. Sim. (2004). The price of robustness. Operations research;52:35-53.

D. Gao, Y. Sun, Y. Lu. (2015). A robust demand response control of commercial buildings for smart grid under load prediction uncertainty. Energy;93:275-283.

D. Gao, Y. Sun. (2016). A GA-based coordinated demand response control for building group level peak demand limiting with benefits to grid power balance. Energy and buildings;110:31-40.

D. Kececioglu. (2002). Reliability engineering handbook (Vol. 1): DEStech Publications, Inc.

D. Massie, J. Kreider, P. Curtiss. (2004). Neural Network Optimal Controller for

Commercial Ice Thermal Storage Systems. ASHRAE Transactions;110.

D. Rumelhart, G. Hinton, R. Williams. (1985). Learning internal representations by error propagation. California Univ San Diego La Jolla Inst for Cognitive Science.

D. Ürge-Vorsatz, L. Cabeza, S. Serrano, C. Barreneche, K. Petrichenko. (2015). Heating and cooling energy trends and drivers in buildings. Renewable and sustainable energy reviews;41:85-98.

D. van der Meer, M. Shepero, A. Svensson, J. Widén, J. Munkhammar. (2018). Probabilistic forecasting of electricity consumption, photovoltaic power generation and net demand of an individual building using Gaussian Processes. Applied Energy;213:195-207.

E. Rajabally, P. Sen, S. Whittle. (2002). A methodology for model dependability assessment. Paper presented at the Proceedings of the Engineering Design Conference.

Electrical and Mechanical Servicess Department. (2018). Hong Kong Energy End-use Data.

F. Sehar, S. Rahman, M. Pipattanasomporn. (2012). Impacts of ice storage on electrical energy consumptions in office buildings. Energy and buildings;51:255-262.

F. Zhao, J. Wang, V. Koritarov, G. Augenbroe. (2010). Agent-based modeling of interaction between commercial building stocks and power grid. Paper presented at the Innovative Technologies for an Efficient and Reliable Electricity Supply (CITRES), 2010 IEEE Conference on.

G. Henze, C. Felsmann, G. Knabe. (2004). Evaluation of optimal control for active and

passive building thermal storage. International Journal of Thermal Sciences;43:173-183.

G. Henze, R. Dodier, M. Krarti. (1997). Development of a predictive optimal controller for thermal energy storage systems. HVAC&R Research;3:233-264.

G. Henze. (2005). Energy and cost minimal control of active and passive building thermal storage inventory. Journal of Solar Energy Engineering;127:343-351.

G. Mavromatidis, K. Orehounig, J. Carmeliet. (2018). Design of distributed energy systems under uncertainty: A two-stage stochastic programming approach. Applied Energy;222:932-950.

G. Zhang, B. Patuwo, M. Hu. (1998). Forecasting with artificial neural networks:: The state of the art. International journal of forecasting;14:35-62.

G. Zhou, M. Krarti, G. Henze. (2004). Parametric analysis of active and passive building thermal storage utilization. Paper presented at the ASME 2004 International Solar Energy Conference.

J. Benesty, J. Chen, Y. Huang, I. Cohen. (2009). Pearson correlation coefficient. Noise reduction in speech processing;1-4, Springer.

J. Birge, F. Louveaux. (2011). Introduction to stochastic programming. Springer Science & Business Media.

J. Cohen, P. Cohen, S. West, L. Aiken. (2013). Applied multiple regression/correlation analysis for the behavioral sciences: Routledge.

J. Nagi, K. Yap, S. Tiong, S. Ahmed. (2008). Electrical power load forecasting using hybrid self-organizing maps and support vector machines. Training;99:31.

J. Rager, F. Maréchal. (2015). Urban energy system design from the heat perspective using mathematical programming including thermal storage. Lausanne, Switserland: EPFL École Polytechnique Fédérale de Lausanne.

J. Sarduy, K. Santo, M. Saidel. (2016). Linear and non-linear methods for prediction of peak load at University of São Paulo. Measurement;78:187-201.

J. Seem. (1995). Adaptive demand limiting control using load shedding. HVAC&R Research;1:21-34.

J. Wang, X. Su. (2011). An improved K-Means clustering algorithm. Paper presented at the Communication Software and Networks (ICCSN), 2011 IEEE 3rd International Conference on.

J. Xie, T. Hong. (2016). GEFCom2014 probabilistic electric load forecasting: An integrated solution with forecast combination and residual simulation. International Journal of Forecasting;32:1012-1016.

J. Yoon, R. Bladick, A. Novoselac. (2014). Demand response for residential buildings based on dynamic price of electricity. Energy and buildings;80:531-541.

K. Drees, J. Braun. (1997). Development and evaluation of a rule-based control strategy for ice storage systems. HVAC&R Research;2:312-334.

K. Herter. (2007). Residential implementation of critical-peak pricing of electricity. Energy

Policy;35:2121-2130.

K. Keeney, J. Braun. (1997). Application of building precooling to reduce peak cooling requirements. ASHRAE transactions;103:463-469.

K. Khan, M. Rasul, M. Khan. (2004). Energy conservation in buildings: cogeneration and cogeneration coupled with thermal energy storage. Applied Energy;77:15-34.

K. Lee, J. Braun. (2008). Development of methods for determining demand-limiting setpoint trajectories in buildings using short-term measurements. Building and Environment;43:1755-1768.

K. Siler-Evans, M. Morgan, I. Azevedo. (2012). Distributed cogeneration for commercial buildings: Can we make the economics work? Energy Policy;42:580-590.

L. Uusitalo, A. Lehikoinen, I. Helle, K. Myrberg. (2015). An overview of methods to evaluate uncertainty of deterministic models in decision support. Environmental Modelling & Software;63:24-31.

L. V. Fausett. (1994). Fundamentals of neural networks: architectures, algorithms, and applications (Vol. 3): Prentice-Hall Englewood Cliffs.

L. Xu, S. Wang. and R. Tang. (2019). Probabilistic load forecasting for buildings considering weather forecasting uncertainty and uncertain peak load. Applied Energy;237:180-195.

M. Aien, A. Hajebrahimi, M. Fotuhi-Firuzabad. (2016). A comprehensive review on uncertainty modeling techniques in power system studies. Renewable and

sustainable energy reviews;57:1077-1089.

M. Ban, G. Krajačić, M. Grozdek, T. Ćurko, N. Duić. (2012). The role of cool thermal energy storage (CTES) in the integration of renewable energy sources (RES) and peak load reduction. Energy;48:108-117.

M. Benedetti, V. Cesarotti, V. Introna, J. Serranti. (2016). Energy consumption control automation using Artificial Neural Networks and adaptive algorithms: Proposal of a new methodology and case study. Applied Energy;165:60-71.

M. Breunig, H. Kriegel, R. Ng, J. Sander. (2000). LOF: identifying density-based local outliers. Paper presented at the ACM sigmod record.

M. Cilimkovic. (2015). Neural networks and back propagation algorithm. Institute of Technology Blanchardstown, Blanchardstown Road North Dublin;15.

M. Evans, N. Hastings, B. Peacock. (2000). Statistical distributions.

M. Piette, O. Sezgen, D. Watson, N. Motegi, C. Shockman, L. Ten Hope. (2004). Development and evaluation of fully automated demand response in large facilities.

M. Raza, A. Khosravi. (2015). A review on artificial intelligence based load demand forecasting techniques for smart grid and buildings. Renewable and sustainable energy reviews;50:1352-1372.

M. Singh, V. Khadkikar, A. Chandra, R. Varma. (2011). Grid interconnection of renewable energy sources at the distribution level with power-quality improvement features. IEEE transactions on power delivery;26:307-315.

M. Yamaha, S. Misaki. (2006). The evaluation of peak shaving by a thermal storage system using phase-change materials in air distribution systems. HVAC&R Research;12:861-869.

N. Sahinidis. (2004). Optimization under uncertainty: state-of-the-art and opportunities. Computers & Chemical Engineering;28:971-983.

N. Wang, J. Zhang, X. Xia. (2013). Energy consumption of air conditioners at different temperature set points. Energy and buildings;65:412-418.

N. Zhu, S. Wang, X. Xu, Z. Ma. (2010). A simplified dynamic model of building structures integrated with shaped-stabilized phase change materials. International Journal of Thermal Sciences; 49:1722-1731.

P. Centolella. (2010). The integration of price responsive demand into regional transmission organization (RTO) wholesale power markets and system operations. Energy;35:1568-1574.

P. Mago, A. Hueffed. (2010). Evaluation of a turbine driven CCHP system for large office buildings under different operating strategies. Energy and buildings;42:1628-1636.

P. McSharry, S. Bouwman, G. Bloemhof. (2005). Probabilistic forecasts of the magnitude and timing of peak electricity demand. IEEE Transactions on Power Systems;20:1166-1172.

P. Tatsidjodoung, N. Le Pierrès, L. Luo. (2013). A review of potential materials for thermal energy storage in building applications. Renewable and sustainable energy

reviews;18:327-349.

P. Xu, P. Haves, M. Piette, J. Braun. (2004). Peak demand reduction from pre-cooling with zone temperature reset in an office building.

P. Xu, P. Haves, M. Piette, L. Zagreus. (2005). Demand shifting with thermal mass in large commercial buildings: Field tests, simulation and audits. Lawrence Berkeley National Laboratory.

R. Qi, L. Lu, H. Yang. (2012). Investigation on air-conditioning load profile and energy consumption of desiccant cooling system for commercial buildings in Hong Kong. Energy and buildings;49:509-518.

R. Rockafellar, S. Uryasev. (2000). Optimization of conditional value-at-risk. Journal of risk;2:21-42.

R. Yin, P. Xu, M. Piette, S. Kiliccote. (2010). Study on Auto-DR and pre-cooling of commercial buildings with thermal mass in California. Energy and buildings;42:967-975.

S. Boonnasa, P. Namprakai. (2010). The chilled water storage analysis for a university building cooling system. Applied Thermal Engineering;30:1396-1408.

S. Coles, J. Bawa, L. Trenner, P. Dorazio. (2001). An introduction to statistical modeling of extreme values. Springer;208.

S. Kalogirou. (2001). Artificial neural networks in renewable energy systems applications: a review. Renewable and sustainable energy reviews;5:373-401.

S. Liu, G. P. Henze. (2004). Impact of modeling accuracy on predictive optimal control of active and passive building thermal storage inventory. ASHRAE transactions;110:151.

S. Morgan, P. Moncef Krarti. (2010). Field testing of optimal controls of passive and active thermal storage. ASHRAE transactions;116:134.

S. Pfenninger, A. Hawkes, J. Keirstead. (2014). Energy systems modeling for twenty-first century energy challenges. Renewable and sustainable energy reviews;33:74-86.

S. Sadineni, R. Boehm. (2012). Measurements and simulations for peak electrical load reduction in cooling dominated climate. Energy;37:689-697.

S. Scalat, D. Banu, D. Hawes, J. Parish, F. Haghighata, D. Feldman. (1996). Full scale thermal testing of latent heat storage in wallboard. Solar Energy Materials and Solar Cells;44:49-61.

S. Wang, X. Xu. (2006). Simplified building model for transient thermal performance estimation using GA-based parameter identification. International Journal of Thermal Sciences;45:419-432.

S. Wang, X. Xue, C. Yan. (2014). Building power demand response methods toward smart grid. HVAC&R Research;20:665-687.

S. Wang. (2016). Making buildings smarter, grid-friendly, and responsive to smart grids. Science and Technology for the Built Environment;22:629-632.

T. Chen. (2001). Real-time predictive supervisory operation of building thermal systems

with thermal mass. Energy and Buildings;33:141-150.

T. Hong, P. Pinson, S. Fan, H. Zareipour, A. Troccoli, R. J. Hyndman. (2016). Probabilistic energy forecasting: Global energy forecasting competition 2014 and beyond: Elsevier.

T. Hong, S. Fan. (2016). Probabilistic electric load forecasting: A tutorial review. International Journal of Forecasting;32:914-938.

V. Gungor, D. Sahin, T. Kocak, S. Ergut, C. Buccella, C. Cecati, G. Hancke. (2011). Smart grid technologies: Communication technologies and standards. IEEE transactions on Industrial informatics;7:529-539.

W. Qureshi, N. Nair, M. Farid. (2011). Impact of energy storage in buildings on electricity demand side management. Energy Conversion and Management;52:2110-2120.

W. Walker, P. Harremoës, J. Rotmans, J. van der Sluijs, M. van Asselt, P. Janssen, M. Krayer von Krauss. (2003). Defining uncertainty: a conceptual basis for uncertainty management in model-based decision support. Integrated assessment;4:5-17.

X. Xue, S. Wang, Y. Sun, F. Xiao. (2014). An interactive building power demand management strategy for facilitating smart grid optimization. Applied Energy;116:297-310.

Y. Sun, S. Wang, F. Xiao, D. Gao. (2013). Peak load shifting control using different cold thermal energy storage facilities in commercial buildings: a review. Energy Conversion and Management;71:101-114.

Y. Sun, S. Wang, G. Huang. (2010). A demand limiting strategy for maximizing monthly cost savings of commercial buildings. Energy and buildings;42:2219-2230.

Y. Wang, D. Gan, M. Sun, N. Zhang, Z. Lu, C. Kang. (2019). Probabilistic individual load forecasting using pinball loss guided LSTM. Applied Energy;235:10-20.

Y. Zeng, Y. Cai, G. Huang, J. Dai. (2011). A review on optimization modeling of energy systems planning and GHG emission mitigation under uncertainty. Energies;4:1624-1656.

Y. Zhang, G. Augenbroe. (2018). Optimal demand charge reduction for commercial buildings through a combination of efficiency and flexibility measures. Applied Energy;221:180-194.

Y. Zhang, G. Zhou, K. Lin, Q. Zhang, H. Di. (2007). Application of latent heat thermal energy storage in buildings: State-of-the-art and outlook. Building and Environment;42:2197-2209.